VSV G H10/A4 MUTANTS AND H2-H10/A4 DOUBLE MUTANTS

CHARACTERIZATION OF THE H10/A4 REGION OF VESICULAR STOMATITIS VIRUS G PROTEIN AND EFFECTS OF H2-H10/A4 MUTATIONS ON FUSOGENIC FUNCTIONS

By

SHAHIRA SHOKRALLA, B.Sc.

A Thesis

Submitted to the School of Graduate Studies

in Partial Fulfilment of the Requirements

for the Degree

Master of Science

McMaster University

MASTER OF SCIENCE (1998)
(Biochemistry)

McMaster University
Hamilton, Ontario

TITLE: Characterization of the H10/A4 region of vesicular stomatitis virus G protein and effects of H2-H10/A4 mutations on fusogenic functions

AUTHOR: Shahira Shokralla, B.Sc. (University of Toronto)

SUPERVISOR: Professor H.P. Ghosh

NUMBER OF PAGES: xvii, 167

PUBLICATIONS

Shokralla, S., He, Y., Wanas, E., and Ghosh, H.P. (1998). Mutations in a carboxy-terminal region of vesicular stomatitis virus glycoprotein G that affect membrane fusion activity. *Virology,* **242,** 39-50.

ABSTRACT

The vesicular stomatitis virus glycoprotein G is responsible for low pH mediated membrane fusion induced by the virus. Four linker insertion mutants (H2, H5, H10, A4) of the G ectodomain were found to disrupt fusion and yet maintained all the requirements for proper folding and cell surface expression (Li et al., 1993). Site specific mutagenesis of residues 123 to 137, surrounding the H2 mutant, either blocked or shifted the pH optima and threshold of fusion to more acidic values with a concomitant reduction in cell-cell fusion efficiency (Zhang and Ghosh, 1994; Fredericksen and Whitt, 1995). The region is highly conserved among vesiculoviruses and was found to insert into lipid membranes by hydrophobic photolabelling (Durrer et al., 1995) suggesting a possible role for this domain as the fusion peptide. Site-directed mutagenesis of residues 190 to 210, surrounding the H5 insertion mutant, did not significantly affect fusion (Fredericksen and Whitt, 1995). Surrounding the H10 and A4 insertion mutants is a conserved region, residues 395 to 424, that does not interact with target membranes (Durrer et al., 1995).

To determine the functional importance of this region, site-directed mutagenesis was employed. Substitution of conserved Gly 404, Gly 406, Asp 409, and Asp 411 with Ala, Ala, Asn, and Asn, respectively, both reduced fusion and caused a shift in the pH of fusion threshold to more acidic values (tested by Y. He as published in Shokralla et al., 1998). In this study, the H10/A4 region is further mutagenized and tested for fusion. Cell surface expression was examined by indirect immunofluorescence and lactoperoxidase catalyzed

iodination. Rates of transport from the endoplasmic reticulum and oligomerization into trimers were tested by resistance to endoglycosidase H and sucrose density gradient centrifugation, respectively. Low-pH induced conformational changes were assayed by resistance to proteolytic digestion. Residues Gly 395, Gly 404, Gly 409 and Ala 418 were substituted with Glu, Lys, Asp, and Lys, respectively. All mutants, with the exception of A418K, were expressed at levels similar to or above wild-type. Mutants G404K and D409A completely abolished fusion. Mutant G395E reduced cell-cell fusion efficiency by 82% and shifted both the pH threshold and optimum of wild type fusion. Although all mutants were capable of trimer formation, alterations in the structure of mutants G404K, D409A, and A418K were detected by slower transport rates. All H10/A4 mutants were more susceptible to trypsin than wild-type at the pH of 6.5, and mutant G404K was completely susceptible at this pH. Reductions in the extent of fusion, along with shifts in the pH optima and thresholds of fusion suggest that the H10/A4 region (residues 395 to 418) of vesicular stomatitis virus G protein is important for G mediated fusion. The region may influence low-pH induced conformational changes.

Double mutants of the H2 and H10/A4 regions were also tested for their effects on fusion. The extents of fusion mediated by double mutant G proteins were severely reduced with levels ranging from 28% wild-type fusion to complete fusion deficiency. Only mutant G131A G404A was capable of 83% wild-type fusion. Mutants G131A G395E, G131A G404A, G131A D411N, D137N G404A, and the fusion defective D137N D411N were expressed at levels above wild-type G protein at the cell surface. Mutants F125Y D411N and

P126L D411N, although capable of very low levels of fusion were not detectable at the cell surface by immunofluorescence and were detected at low levels by lactoperoxidase catalyzed iodination of cell surface proteins. These two mutants, along with G131A G404A, also showed slower transport rates than wild-type G. All double mutants showed increased sensitivity to trypsin at the pH of 6.5 with mutant F125Y D411N showing complete susceptibility. They were also all capable of trimer formation by sucrose density gradient centrifugation. In comparing the fusion profiles of double mutants with those of their component single mutants, it was found that in most cases the pH threshold of fusion by double mutants was greater than the sum of the single mutants and that the pH optimum of fusion corresponded to that of the constituent H2 single mutant. Although, the regions are functionally independent, they may indirectly affect one another through alterations in protein structure.

ACKNOWLEDGEMENTS

These studies would not have been possible without the help and encouragement of my supervisor, Dr. H.P. Ghosh. Thanks for all the advice. For technical assistance, I thank Kakoli Ghosh, Derek Odell, Essam Wanas, and Sue Efler. Thanks for passing on all the 'tricks' to science.

This work is dedicated to my parents for their endless support, strength, and patience.

TABLE OF CONTENTS

LIST OF ILLUSTRATIONS

LIST OF TABLES

LIST OF ABBREVIATIONS

ATP	Adenosine triphosphate
BHA	Bromelain treated hemagglutinin
BiP	Immunoglobulin heavy chain binding protein
BSA	Bovine serum albumin
CIAP	Calf intestinal alkaline phosphatase
dATP	Deoxyadenosinetriphosphate
dCTP	Deoxycytidinetriphosphate
dGTP	Deoxyguanosinetriphosphate
DMSO	Dimethyl sulfoxide
DNA	Deoxyribonucleic acid
dTTP	Deoxythymidinetriphosphate
DTT	Dithiotreitol
EDTA	Ethylenediaminetetraacetic acid
EGTA	Ethyleneglycol-bis(β-aminoethylether) N,N,N',N' tetraacetic acid
ER	Endoplasmic reticulum
E. coli	Escherichia coli
EDTA	Ethylenediaminetetraacetic acid
Endo H	Endoglycosidase H
FITC	Fluorescein isothiocyanate
GPI	Glycosylphosphatidylinositol
HA	Hemagglutinin
HEPES	N-2-hydroxyethylpiperazine-N'-2-ethanesulfonic acid
HGD	High glucose Dulbecco's
HIV	Human immunodeficiency virus
LB	Luria Bertani
MES	2-[N-Morpholino]-ethanesulfonic acid
MMTV	Mouse mammary tumour virus
MoMuLV	Moloney murine leukemia virus
MOPS	3-[N-Morpholino]-proanesulfonic acid
NEB	New England Biolabs Ltd.
PBS	Phosphate buffered saline
PMSF	Phenylmethylsulfonyl fluoride
RAIN	rabies G mutants resistant to acid induced neutralization
SDS	Sodium dodecylsulfate
SFV	Semliki Forest virus
SIV	Simian immunodeficiency virus
SU	Surface protein of retroviruses
TBE	Tick-borne encephalitis virus

$TBHA_2$	Bromelain, trypsin and thermolysin treated hemagglutinin
TE	Tris-EDTA buffer
TEMED	N,N,N',N' Tetramethyl-ethylenediamine
TM	Transmembrane protein of retroviruses
VSV	Vesicular stomatitis Virus
VSV G	Vesicular stomatitis Virus glycoprotein G

1. INTRODUCTION

1.1 Membrane Fusion

Membrane fusion is the unification of two separate membrane bound compartments resulting in joining of lipid membranes and content mixing. It is required for many cellular functions including protein transport, endocytosis, and phagocytosis. Fusion may be endocytoplasmic or exocytoplasmic depending on the bilayer leaflet making first contact. The first involves initial contact with the cytoplasmic surface of cellular membranes, whereas in the latter process initial contacts are made by external surfaces of cellular membranes or the lumenal surfaces of intracellular compartments (Stegmann et al., 1989). The process is energetically unfavourable, and therefore requires an aid to overcome repulsive hydration forces and/or to promote attractive hydrophobic ones (White, 1990; Stegmann et al., 1989). It is thus postulated that cellular proteins are responsible for bridging the gap between two opposing bilayers. Viral membrane fusion mediating proteins can be more easily identified, manipulated, and examined, than their cellular counterparts without having significant effects on cell survival or function. Extensive studies are, therefore, currently ongoing to understand the fusogenic mechanisms of such proteins. These have lead to a working hypothesis of membrane fusion as follows: a conformational change in an oligomerized fusion protein is induced following exposure to an external stimulus, peptide domains within the protein make initial contacts with the target membrane probably at an oblique angle, clustering of oligomers, mixing of only the external leaflets in both the viral and target membranes (termed

hemifusion), opening and dilation of a fusion pore (Hernandez et al., 1996; Durell et al., 1997; White, 1992). A glycophosphatidylinositol (GPI) lipid tail that was substituted for influenza HA transmembrane and cytoplasmic tail was capable of mixing the outer lipid layer but not of complete fusion (Kemble et al., 1994; Melikyan et al., 1995). This suggests that pore formation and dilation require at least a transmembrane anchor. Although GPI-linked vesicular stomatitis virus (VSV) G was incapable of hemifusion, a transmembrane anchor was also found to be required for complete fusion (Odell et al., 1998). Similar to influenza, the transmembrane sequence itself was found not to be important (Schroth-Diez et al., 1998; Odell et al., 1998). The best characterized fusion mediating viral glycoprotein is hemagglutinin (HA) of influenza virus. This is because crystall structures of both fusion inactive and active forms have been solved (Wilson et al., 1981; Bullough et al., 1994). The fusion active forms of human immunodeficiency virus gp41 (Weissenhorn et al., 1997; Chan et al., 1997) and Moloney murine leukemia virus TM (Fass et al., 1996) have recently also been characterized. The G glycoprotein of vesicular stomatitis virus differs from the above-mentioned glycoproteins in the location of the fusion mediating domain and in its response to similar environmental conditions. Studies of G protein would, therefore, broaden our understanding of different classes and modes of action of fusogenic proteins.

1.2 pH Dependence

Fusion of a viral envelope with a cellular lipid bilayer can take place either under acidic or neutral pH conditions (White, 1990). Viruses that require a low-pH to induce fusion include VSV, rabies virus, Semliki Forest virus (SFV), and influenza virus. Once exposed to

the acidic environment of the endosome, following receptor mediated endocytosis, a conformational change is induced within the fusion protein that is responsible for mediating fusion between the viral and endosomal membranes. Viruses that do not require an acidic-pH generally induce fusion under neutral pH conditions, at the cell surface, where a fusion active conformation of the glycoprotein is presumably triggered by binding to a cell surface receptor. These viruses can also induce fusion under the influence of the acidic pH of the endosome. pH-independent fusion can be mediated by the glycoproteins of human immunodeficiency virus (HIV), paramyxoviruses, and herpesviruses. It is the viral fusion protein that is responsible for the pH dependence of fusion.

1.3 Viral Fusion Proteins

Fusion proteins catalyze the formation of fusion pores. Properties of viral fusion proteins are summarized in reviews by White (1990) and Hernandez, et al. (1996). Overall, all viral fusion proteins are composed of class I integral membrane proteins with greater than 85% of the protein mass external to the viral membrane. They are also post-translationaly modified with N-linked oligosaccharides, and many are fatty acylated (White et al., 1990; Hernandez et al., 1996). Many of these are synthesized as large precursors that are proteolyticaly cleaved to form two non-covalently or disulfide linked subunits. The fusion peptide is normally located at the amino terminus of the membrane subunit. In some cases, however, the fusion peptide is internally located. Examples of fusion proteins include influenza hemagglutinin (HA) which is cleaved to generate the HA_1 and HA_2 subunits. The HA_2 subunit is membrane anchored and carries the fusion peptide at its amino-terminus. The

Sendai virus F protein is cleaved into the F_1 and F_2 subunits with the membrane anchored F_2 subunit containing the fusion peptide. This is also the case for the HIV gp160 glycoprotein that is cleaved into its gp120 and gp41 subunits. The gp41 subunit is membrane anchored and contains the fusion peptide at the N-terminus. VSV G, rabies G, and tick-borne encephalitis (TBE) virus E fusion proteins are composed of a single subunit with the fusion peptide found internally within the glycoprotein. The Semliki Forest virus protein is synthesized as a p62 precursor that heterodimerizes with the E1 fusion protein. The precursor is later cleaved into an E2 and E3 subunits. Both E1 and E2 are membrane anchored. Although fusion proteins differ in the number of subunits and fusion peptide location, the peptide is always present within a membrane anchored subunit. Viral fusion mediating proteins are present on the cell surface as oligomers at a high density.

1.4 Fusion Peptides

Mediating initial interactions between the viral envelope and target membrane is the fusion peptide. It may be found at the amino terminus or internally within the fusion protein, but the location does not correlate with the pH dependence of the fusion process. In general, fusion peptides are relatively short hydrophobic stretches of amino acids conserved within virus families (White, 1990). Amino terminal fusion peptides are typically 20 to 36 amino acids in length and terminate at the first positively charged residue (White, 1990; Durell et al., 1997). An internal fusion peptide is characterized as a region of 16 to 20 apolar amino acids with a positively charged residue at the amino terminal end and either a basic or acidic amino acid at the carboxy terminal end (White, 1990; Durell et al., 1997). The peptides of human

immunodeficiency and influenza viruses can be modelled as amphipathic alpha-helices rich in alanine and glycine (White, 1990; Durell et al., 1997). Internal fusion peptides may also contain proline near the centre (White, 1992). Fusion peptides are thought to help induce coalescence of apposing membrane bilayers by induction of localized lipid perturbations prior to the formation of lipid pores (Durell et al., 1997).

For VSV no stretches of hydrophobic amino acids were detected in the ectodomain other than the cleaved signal sequence. The amino terminus is hydrophilic and mutagenesis of the N-terminal amino acid did not alter the fusogenic activity of G protein (Woodgett and Rose, 1986). That the fusion peptide may be internal was first suggested by Ohnishi, 1988, based on conservation of residues 116 to 148 between Indiana and New Jersey VSV serotypes. The presence of an additional N-linked oligosaccharide at residue 117 was sufficient to cause loss of fusion (Whitt et al., 1990). Immediately adjacent to residue 117 is a region of uncharged amino acids (residues 118-136) postulated to constitute the internal fusion peptide. Linker insertion mutagenesis (Li et al., 1993), identified four fusion defective mutants in regions conserved between VSV serotypes within G ectodomain. These were termed the H2, H5, and H10/A4 regions with insertion mutations at residues 123, 194, 410, and 415 respectively (Fig. 1A). The H2 mutation is present within the uncharged 19 amino acid candidate fusion peptide. The H10 and A4 mutations also lie within a region conserved between VSV serotypes, residues 395 to 424. Some hydrophobic character is present in the region surrounding the H5 insertion mutation (residues 191-215). The H2 and H10/A4 regions are also somewhat hydrophobic. Site directed mutagenesis of residues 118 to 139 surrounding the H2 mutation resulted in complete fusion inhibition or a shift in the pH

optimum and threshold of fusion (Zhang and Ghosh, 1994; Fredericksen and Whitt, 1995, 1996). The region was therefore postulated as a putative fusion peptide. Glycine, alanine, proline, and aspartic acids were critical to fusion. The spatial arrangement of these residues is similar to that of the Semliki Forest virus E1 protein that is also responsible for low-pH mediated fusion (Zhang and Ghosh, 1994). These residues are also largely conserved among alphaviruses (Kielian, 1993). Mutagenesis of these residues resulted in a pH shift to more acidic values for both SFV (Levy-Mintz and Kielian, 1991) and VSV, suggesting a common structural requirement. Hydrophobic photolabelling experiments (Durrer et al., 1995) have revealed that a region within residues 59 to 221 of G protein interacts with target membranes upon acidification of the surrounding medium. The labelled fragment contained the H2 region within it, supporting the premise that this region is the fusion peptide. Also labelled was the H5 region (residues 191 to 215), but site directed mutagenesis in this region did not alter the fusogenic properties of G protein (Fredericksen and Whitt, 1995). The H5 region is also not sufficiently conserved within the G proteins of four vesiculoviruses (Li et al., 1993). The H10/A4 region was not photolabeled, and therefore is not directly involved in target membrane fusion. Hydrophobic photolabeling was also used to label the putative fusion peptides of rabies (Durrer et al., 1995) and influenza (Harter et al., 1989).

1.5 The Vesicular Stomatitis Virus

Vesicular stomatitis virus belongs to the *Vesiculovirus* genus of the *Rhabdoviridae* family. Wagner and Rose (1996) provide a review of the structure, life cycle, and pathogenesis of the virus. The virion is bullet shaped with a ribonucleoprotein core

surrounded by a lipid bilayer envelope from which glycoprotein spikes protrude (Fig. 1B). The ribonucleoprotein (RNP) core consists of unsegmented single stranded negative sense RNA that is tightly wound by the N (nucleocapsid) protein. Within the genome are five anti-sense genes, in the order 3'-N,P,M,G,L-5', coding for the nucleocapsid, phosphoprotein, M (matrix), G (glycoprotein), and L protein. Associated with RNP is the P (phosphoprotein) and L (large) protein that together with the N protein serve as the viral transcriptase.

G protein is responsible for receptor recognition and binding to target cells. Following adsorption, a virus particle is endocytosed via clathrin coated pits by endocytosis. The acidic pH of the endosome triggers a conformational change in G that allows the protein to mediate fusion of the viral envelope with that of the endosome, so that the ribonucleocapsid is released into the cytoplasm. P and L proteins together serve as the polymerase for transcription of the genomic RNA associated with the nucleocapsid protein. Transcription is polar such that genes closer to the 3' end of the genomic RNA are transcribed in greater quantities than those closer to the 5' end. A 30% decrease in transcription of a gene relative to its upstream neighbour is evident (Iverson and Rose, 1981). The RNP complexed with L and P proteins also serves as the viral replicase. Unlike transcription, replication requires concomitant translation. This is because, large amounts of N protein are required to encase newly synthesized genomes. Translation of P protein is also required. Matrix protein binds to progeny nucleocapsid in the cytoplasm and associates with plasma membrane regions enriched with the G glycoprotein. Both M and G are thought to contribute to the budding process (section 1.7).

Fig. 1. (A) The amino-terminal and carboxy-terminal predicted heptad repeats are indicated as arrows labelled HR1 and HR2, respectively. The transmembrane (TM) and cytoplasmic (CT) domains are alsc represented. An arrow the site of signal sequence cleavage. The diagram is not to scale. (B) The vesicular stomatitis virus with a schematic representation of its genome. Adapted from Wagner and Rose (1996). Schematic representation of G protein. The H2, H5, and H10/A4 regions are indicated.

A

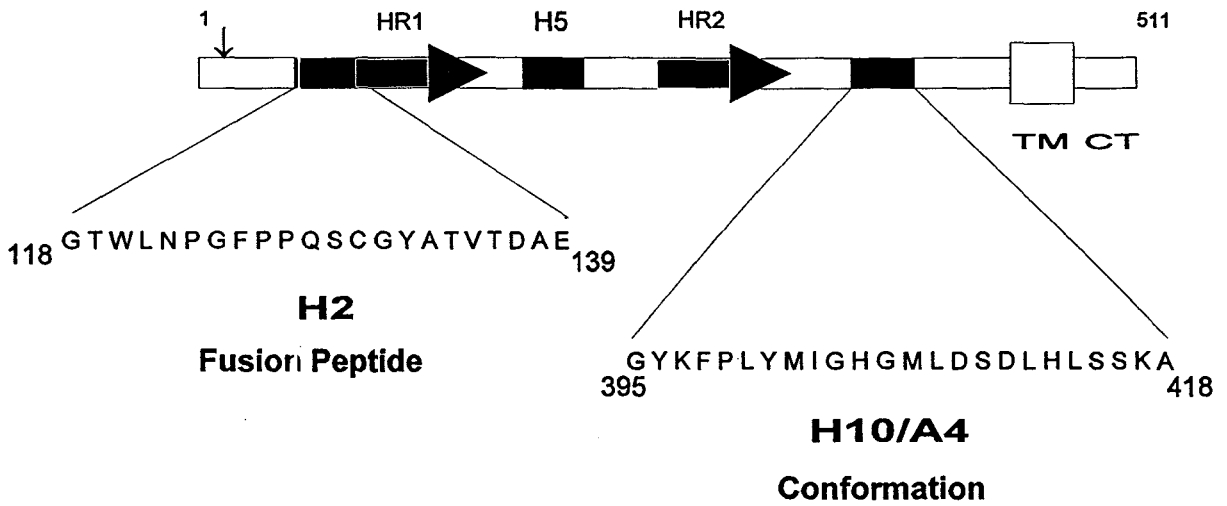
1
HR1
H5
HR2
511
TM CT
118 GTWLNPGFPPQSCGYATVTDAE 139
H2
Fusion Peptide
GYKFPLYMIGHGMLDSDLHLSSKA
395
418
H10/A4
Conformation

B

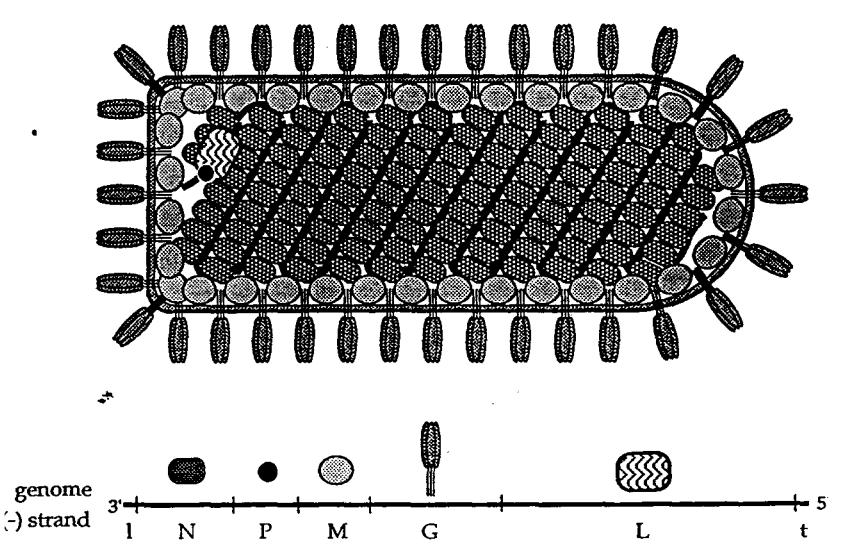
genome
(-) strand
3'
5
l
N
P
M
G
L
t

1.6 Pathway of G Protein Synthesis and Maturation

The G protein of vesicular stomatitis virus Indiana serotype is 511 amino acids in length with a 20 amino acid transmembrane region and a 29 amino acid cytoplasmic tail (Fig. 1A). Within the ectodomain is a 16 residue amino terminal signal sequence, two glycosylation sites, and two predicted regions of a-g heptad repeats (Rose and Gallione, 1981; Coll, 1995).

The protein is synthesized on the rough endoplasmic reticulum. It is inserted into the ER and is glycosylated (Knipe et al., 1977). ER associated glucosidase and mannosidase activities modify the two N-linked core oligosaccharides (Tabas and Kornfeld, 1978; Atkinson and Lee, 1984). Further trimming and modification of the sugar moieties take place in the Golgi network (Balch et al., 1986). Oligomerization of monomeric G proteins into non-covalently linked trimers also takes place in the endoplasmic reticulum and is required for transport out of the ER and to the cis-Golgi network (Doms et al., 1987). Transport is blocked with depletion of adenosine triphosphate (ATP). Much of the details of folding within the endoplasmic reticulum were studied using the temperature sensitive mutant ts045. This mutant fails to oligomerize and transport out of the ER at the non-permissive temperature (Kreis and Lodish, 1986). When the temperature is lowered to a permissive one, however, the mutant protein is capable of trimer formation and transport. Failure to transport is due to formation of aggregates that dissociate to monomers and trimerize under a permissive temperature (Doms et al., 1987). Aggregates also fail to dissociate upon ATP depletion. The protein was found to incorrectly fold at the non-permissive temperature with incomplete intra-chain disulfide bonds. In addition, epitope recognition by monoclonal antibody failed and the protein was permanently associated with the immunoglobulin heavy

chain binding protein (BiP) and calnexin chaperones (de Silva et al., 1990; de Silva et al., 1993; Hammond and Helenius., 1994). All properties were reversed upon exposure to the permissive temperature. BiP and calnexin were also found to transiently bind to wild type G protein during folding and permanently to a number of irreversible G protein mutants (Machamer et al., 1990; Mathieu et al., 1996). Newly synthesized wild type G polypeptides are thought to interact with BiP and calnexin immediately after chain termination and are released one to four minutes later as trimerization competent monomers (de Silva et al., 1993; Machamer et al., 1990, Hammond and Helenius, 1994).

Although not absolutely required, the cytoplasmic domain of G protein has been shown to regulate rates of transport. Deletion mutants lacking both the transmembrane and cytoplasmic domains were capable of trimer formation and secretion out of cells, albeit at a reduced rate (Rose and Bergmann, 1983; Crise et al., 1989; Guan et al., 1988). Glycophospholipid anchored G protein was capable of trimer formation and cell surface expression, but was also reduced in its rate of transport as compared to wild-type G protein (Crise et al., 1989; Odell et al., 1997). Considerably shorter substitution mutants of the cytoplasmic domain that had little effect on protein folding or oligomerization were either retained in the endoplasmic reticulum or slowly transported to the cell surface (Doms et al., 1988; Guan et al., 1988). Balch et al., 1994, detected accumulation of G in vesicles during vesicular budding from the endoplasmic reticulum. The tail of G protein does not contain a specific transport signal, but may contain one that aids in clustering at sites of transport vesicle formation (Guan et al., 1988).

1.7 A Role for G Protein in Budding

Following modifications in the Golgi, G is inserted into the plasma membrane where it awaits interaction with progeny viral nucleocapsids. A role for the glycoprotein of vesicular stomatitis virus in budding of mature virion from a host cell plasma membrane was first elucidated using complementation studies of the temperature sensitive mutant ts045. A hybrid composed of the extracellular and transmembrane domains of HIV-1 env glycoprotein, and the tail of VSV G was able to rescue ts045. This was not true for wild type env or env protein with the same length tail as that of G. Thus, the cytoplasmic domain and not the extracellular or transmembrane domains was responsible for rescue (Owens and Rose, 1993). G proteins with tails shortened to either the membrane proximal nine amino acids or membrane distal twelve amino acids were found to rescue ts045 at the non-permissive temperature. The presence of one or three amino acids was not sufficient, indicating that at least part of the cytoplasmic tail is required for efficient budding (Whitt et al., 1989). Similar results were obtained when Schnell et al. (1998) also recovered vesicular stomatitis virion expressing these constructs. Schnell et al. (1998), however, was also able to recover VSVs expressing chimeric G with transmembrane and cytoplasmic tails derived from CD4 (termed GCC). Hybrid G protein containing CD4 cytoplasmic tail (GGC) budded with equal or near efficiency as that of wild type, whereas the chimera GCC budded with approximately half the efficiency of wild type G. This has led to a model for VSV budding in which a short cytoplasmic tail but not a specific sequence is required.

The VSV M and G proteins have each been shown solely to drive budding without the requirement of other viral proteins. The M protein was reported to bind to the plasma

membrane and to induce exocytotic budding of vesicles (Chong and Rose, 1993, 1994; Li et al., 1993a; Justice et al., 1995). The exocytotic activity of G protein has been implied by the generation of infectious vesicles containing naked Semliki forest virus RNA and G spikes (Rolls et al., 1996). Budding of rabies virus in the absence of glycoprotein G was observed by Mebatsion et al. (1996) but with a reduction in efficiency of about 30-fold. Budding efficiency was also decreased by approximately 24-fold when the cytoplasmic tail of G was omitted. Mebatsion et al. (1996) has proposed that efficient budding of rhabdoviruses is a concerted effort between the matrix and spike proteins. The M protein might induce bending of the plasma membrane from within the cellular interior; whereas G protein would induce bending from the exterior. The tails of oligomeric G protein may interact with a "pocket or groove" in the viral nucleocapsid or matrix to form a structure that would enhance envelopment of viral cores and overall budding (Schnell et al., 1998).

1.8 Lipid Requirements for G Mediated Binding and Fusion

VSV G does not only mediate fusion of the viral envelope with that of the endosome, but is also responsible for receptor recognition on the cell membrane. Removal of the viral glycoprotein by trypsinization reduced adsorption of viral particles to cells (Schloemer and Wagner, 1975). Sialoglycoproteins and sialoglycolipids were both excluded as possible VSV receptors, since treatment of cells with either trypsin or neuraminidase resulted in an increase in the number and rate of virion attachment (Schloemer and Wagner, 1975; Yamada and Ohnishi, 1986). Detergent extracts of Vero cells were also tested for inhibition of VSV binding to Vero cells (Schlegel et al., 1983). The binding factor was found to be resistant to

trypsin, pronase, neuraminidase, and heating to 100°C for 10 minutes. It was, however, soluble in chloroform-methanol and susceptible to phospholipase C, suggesting that the inhibitory activity was in fact a phospholipid. Liposomes of purified phoshpatidylserine were the most effective phospholipid in inhibition of VSV binding with 10μM concentrations resulting in complete inhibition. As well, spin-labelled VSV bound preferentially to phoshpatidylserine liposomes (Yamada and Ohnishi, 1986) over those containing phoshpatidylcholine, without any dependence on acyl-chain composition. The serine phosphoglycerol head alone did not inhibit binding, suggesting that both the head group and fatty acid moieties are required for binding. The amount of virus bound to liposomes at acidic pHs was similar to that bound at pH 7.0, but decreased at pH values greater than 7.0 (Yamada and Ohnishi, 1986). This may help to ensure that dissociation of the viral glycoprotein from the target membrane does not take place under the acidic conditions of the endosome (Lenard, 1993). Studies with liposomes by Yamada and Ohnishi (1986) have revealed that binding is dependent on the phosphate head group of lipids, with a greater affinity toward phosphatidylserine than to phosphatidylcholine, and is not dependent on the acyl chains. However, the difference is observed only when small amounts (0.1-2mM quantities/40μg virus) of liposomes are used. Otherwise, binding efficiency to both phoshpatidylcholine and phoshpatidylserine was similar. It was suggested by Schlegel et al., 1983, that the saturation of VSV binding to 4000 sites may be due to the predominant localization of phoshpatidylserine to the inner membrane leaflet of the cellular bilayer. Phosphatidylcholine rich domains, on the cell surface, may also serve as binding sites for VSV G protein. Cholesterol was found not to influence VSV binding (Yamada and Ohnishi, 1986).

Yamada and Ohnishi (1988) examined the fusion of spin-labelled VSV with various phospholipid liposomes. They found that lipid head groups do not influence fusion, and that fusion was greater with cis-unsaturated fatty acid chains than with saturated ones. Conversion of phosphatidylserine in lipid-symmetric erythrocyte ghosts into phosphatidylethanolamine, resulted in erythrocyte ghost target membranes that did not alter the fusogenic capabilities of VSV (Herrmann et al., 1990). These studies suggest that fusion is independent of lipid head groups. Contradictory to this, Herrmann et al., 1990, also found that fusion is rapid with lipid-symmetric erythrocyte ghosts but not with asymmetric ghosts. However, this was attributed to mobility of acyl chains. Those of the lipid-symmetric erythrocyte ghosts were found to be more mobile than those of the lipid asymmetric ghosts or intact erythrocytes (Herrmann et al., 1990). The results of Herrmann et al. (1990) are in agreement with those of Yamada and Ohnishi (1986) in that fusion of VSV is independent of phospholipid head groups, but is dependent on acyl chain composition with a preference for cis-unsaturated fatty acids. Cholesterol appeared to enhance fusion as not only did inclusion of the molecule in liposomes along with cis-unsaturated fatty acids increase fusion (Yamada and Ohnishi, 1986), but its removal from lipid-symmetric erythrocyte ghosts decreased fusion (Herrmann et al., 1990).

1.9 Models of Viral Fusion Mediating Proteins

Common elements to viral fusion mediating proteins have recently emerged by examination of crystal structure portions of influenza hemagglutinin, HIV-1 gp41, and the Moloney murine leukemia virus (MoMuLV) transmembrane (TM) subunit (Wilson et al.,

1981; Bullough et al., 1994)(Carter et al., 1984; Weissenhorn et al., 1997; Fass et al., 1996).

1.9.1 Influenza Virus Hemagglutinin

The most characterized viral fusion protein, thus far, is that of influenza virus. This is because the crystal structures of both the neutral (Wilson et al., 1981) and low pH forms (Bullough et al., 1994) of proteolyticaly digested hemagglutinin have been solved. Because of the extensive studies performed on the hemagglutinin protein, many reviews have been written on the subject that should be consulted for more extensive analysis as only a synopsis is provided below. These include Hughson (1997), Skehel, et al. (1995), White (1992), Carr and Kim (1994), Hernandez et al. (1996), and Gaudin et al. (1995). Mature hemagglutinin (HA) consists of two subunits HA1 and HA2 that are bound together through a single disulfide bond following cleavage of the HA_0 precursor (Lazarowitz et al., 1971; Skehel and Waterfield, 1975), and are present as trimers on the cell surface. The HA1 subunit is responsible for receptor recognition on target membranes, whereas HA2 is the transmembrane bound subunit of the glycoprotein that also houses the fusion peptide. Influenza virus enters the target cell via the endocytic pathway, following interaction of the HA1 subunit with a sialic acid receptor on the target cell surface at neutral pH. Once exposed to the low pH environment of the endosome, HA undergoes a conformational alteration that renders it capable of fusing the viral envelope with that of the endosome.

The crystallographic structures shown in Figs. 2 c and d (Weissenhorn et al., 1997) are those of the HA2 subunit in the low pH and neutral pH conformations, respectively. In the native state (neutral pH structure), bromelain treated influenza HA (BHA) shows a central

30Å long coiled coil stalk composed of three monomeric long alpha-helices wound around each other (Wilson et al., 1981). Bromelain cleaves each HA2 subunit next to the carboxyl end of the ectodomain to generate soluble trimers lacking the transmembrane and cytoplasmic domains (Brand and Skehel, 1972; Skehel and Waterfield, 1975). Each long alpha-helix, from a single monomer, is connected to the corresponding short alpha-helix of the same monomer with a connecting loop region. The majority of contacts between the HA2 subunit and the HA1 globular head domains are made through the loop region (Wilson et al., 1981). The short alpha-helices are on the outside and toward the carboxy-terminal end of the central three-stranded coiled coil such that the loop region is in a hairpin form. The fusion peptide from each monomer, at the amino terminus of each short alpha-helix, is buried within the hydrophobic interior of the central stalk region. This places the fusion peptide at approximately 100Å from the distal tip of the HA molecule and about 35Å from the base of the BHA molecule. Hemagglutinin fusion peptides are thus unable to mediate lipid mixing under a neutral pH environment. In this structure, each HA1 subunit is disulfide bonded to an HA2 subunit near the base of the trimer, and extends upwards where a globular head domain is formed. Interactions with a sialic acid receptor are made through the globular head domains (Weis et al., 1988).

The structure of HA at the pH of fusion was elucidated by X-ray crystallography of the $TBHA_2$ molecule (Bullough et al., 1994). As the BHA molecule aggregates upon exposure to low pH, treatment of BHA with thermolysin in order to release the amino-terminal fusion peptides from HA2 subunits was necessary. The molecule was also treated

Fig. 2. Representations of trimeric structures of (a) HIV-1 gp 41 GCN4/gp41 hybrid, (b) Moloney murine leukemia virus transmembrane subunit, (c) low-pH induced conformation of influenza virus HA2, (d) neutral pH conformation of influenza virus HA2. Adopted from Weissenhorn et al., 1997.

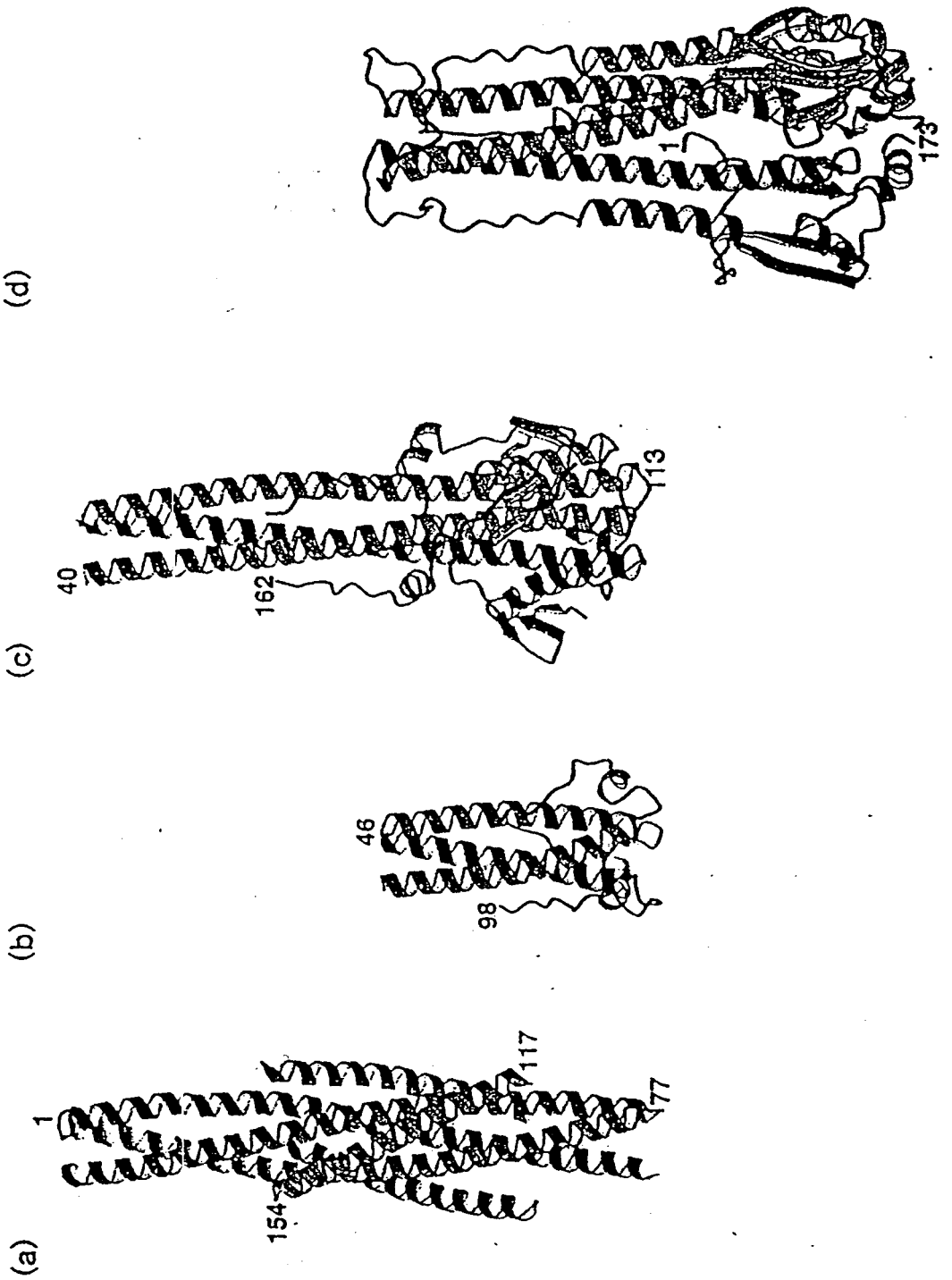
(a)
1
117
77
154
(b)
46
98
(c)
40
162
113
(d)
1
173

with trypsin, and the resultant trimeric complex consisted of residues 1-27 of the HA1 chain and residues 38-175 of the HA2 chain for each monomer. That is, the globular head and most of the connecting stalk of the HA1 subunit are lacking, with only a region near to the disulfide bond retained. In addition to the transmembrane and cytoplasmic domains of the HA2 subunit, the fusion peptide is also absent. The major transformation of HA2, under an acidic environment, is the rearrangement of the hairpin loop connecting the long and short alpha helices into a helical conformation. The short alpha-helix (residues 38-55) of BHA is thrust upwards to the top of the viral membrane distal end of the trimeric $TBHA_2$ molecule by a distance of 100Å. This forms a much longer central coiled-coil, than in the native BHA model. The fusion peptide (residues 1-23) and two β-strands (residues 24-37), are also postulated to relocate to the distal end of the $TBHA_2$ molecule. The fusion peptide would therefore be displaced from its original position by 100Å, in a position ideal for interaction with a target membrane. This in fact, is the essence of the "spring-loaded" model of conformational change in influenza hemagglutinin that was first suggested by Carr and Kim (1993). Carr and Kim (1993) identified the loop region in the native structure to be one containing hydrophobic repeats with potential of forming a coiled coil structure. The rearrangement of the loop region in the BHA structure to that of a coiled coil under low pH, makes it extremely difficult to maintain contacts between the HA2 subunit and HA1 globular heads. It is postulated that the globular heads of HA1 are removed away from the hemagglutinin trimer, under the influence of low pH, such that the fusion peptide becomes unhindered to contact a target lipid bilayer (Carr and Kim, 1994). In addition, part of the long alpha-helix in BHA (residues 106-112), that had previously made contacts with the

fusion peptide, refolds to form a loop that connects the $TBHA_2$ trimeric coiled coil to a new short alpha helix (residues 113-126). This new short helix was previously the carboxy-terminal end of the BHA trimeric coiled coil. It now packs in an antiparallel manner exterior to the trimeric coiled coil of $TBHA_2$. The carboxy terminal loop region in the$TBHA_2$ model is postulated to mediate intermolecular interactions between hemagglutinin trimers under the influence of low-pH (Kim et al., 1998).

1.9.2 Human immunodeficiency virus gp41

Recently, the crystallographic studies of protease resistant fragments of HIV gp41 have revealed similarities to the low-pH induced form of influenza hemagglutinin. The HIV envelope glycoprotein consists of non-covalently linked gp120 (SU) and gp41 (TM) subunits that are proteolyticaly processed from the gp160 precursor (Freed and Martin, 1995). gp120 is responsible for receptor and co-receptor recognition (Hernandez et al., 1996; Wilkinson, 1996). This triggers the gp41 subunit into promoting fusion at neutral pH. The general structure of gp41 is similar to that of HA2 with an amino-terminal fusion peptide followed by a 4-3 heptad repeat segment of high alpha helical propensity (Chambers et al., 1990), a transmembrane domain, and cytoplasmic tail. Digestion of bacterially expressed gp41 ectodomain with proteinase K, by Lu et al. (1995), generated two peptide fragments termed N51 (residues 28-78) and C43 (residues 112-154) at the amino and carboxy terminal ends, respectively. The sequence of C43 also contained a 4-3 hydrophobic repeat. Protease resistance of C43 was dependent on the presence of N51 with maximum protection at a stoichiometry of one to one. Circular dichroism revealed a helical and thermodynamically

stable complex, and sedimentation equilibrium centrifugation showed that the complex consisted of three molecules each of N51 and C43. The complex was hypothesized to consist of a trimer of N51 and C43 anti-parallel dimers arranged in a helical conformation with the N51 peptides packed within the interior of the coiled coil (Fig. 2a). This was confirmed by two independent crystallization studies. Chan et al., 1997, solved the crystall structure of a stable complex formed from slightly smaller proteolyticaly resistant subdomains of N51 and C43 termed N36 and C34. The structure consisted of an internal parallel trimeric coiled coil of N36 helices around which three C34 helices wrapped in an anti-parallel orientation. As well, the atomic structure of a bacterially expressed trimeric GCN4 isoleucine zipper (residues 30-79) and gp41 (residues 117-154) hybrid revealed a 115Å central alpha-helical coiled coil mapping to N51 and anti-parallel outer alpha-helices 60Å long (Weissenhorn et al., 1997). The GCN4 sequence was a substitute for the amino terminal fusion peptide (Fig. 2a). The carboxy-terminal helices followed the grooves formed by interacting amino-terminal helices and map to C43.

The conformation is thought to correspond to the fusion-active state of gp41since it is extremely thermostable and occurs in the absence of gp120. Shedding of gp120 following binding of the CD4 receptor has been observed in laboratory isolates of the virus (Moore et al., 1990; Hart et al., 1991). Conformational changes in gp41, induced by CD4 binding, have also been observed and thought to induce the exposure of domains involved in membrane fusion (Freed and Martin, 1995). The dissociation of gp120, therefore, is expected to accompany the conversion from a non-fusogenic to a fusion active form of gp41 (Wilkinson, 1996). As well, that the heptad repeat regions do not merely act as oligomerization domains

with interactions present in both the fusion inactive and active forms of gp41 is postulated through peptide inhibition studies. Peptides corresponding to regions including or overlapping with N36 and C34 inhibit HIV-1 infection and fusion (Wild et al., 1992, 1994; Jiang et al., 1993; Lu et al., 1995), with C-terminal peptides acting as more potent inhibitors. N-terminal peptides tend to aggregate in solution (Lu et al., 1995), and decrease the inhibitory activity of C-terminal peptides. Thus, the peptides may act in a negative dominant manner by interacting with the HIV-1 glycoprotein en route to reaching the more stable fusion active conformation described above (Chan et al., 1997; Hughson, 1997; Weissenhorn et al., 1997).

1.9.3 Moloney murine leukemia virus TM

As with HIV-1, MoMuLV is a neutral-pH retrovirus with an envelope protein consisting of disulfide linked surface and TM subunits. The TM subunit is composed of an amino-terminal fusion peptide, an amino terminal 4-3 heptad repeat, a transmembrane domain, and a cytoplasmic domain. Fass et al., 1996, crystallized a bacterially expressed 55 residue peptide (Mo-55, residues 46 to 97) fragment of the TM subunit including the 4-3 heptad repeat and lacking the fusion peptide (Fig. 2b). The fragment had been previously shown to be trimeric and thermostable (Fass and Kim, 1995). The structure revealed an internal trimeric coiled coil (residues 46-79) corresponding to the N-terminal heptad repeat region, and a 4 residue alpha-helix (residues 85-89) perpendicular to the coiled coil. The small alpha helix is anti-parallel to and hydrophobicaly interacts with the internal coiled coil. The remaining residues 90-97 pack against the internal coiled coil. By analogy to HIV-1, this

structure was proposed to be the core of the fusion active conformation of the MoMuLV TM subunit due to the lack of the receptor binding SU subunit.

1.9.4 A Common Fusogenic Conformation

Examination of the crystallized derivatives of influenza hemagglutinin, human immunodeficiency virus gp41, and moloney murine leukemia virus TM protein reveal common structural arrangements in fusion-active conformations (Weissenhorn et al., 1997). Amino terminal fusion peptides are situated at the tip of a triple stranded coiled coil, and may have been displaced from a previously buried site as has been revealed from studies with influenza HA. In addition, the polypeptide chain reverses direction and proceeds toward the amino terminus such that antiparallel helices surround the internal alpha helical coiled coil toward its base. The region connecting the crystallized structures and transmembrane anchor is probably flexible as it is susceptible to proteolysis and structurally disordered in the acid induced HA conformation. As well, the structures represent the final stable conformation attainable by the glycoproteins under fusogenic conditions. This is such that the transmembrane and fusion peptides would both reside in fused target and viral membranes. For HA, the C-terminal end is only 23 residues from the transmembrane anchor, 18 residues for HIV-1, and 37 residues for MoMuLV. This presents a model where, once triggered to undergo a fusogenic conformation, the glycoprotein presents the fusion peptide for interaction with a target membrane via a coiled coil extension. A carboxy-terminal rearrangement brings the transmembrane and fusion peptide domains into close proximity, while simultaneously bridging the gap between target and viral membranes. The final stable conformation would

involve the two membrane associating domains interacting with what has now become a single membrane lipid bilayer (Hughson, 1997).

1.10 Conformational states of rabies G and VSV G proteins

Both rabies and vesicular stomatitis viruses are members of the *Rhabdoviridae* family, although rabies belongs to the *Lyssavirus* genera whereas VSV belongs to the *Vesiculoviruses*. Despite the classification differences, G proteins of both viruses share the same basic structures including an internal fusion peptide, two N-linked oligosaccharides, two regions of newly defined heptad repeats, oligomerization into trimers, and approximately 20% amino acid identity (Rose et al., 1982; Coll, 1995; Durrer et al., 1995). In addition, fusion is low-pH mediated and the conformational change responsible for fusion is reversible. For influenza HA, fusion is irreversible (Morris et al., 1988). It is therefore helpful to discuss elements of rabies G relating to fusion, since these have been more extensively analyzed than those of vesicular stomatitis virus G protein.

Similar to VSV G, rabies G fusion appears at pHs below 6.2 and is maximal at a pH of 5.5 (Gaudin et al., 1991; Whitt et al., 1991). For both viruses, fusion is reversible such that incubation of virion under neutral pH arrests fusion following activation under acidic conditions and in the absence of target membranes (Gaudin et al., 1991; Gaudin et al., 1993; Blumenthal et al., 1987; Puri et al., 1988; Crimmins et al., 1983). For rabies G the conformational change leading to fusion was found to be reversible using protease resistance and recognition by monoclonal antibody experiments (Gaudin et al., 1991). A reversible conformational change was also hypothesized for VSV G (Crimmins et al., 1983; Blumenthal

et al., 1987; Puri et al., 1988; Clague et al., 1990). As well, hydrophobic photolabelling studies were used to demonstrate direct interaction of G proteins with target membranes for both rabies and VSV and to confirm the three conformational states (Durrer et al., 1995; Pak et al., 1997). Labelling of the proteins in the ectodomain did not take place at neutral pH, but did occur under pre-fusion conditions of pH 6.4 , 0°C, and fusogenic conditions. These results were confirmed for VSV G by Pak et al. (1997) who also demonstrated reversibility of protein and target membrane interactions.

There exists three states of the rabies virus glycoprotein which have been detected with monoclonal antibodies, electron microscopy, and protease resistance studies. These are the native (N), active (A), and inactive (I) conformations (Gaudin et al., 1993, 1991). The native (N) state is detected at the viral surface at a pH above 7. Electron microscopy was able to distinguish between the native and inactive forms of G as the inactive form is 32Å longer than the native one. The three states are in equilibrium with one another depending on environmental conditions, with the equilibrium shifting towards the I state following prolonged incubation under acidic conditions. Fusion inhibition takes place at 0.5 pH units (pH 6.7) above the pH of fusion threshold, where the number of spikes in the I state is 50% (Gaudin et al., 1993). This number increases to about 90% when virus is pre-incubated at a pH of 6.4. The conformational change associated with fusion inactivation is, however, irrelevant to the fusion process, and it is thought that the I state functions to prevent pre-mature fusion of newly synthesized G proteins with acidic Golgi compartments (Guadin et al., 1995, 1996). The active state is more hydrophobic, is detectable immediately following acidification, and causes formation of aggregates under low pH and low temperature in the

absence of target membranes (Gaudin et al., 1993). This state is detectable at the pH of 6.7, but fusion is present at a pH of 6.2 or lower. Therefore, a second step of protonation is required to induce fusion. The A state is the first step in a pathway leading to insertion of the fusion peptide into a target membrane (Gaudin et al., 1993). The protein acquires its native structure at the cell surface and once exposed to an acidic environment the majority of spikes can shift either to the active or inactive conformations depending on the duration of exposure. The kinetics of conformational change from the active to inactive state are sufficiently slow to allow for interaction with an endosomal target membrane (Gaudin et al., 1993, 1995).

The same three states were also hypothesized for VSV G on the basis of fusion kinetic studies (Puri et al., 1988; Clague et al., 1990). The neutral (N), active (A), and inactive (I) states of rabies virus correspond to the tense (T), relaxed (R) and desensitized (D) states of vesicular stomatitis virus G protein. The tense and relaxed states were proposed to account for the absence and presence of fusion, respectively. The desensitized state, on the other hand, was hypothesized to account for pH-dependent extents of fusion. Using fluorescently labelled octadecylrhodamine fatty acid probe to monitor fusion, a lag period dependent on pH and temperature was observed before the onset of fusion. The duration of this lag decreased with decreasing pH and increasing temperature (Clague et al., 1990). In addition, the initial rate of fusion increased with decreasing pH. Lag times were interpreted to reflect G oligomer rearrangements into fusogenic states thereby reflecting a multistate model where G protein has to undergo conformational alterations. Given the similarities between vesicular stomatitis virus and rabies G proteins, there exists considerable evidence towards a three-state conformational model of low-pH-induced G protein fusion.

To help define regions influencing the low-pH triggered conformational alterations, substitution mutagenesis of conserved regions within VSV G ectodomain was employed. In addition to the fusion peptide, linker insertion mutagenesis of the VSV G ectodomain resulted in the identification of residues 395 to 424 as a region possibly affecting fusion (Li et al., 1993). Residues conserved within the H10/A4 region (residues 395 to 424), therefore, were mutated. Mutant glycoproteins were expressed in COS cells and tested for their capacity to induce cell-cell fusion. Transport to the cell surface, oligomerization into trimers, and low-pH induced proteolytic resistance were also examined for indications of conformational deviations. Substitution of glycine 404 and aspartate 409 to lysine and asparagine, respectively, completely abolished cell-cell fusion. Low-pH triggered alterations of mutant G404K were also dramatically altered from those of wild type, as tested by resistance to tryptic digestion. Mutant G395E caused a severe reduction in fusion efficiency, along with shifts in the pH optimum and threshold of fusion to more acidic values. This, along with previous mutagenesis (Shokralla et al., 1998), provides evidence toward a functional role for the H10/A4 region in G protein mediated low pH fusion. Glycoproteins mutated in both the fusion peptide and H10/A4 regions were also expressed in COS cells and tested for fusion, transport, oligomerization, and conformational alterations. The double mutants, including P126L D411N, G131A D411N, and D137N D411N caused a shift in the pH of fusion threshold that are more acidic than either of their constituent single mutants. Shifts in the pH optima of fusion of mutants G131A G404A, G131A D411N, and D137N G404A corresponded to those of the H2 mutants. As well, mutant D137N D411N was completely incapable of membrane fusion. The data suggest that the regions may be functionally

independent but could indirectly affect each another.

2. MATERIALS AND METHODS

2.1 Chemicals and Reagents

Chemical	Supplier
Acetone	BDH
Acrylamide	Research Organics Inc.
Agarose	Gibco/BRL
Ammonium acetate	BDH
Ammonium persulfate	BDH
Ampicillin	Sigma
Bacto-tryptone	Difco
Bacto-yeast extract	Difco
Bacto-agar	Difco
Bovine serum albumin	Sigma
Calcium chloride	BDH
Calf serum	GIBCO/BRL
Cesium chloride	Research Organics Inc.
Chloramphenicol	Sigma
Chloroform	Caledon
Dimethyl sulfoxide	BDH
Dithiotreitol	Calbiochem
Ethidium bromide	Sigma
Ethylenediaminetetraacetic acid	BDH
Ethylene glycol-bis (β-aminoethylether) N,N,N',N' tetra acetic acid	Sigma
Fluorescein isothiocyanate (FITC)	Coppel Laboratories
Glycerol	BDH
Isoamyl alcohol	Fisher Scientific
L-glutamine	GIBCO/BRL
L-methionine	General Biochemicals
MEM-vitamins	GIBCO/BRL
2-[N-morpholino]-ethanesulfonic acid (MES)	Sigma
3-[N-morpholino]-propanesulfonic acid (MOPS)	Sigma
N-2-hydroxyethylpiperazine-N'-2-ethanesulfonic acid (HEPES)	Boehringer Mannheim
N,N-methylenebisacrylamide	GIBCO/BRL
N,N,N,N,-tetramethylethylenediamine (TEMED)	GIBCO/BRL
Nonessential amino acids	GIBCO/BRL

Chemical	Supplier
Nonidet P-40	BDH
Paraformaldehyde	Sigma
Penicillin/streptomycin solution	GIBCO/BRL
Phenol	Fisher Scientific
Phenylmethylsulfonyl fluoride (PMSF)	Sigma
Polyethylene glycol 8000	BDH
Protein-A-Sepharose	Pharmacia
Rubidium chloride	Sigma
RNase A (DNase-free)	Sigma
Salicylic acid	Sigma
Sodium acetate	BDH
Sodium bicarbonate	BDH
Sodium deoxycholate	Calbiochem
Sodium dodecylsulfate (SDS)	BDH
Sucrose	BDH
T4 gene 32 protein	Pharmacia
Trasylol (aprotinin)	Miles Canada Inc.
Tris (hydroxymethyl) aminomethane (Tris)	Boehringer Mannheim
Triton X-100	Bio-Rad
Trypsin-EDTA solution	GIBCO/BRL
Urea	Bio-Rad
Xylene cyanol FF	Baker Chemical
Yeast extract	Difco

2.2 Enzymes

Calf intestinal alkaline phosphatase	Pharmacia
Endo H_f	NEB
Endoglycosidase H	G enzyme
Glucose oxidase	Boehringer Mannheim
Lactoperoxidase	Sigma
Restriction endonucleases	Pharmacia, NEB, GIBCO/BRL, Boehringer Mannheim
Sequenase Version 2.0 T7 DNA polymerase	USB
T4 polynucleotide kinase	NEB
T4 DNA ligase	Bio-Rad
T4 DNA polymerase	Bio-Rad
TPCK-trypsin	Millipore

2.3 Radiochemicals

[α-^{35}S]dATP	Dupont-NEN
[^{35}S]methionine	Dupont-NEN
Na[^{125}I] carrier free	Dupont NEN

2.4 Multi-Component Systems

BCA* Protein Assay kit	Pierce
Geneclean II® kit	BIO 101 Inc.
Muta-Gene® M13 In Vitro Mutagenesis Kit, Version, 2	Bio-Rad
Sequenase Version 2.0 DNA Sequencing Kit	USB

2.5 Plasmids, Bacterial Strains, Bacteriophages, and Cell Lines

	Supplier	Properties
pXMG	Dr. H.P. Ghosh	pXM plasmid originally obtained from Dr. G.G. Wong (Genetics Institute, Cambridge, MA) with the G glycoprotein gene of VSV Indiana serotype subcloned into the EcoRI multiple cloning region site by C.Drone
pXMG(AXB)	Dr. H.P. Ghosh	pXMG plasmid with added ApaI, XhoI, and BssHII sites at nucleotides 299, 1416, 1473, respectively. Plasmid was constructed by E. Wanas.
DH5α	Gibco/BRL	*E. coli*
MV1190	Bio-Rad	*E. coli*. Lactose and proline synthesis genes are deleted from the chromosome. The F' plasmid carries the *lac* operon with an incomplete β-galactosidase gene, and proline synthesis genes
CJ236	Bio-Rad	*E. coli*. *dut* and *ung* double mutant bacterium. The dUTPase and uracil N-glycosylase enzymes are inactivated. The pili manufacturing F' pCJ105 plasmid carries genes for chloramphenicol resistance

M13G(XB)	Dr. H P. Ghosh	M13 phage (Bio-Rad) carrying the 629 bp fragment, obtained by KpnI and EcoRI restriction endonuclease digestion of pXMG. The fragment contains additional XhoI and BssHII restriction endonuclease sites created by site directed mutagenesis at nucleotide positions 1416 and 1473, respectively. Constructed by E. Wanas
COS-1	M. Butcher	Monkey kidney cells transformed with the Simian Virus 40 large T antigen

2.6 Growth Media and Buffers

	Composition
Detergent lysis buffer	10mM Tris pH 7.4, 66mM EDTA, 0.4% deoxycholic acid, 0.02% sodium azide, 1% Triton X-100
Glucose-Minimal media	1.5%KH_2PO_4, 0.45% K_2HPO_4, 0.05% NaCl, 0.1% NH_4Cl
H media	1% Bacto-tryptone, 0.5% NaCl
HGD media	purchased from GIBCO/BRL
HeBS	1.6% NaCl, 0.076% KCl, 0.02% Na_2HPO_4, 1.0% HEPES, 0.2% dextrose. The solution is adjusted to pH 7.1
High Salt Buffer	300mM NaCl, 100mM Tris pH8.0, 1 mM EDTA pH 8.0
SDS-PAGE Loading Buffer 2X	100mM Tris-HCl pH 6.8, 200mM DTT, 4% SDS, 0.2% bromophenol blue, 20% glycerol. 10%β-mercaptoethanol is added immediately before use
LB media	1% Bacto-tryptone, 0.5% Bacto-yeast extract, 1% NaCl
Lysis buffer	1% NP40, 0.4% NaDeoxycholate, 66mM EDTA, 10mM Tris pH 7.4
MNT (4X)	80mM MES, 120mM Tris-HCl, 400mM NaCl, 4mM EDTA, 4mM EGTA
PBS	137mM NaCl, 2.68mM KCl, 8.1mM Na_2HPO_4, 1.5mM KH_2PO_4

RIPA	1% NP40, 0.4% sodium deoxycholate, 12.5mM EDTA, 50mM Tris-HCl
TBE	90mM Tris-borate, 2mM EDTA
2XYT	1.6% Bacto-tryptone, 1% yeast extract, 0.5% NaCl

To prepare agar plates of the above media, 1.5% Bacto-Agar is added to the mixture before autoclaving. To prepare top-agar, 0.7% Bacto-Agar is added before autoclaving.

2.7 Oligonucleotides

Oligonucleotides used for DNA sequencing and mutagenesis reactions were synthesized by the Central Facility of the Institute for Molecular Biology and Biotechnology, McMaster University.

Primer	Sequence (5' to 3')	Properties
AB2449 nucleotides 1150-1167	ATGACTGGGCACC ATATG	Sense primer. Used to sequence the double stranded form of the H10/A4 G395E, G404K, D409A, and A418K mutants
AB6809 nucleotides 1490-1461	ATGGATACCAACT CGGAGAACCAAGA ATAG	Antisense primer. Used for sequencing single stranded G395E, G404K, D409A, and A418K M13G(XB) phage DNA
AB7387 nucleotides 1225-1200	GGAAACTTATATtC TGAACTGGTCCT	Antisense primer. A dGTP at position 1213 is replaced by a dATP resulting in an amino acid replacement of glycine by glutamate. Used to generate mutant G395E
AB7388 nucleotides 1253-1219	CAACATACCATGTt tAATCATGTATAA	Antisense primer. Two dGTPs at positions 1239 and 1240 are replaced by dATPs resulting in an amino acid replacement of glycine by lysine. Used to generate mutant G404K
AB7389 nucleotides 1266-1240	GAAGATCGGAGgC CAACATACCAT	Antisense primer. A dATP at position 1255 is replaced by a dCTP resulting in an amino acid replacement of aspartate by alanine. Used to generate mutant D409A

AB7390 nucleotides 1296-1270	GTTCGAACACCTGt ttCTTTGAGCTAA	Antisense primer. A dGTP, dCTP, and dTTP, at positions 1281, 1282, and 1283 respectively, were replaced by three dATP residues resulting in an amino acid replacement of alanine by lysine. Used to generate mutant A418K
AB10028 nucleotides 357-377	GCGCGAATTCGAA AGCATTGAACAAA CGAA	Sense primer. Includes additional GCGC clamp and GAATTC EcoRI restriction endonuclease sequences. Used to sequence the double stranded H2-H10/A4 P126L D411N, G131A G404A, D137N G404A double mutants in the H2 region
AB10029 nucleotides 533-513	GCGCGGATCCTTT TCCGTTGATGAAC TGTGA	Antisense primer. Includes additional GCGC clamp and GGATCC BamHI restriction endonuclease sequences. Used to sequence the double stranded H2-H10/A4 F125Y D411N double mutant in the H2 region

All nucleotide and amino acid references correspond to the sequence of vesicular stomatitis virus, Indiana serotype, glycoprotein G (Gallione and Rose, 1983). Mutated residues are shown in lowercase letters. Mutants are named according to the wild type residue, amino acid position, and replacement residue.

2.8 Antibodies

Polyclonal antibodies to VSV G, Indiana serotype, were obtained from E. Wanas. Rabbits were injected with a recombinant adenovirus vector expressing G protein (Dr. L. Prevec, McMaster University), and antibody containing serum was harvested. Ammonium sulfate purified antibodies used in immunofluorescence experiments were obtained from K. Ghosh. Goat anti-rabbit IgG antibody conjugated to fluorescein isothiocyanate was purchased from Coppel Laboratories.

2.9 Molecular Weight Markers

For approximation of DNA fragment sizes by agarose gel electrophoresis, a 1KB DNA ladder was purchased from Gibco/BRL, and visualized by incorporation of ethidium bromide into the agarose gel preparation. A radioactive VSV Indiana serotype marker was used for SDS-polyacrylamide gel electrophoresis of radioactive protein preparations. The marker was prepared by infection of COS-1 cells with VSV and labelled with [^{35}S]methionine. Cells were lysed with detergent lysis buffer and cellular debris was removed by centrifugation at 14,000g, 5min, and 4°C. To the supernatant containing radioactive viral proteins was added an equal volume of 2X loading buffer (100mM Tris-HCl pH 6.8, 4% SDS, 0.2% bromophenol blue, 20% glycerol, 10% β-mercaptoethanol). The preparation was boiled for 3 min. and stored at -20°C. Upon electrophoresis and exposure by autoradiography, five bands were evident: L protein (190kDa), G protein (69kDa), N protein (50kDa), P protein (49kDa) bands immediately below N and is indistinguishable from the latter, and M protein (29kDa).

2.10 Restriction Endonuclease Digestions

Digestions with restriction enzymes were carried out according to the enzyme manufacturers' guidelines. Unless otherwise stated, DNA, enzyme, 1X restriction enzyme buffer, and sterile ddH_2O were mixed and incubated at 37°C for 1-2hrs. Reactions were arrested by storage at -20°C and by the addition of 6X loading buffer prior to analysis by agarose gel electrophoresis.

2.11 Agarose Gel Electrophoresis

Agarose gels were prepared by dissolving 0.7 to 1.0% (w/v) electrophoresis grade agarose in TBE buffer. The mixture was microwaved for a few minutes to dissolve the agarose and cooled to less than 60°C at room temperature. Ethidium bromide was added to a final concentration of 0.5μg/ml, mixed by swirling, and the solution was immediately poured into a gel mold to harden. Samples were mixed with 6X loading buffer (0.25% bromophenol blue, 0.25% xylene cyanol FF, 30% glycerol), loaded into agarose wells, and the gels run long enough to allow separation of DNA fragments at 100V. DNA was visualized by short wave ultraviolet light and a photograph was taken using a Polaroid Photodyne Inc. camera to record the results. Long wave ultraviolet light was used, during cloning procedures, to visualize digested products and photographs were taken only after excision of DNA.

2.12 Concentrating Nucleic Acids

To precipitate double stranded DNA, 0.1 volumes of 3M sodium acetate pH 5.2 and two volumes of 95% ethanol are added to and mixed with the DNA solution. The solution was then incubated for either a minimum of 30 min at -70°C or 60 min at -20°C. DNA was pelleted by centrifugation in a microcentrifuge at 14000g, 4°C, and 20 min. The supernatant was removed by aspiration and the pellet and walls of the centrifuge tube were washed with 70% ethanol. This was also removed by aspiration. The pellet was allowed to dry completely and was then resuspended in the desired volume of TE pH 8.0 or ddH_2O.

2.13 Purification of DNA from Agarose Gels

For isolation of DNA fragments from agarose gels, the Geneclean II® kit (BIO 101 Inc.) was utilized. All reagents were supplied with the kit. Glassmilk® silica matrix binds both single and double stranded DNA without inclusion of contaminants. DNA was visualized under long-wave ultraviolet light. An agarose slice, containing the desired DNA, was removed using a sterile razor blade and transferred to a 1.5ml microcentrifuge tube. The slice was weighed to determine reagent volumes required in subsequent steps. To the agarose were added ½ volumes of TBE modifier™ and 4.5 volumes of 6M NaI. The mixture was placed in a 55°C water bath and periodically mixed to facilitate dissolution of the slice. To ensure suspension of the silica matrix, Glassmilk® was vortexed in a horizontal position before use. Five micoliters of matrix were added for 5μg or less of DNA. An additional microliter was added for every 0.5μg of DNA above 5μg. The mixture was vortexed, incubated on ice for 15 min. with periodic mixing, and pelleted by brief centrifugation at 4°C. The NaI supernatant was transferred to a separate tube. The pellet was washed three times with 500μl of ice cold NEW WASH buffer (NaCl, Tris, and EDTA in ethanol pH 7.0-8.5). For each wash, the pellet was resuspended by pipetting and re-pelleted by centrifugation. To elute DNA from the Glassmilk®, 5μl of TE pH 8.0 were used to resuspend the matrix and the mixture was incubated at 55°C for 3 min. Silica was removed from suspension by centrifugation at 14000g for 30 sec. in a microcentrifuge, and the supernatant containing eluted DNA was transferred to a new microcentrifuge tube. A second elution was also carried out to increase the efficiency of DNA recovery. An aliquot of the eluted DNA was electrophoresed, along with standards of varying amounts, to visually quantify recovered

DNA. Typically, an 80% recovery of the nucleic acid was obtained.

2.14 Dephosphorylation of DNA

Vector DNA digested with a single endonuclease was subjected to treatment by calf intestinal alkaline phosphatase (CIAP) prior to ligation. Removal of the 5' phosphate prevented re-circularization of plasmid DNA, thereby reducing the number of false positives obtained during transformation. The restriction enzyme was heat inactivated for 15 min. and cooled on ice. Pharmacia One Phor All buffer was added to the DNA at a final concentration of 1X, and a single unit of CIAP (Pharmacia) was used to dephosphorylate 1-10μg of DNA at 37°C for 30min. The mixture was genecleaned to purify the DNA.

2.15 Ligations

Purified vector and insert were mixed at a molar ratio of 1:3, and warmed at 45°C for 5 min to melt any cohesive termini that may have reannealed. One microliter T4 DNA ligase (1unit/μl) and 2μl of 5X T4 DNA ligase buffer (250mM Tris-HCl pH 7.6, 50mM ATP, 5mM DTT, 25% (w/v) polyethylene glycol-8000) were also added. The reaction was brought to a final volume of 10μl with sterile ddH_2O and incubated overnight at a temperature of 16°C. Negative control reactions containing either only the vector or insert DNA were also set up. Depending on the amount of DNA present, an appropriate volume of the ligation mixture was used to transform competent DH5α cells.

2.16 Preparation of Competent Cells

E. coli DH5α cells were made competent by two methods, one utilizing calcium chloride as the functional agent and the other utilizing rubidium chloride. The calcium chloride method was performed as outlined in Sambrook et al., (1989). Transformation efficiencies of 10^5 were obtained with both methods. DH5α cells were plated on LB agar and grown overnight in a 37°C incubator. A single colony was selected and grown overnight in 5 ml of LB broth and 37°C. The culture was then added to 500 ml of prewarmed LB broth in a 2L flask and grown in a 37°C rotary shaker, with aliquotes of 1ml periodically removed and tested for an OD_{600} of approximately 0.4 using a Beckman model 25 spectrophotometer. Once such an optical density had been reached, the culture was placed on ice to help arrest cellular growth. All subsequent steps were performed on ice with pre-chilled materials to maintain the proper cell density and therefore competency. Cells were transferred to 250 ml polypropylene tubes, and centrifuged at 4000 rpm for 10 min at 4°C in a Sorvall GSA rotor. The resultant LB broth supernatant was decanted and the remaining traces aspirated. Each bacterial pellet from 250 ml of culture was resuspended with pipetting in 50 ml of ice-cold 0.1 M $CaCl_2$ and incubated on ice. The cells were pelleted again at 4000 rpm, 4°C, and 10 minutes. The supernatant was once again decanted, and the resultant pellet from 250 ml of original culture was resuspended, by pipetting, in 10 ml of ice-cold 0.1M $CaCl_2$ including 15% glycerol. One hundred to two hundred microliter aliquotes of competent cells were transferred to pre-chilled Eppendorf centrifuge tubes on ice, flash frozen in liquid nitrogen, and stored at -70°C.

For the rubidium chloride method, a single colony of E.coli DH5α or MV1190 cells was also picked from an LB agar plate and grown overnight in a 37°C shaking incubator, in 5 ml of LB broth. The overnight culture was then diluted 1 in 100, in LB broth containing 20mM $MgSO_4$, to a final volume of 500 ml and grown to an OD_{600} of 0.4. Cells were then placed on ice to maintain the appropriate growth phase. All subsequent steps were performed using pre-chilled materials. The cells were pelleted by centrifugation at 4°C, 5min, and 5000rpm in a Sorvall GSA rotor using 250ml polypropylene tubes, and the supernatant removed by aspiration. Each pellet obtained from 250ml of original culture was gently resuspended by pipetting in 100ml of TFBI solution. Cells were transferred to 50ml polypropylene tubes, incubated on ice for 5min, and centrifuged using a Sorvall SS34 rotor for 5min, 4°C, and 5000rpm. Pelleted cells, from 125ml original culture, were resuspended in 5ml of TFBII solution and incubated on ice for 15 min. Competent cell aliquotes of 100-200μl were transferred to 1.5ml centrifuge tubes, frozen in liquid nitrogen, and placed at -70°C for storage. The procedure is as described by Hanahan (1985).

2.17 Transformation of Competent Cells

Frozen competent cells were thawed on ice and transformed with plasmid DNA using one of two methods that differ in the temperature and duration of heat shock. Using a chilled pipette tip, the appropriate amount of DNA was added and gently stirred using the pipette tip. The mixture was then stored on ice from 30 to 60min. Cells were heat shocked by placing the mixture in either a 42°C water bath for exactly 90 sec or 45 sec at 37°C without shaking. Following heat shock, cells were incubated on ice for 2 min, diluted to a final volume of 1 ml

by addition of LB broth, and grown for 20 to 45 min at 37°C in a rotary shaker. One hundred microliters of transformed cells were plated onto LB agar plates containing the appropriate antibiotic (frequently 50μg/ml ampicillin). The remaining 900μl of culture were centrifuged at 4°C in a microcentrifuge to pellet the transformed cells and resuspended in 100μl of LB broth to facilitate plating. Plates were inverted and incubated overnight at 37°C.

2.18 Small-Scale Preparations of Plasmid DNA

The lysis by alkali method, as presented in Sambrook et al. (1989), was used for minipreparations of plasmid DNA. The procedure is a modification of protocols by Birnboim and Doly (1979) and Ish-Horowicz and Burke (1981) and was used for minipreparations of plasmid DNA. Using a sterile toothpick, a single colony of transformed DH5α was selected and transferred to a loosely capped 13ml Falcon tube containing 5ml of LB media with the appropriate antibiotic. Cells were grown overnight at 37°C in a rotary shaker. Following the overnight incubation, 1.5ml of the culture was transferred to an Eppendorf microcentrifuge tube and centrifuged at 14000g for 30 sec in a microcentrifuge to pellet the bacteria. The remaining overnight culture was stored at 4°C. The medium was removed by aspiration and the pellet resuspended in 100μl of ice-cold solution I (50mM glucose, 25mM Tris-HCl pH8.0, and 10mM EDTA pH8.0) by vortexing. Two hundred microliters of freshly made solution II (0.2N NaOH, and 1% SDS) were added and the tubes inverted several times gently to mix the preparation. To the bacterial lysate, was added 150μl of ice-cold solution III (3M KOAc, and 11.5% glacial acetic acid) and the solution was inverted to mix and stored on ice for 5min. The white precipitate was pelleted and removed by centrifugation at 14000g and 4°C

for 5 min. To remove cellular proteins, the supernatant was extracted once by addition of an equal volume of phenol:chloroform:isoamyl alcohol (50:49:1 as described in Sambrook et al., 1989). The solution was vortexed, centrifuged for 2 min at 14,000g and 4°C, and the aqueous phase transferred to a new microcentrifuge tube, being careful not to remove any proteins present at the interphase of inorganic phenol and aqueous TE phases. Two volumes of 95% ethanol were added to the aqueous phase to precipitate the double stranded plasmid DNA, and incubated at room temperature for 2 minutes. The DNA was pelleted by centrifugation for 5 min, 4°C, and 14000g in a table top microcentrifuge. The alcohol was aspirated and the DNA washed with 70% ethanol to remove salts. The dry pellet was resuspended in 50μl of TE buffer pH8.0 and stored at -20°C.

2.19 Large-Scale Preparations of Plasmid DNA

2.19.1 Lysis by alkali

The lysis by alkali procedure, as presented in Sambrook et al., (1989), was used for maxi-prepping and isolating plasmid DNA. 500ml of pre-warmed LB media, containing the proper selective agent, were inoculated with 1ml of overnight culture originating from a single colony of E. coli carrying the appropriate plasmid. The inoculate was grown overnight at 37°C. Following transfer to 250ml polypropylene centrifuge tubes, cells were harvested from the culture by centrifugation at 4000rpm, 15min, and 4°C in a Sorvall GSA rotor. The supernatant was discarded and any remaining droplets removed by aspiration. Each bacterial pellet from 250ml of original culture was resuspended, by vigorous vortexing, in 5ml of ice-cold solution I (50mM glucose, 25mM Tris-HCl pH8.0, and 10mM EDTA pH 8.0). Ten

milliliters of freshly prepared solution II (0.2N NaOH, 1% SDS) were added to the resuspended cells, mixed by gentle inversion and stored at room temperature for 10 min. To the cell lysate was added 7.5ml of solution III (3M KOAc and 11.5% glacial acetic acid) and the solution mixed by shaking followed by a 10 min incubation on ice. The resultant precipitate was removed from solution by centrifugation at 4000 rpm, 15 min, at 4°C in a Sorvall GSA rotor. The supernatant was filtered through four layers of cheesecloth, into 50ml polypropylene centrifuge tubes, and 0.6 volumes of isopropanol were added, mixed by vortexing, and stored for 30 min at room temperature to precipitate nucleic acids. Nucleic acids and proteins were pelleted by centrifugation at 10,000 rpm, 30 min, and room temperature in a Sorvall SS34 rotor. The supernatant was removed by aspiration, and the pellet and walls of the centrifuge tube were washed with 70% ethanol. The ethanol was drained off and any remaining droplets removed by aspiration. The centrifuge tube was placed in an inverted position to allow the last remaining traces of ethanol to evaporate and the pellet was dissolved in 8ml of TE buffer pH 8.0. Plasmid DNA was purified by equilibrium centrifugation in CsCl-ethidium bromide gradients.

2.19.2 Purification by CsCl-Ethidium Bromide density gradients

The procedure followed was that presented in Sambrook et al. (1989). To the 8ml of nucleic acid and protein solution obtained by alkali lysis were added 8.8g of cesium chloride that was dissolved by vortexing. To the resultant 10ml solution was added 0.8ml of a 10mg/ml solution of ethidium bromide that was immediately vortexed to disperse the ethidium bromide. Using a 5ml syringe and a 10 gauge needle, 5 ml of solution was

transferred to a 13 X 51mm Quick-Seal Beckman centrifuge tube and the tubes balanced and sealed. The mixture was centrifuged for a minimum of 16 hrs, at 45,000 rpm, and at 20°C using a Vti65 Beckman vertical rotor in a Beckman L8-70M ultracentrifuge.

The closed circular plasmid DNA appeared as a thick band across the centre of the centrifuge tube and was visualized either by ordinary light, if present in sufficient quantities, or by long wave ultraviolet light. To collect the DNA, a 21 gauge needle was inserted into the top of the tube to allow air to enter and the band was collected by an 18 gauge needle and syringe. The needle was inserted below the band and collected into a 13ml polypropylene Falcon tube. Plasmid DNA was purified from the ethidium bromide solution by extraction with 1-butanol saturated with water.

To the DNA-ethidium bromide solution was added an equal volume of 1-butanol that was mixed by vortexing. The upper phase, containing ethidium bromide and butanol, was removed and the extraction procedure repeated until the ethidium bromide could no longer be visualized in the organic phase. The DNA containing aqueous phase was transferred to a 50ml polypropylene centrifuge tube, diluted with three volumes of double distilled water and eight volumes of 95% ethanol, and incubated overnight at -20°C to precipitate plasmid DNA. The nucleic acid was pelleted by centrifugation at 10,000 rpm, 30 min, and 4°C in a Sorvall SS34 rotor, and the supernatant decanted. The pellet and walls of the centrifuge tube were washed with 70% ethanol, and any remaining ethanol was allowed to evaporate. The pellet was resuspended in 500μl of TE buffer, pH 8.0. The OD_{260} and OD_{280} were measured, using a Beckman model 25 spectrophotometer, to determine the DNA concentration and purity, and the plasmid was stored at -20°C.

2.20 Site Directed Mutagenesis

For oligonucleotide mediated mutagenesis, the Muta-Gene® M13 In Vitro Mutagenesis Kit, Version 2, as based on the method of Kunkel (1987), was utilized.

2.20.1 Growth of Bacterial Strains

Growth of both MV1190 and CJ236 *E. coli* strains took place at 37°C, as growth below 35°C would not allow for manufacturing of pili required for entry of M13 phage into bacterial cells. MV1190 cells were streaked on glucose-minimal medium plates to maintain selective pressures for preservation of the proline synthesizing F' plasmid. CJ236 cells were streaked on LB plates containing chloramphenicol, at a concentration of 30μg/ml, and inoculated in liquid media containing the drug to maintain selection for the F' drug resistant plasmid.

2.20.2 Phage Titrations

Whereas uracil-containing phage could only be titered on CJ236 cells, non-uracil-containing phage was titered on both MV1190 and CJ236 cells. CJ236 cells allow for the substitution of thymine with uracil in DNA due to mutations in the *dut* and *ung* genes that result in inactivation of dUTPase and uracil N-glycosylase enzymes. MV1190 cells were streaked on a glucose-minimal medium plate, and grown overnight at 37°C. A single isolated colony was used to inoculate 20ml of LB, and grown overnight with vigorous shaking at 37°C. For CJ236 cells, 20ml of LB containing chloramphenicol (30μg/ml) was inoculated from a single colony obtained from an LB-chloramphenicol (30μg/ml) plate, and grown

overnight at 37°C with agitation. For each strain, 200μl aliquotes of the overnight cultures were prepared in 13 ml Falcon tubes. One hundred fold serial dilutions of the M13G(XB) phage stock were prepared in LB. For titration on MV1190 cells, 100μl of the 10^4, 10^6, and 10^8 fold phage dilutions were added to 200μl aliquots of MV1190 overnight culture. For titration on CJ236 cells, 100μl of the 10^8, 10^{10}, and 10^{12} fold phage dilutions were added to 200μl aliquots of CJ236 overnight culture. Negative controls, lacking phage, were also prepared. Following a 5 min. incubation at room temperature, 2.5ml of pre-warmed LB top agar were added to each Falcon tube, mixed by inversion, poured onto an LB agar plate, and swirled to distribute the mixture evenly. The top agar was allowed to harden for a minimum of 15 min. and the plates incubated overnight at 37°C in an inverted position. Phage titer was calculated in pfu/ml, according to the formula: titer = No. of plaques X 10 X dilution factor.

2.20.3 Growth of Uracil-Containing Phage

CJ236 cells were streaked on an LB plate containing 30μg/ml chloramphenicol, and grown overnight at 37°C. A single colony was picked with a sterile toothpick and used to inoculate 20ml of LB containing chloramphenicol at a concentration of 30μg/ml. The culture was grown overnight at 37°C with agitation. The following day, 1 ml of the overnight culture was used to inoculate 50ml of 2XYT media with 30μg/ml chloramphenicol. The diluted culture was grown at 37°C with shaking to an OD_{600} of 0.3, corresponding to approximately 10^8cfu/ml. Uridine was added to a final concentration of 0.5μg/ml, and M13G(XB) phage was added to a multiplicity of infection of 0.2 phage/cell. The culture was further incubated with shaking, at 37°C, for 4-6 hours. Two 25ml of culture were transferred to 50ml

polypropylene centrifuge tubes and the bacterial cells were pelleted by centrifugation at 12,000 rpm, 4°C, and 15 min in a Sorvall SS34 rotor. The supernatant containing phage was transferred to a fresh polyallomer centrifuge tube and 150μg of DNase-free RNase A were added. Following a 30 min room temperature incubation, 6.5 ml of a solution of 3.5M ammonium acetate and 20% PEG 8000 were added to every 25 ml of supernatant. The resultant solution was mixed and incubated on ice for a minimum of 30 min. The phage was recovered by centrifugation at 12,000 rpm, 15 min, and 4°C in a Sorvall SS34 rotor, and the supernatant removed by aspiration. Phage was resuspended in 500μl of high salt buffer, transferred to a microcentrifuge tube, and incubated on ice for 30 minutes. The suspension was centrifuged for 2 min in a microcentrifuge to remove any insoluble material and the supernatant transferred to a fresh Eppendorf tube. Stocks were stored at 4°C, and the DNA extracted within one week. The phage was titered on both CJ236 and MV1190 to determine if the phage DNA contains ample uracil for inactivation by MV1190 cells. A 10^4 reduction of titer on MV1190 as compared to CJ236 is desired.

2.20.4 Extraction of Viral DNA

To release the uracil-containing viral DNA from within viral nucleocapsids, phage stocks were extracted twice by the addition of neutralized phenol (equilibrated with TE pH 8.0), 30 min of vortexing, and a 2 min centrifugation at 14,000g and 4°C in a microcentrifuge. Following centrifugation, the organic and DNA containing aqueous phases were separated by a protein interphase. The aqueous phase was transferred to a new microcentrifuge tube, and the process was repeated once with phenol:chloroform:isoamyl alcohol prepared in a

50:49:1 (v/v/v) ratio. Several extractions were then performed with chloroform:isoamyl alcohol (49:1, v/v) until an interphase was no longer visible, and then once more. Each step was also back-extracted by addition of 100μl TE, pH 8.0. All aqueous phases were pooled in a 1.5 ml microcentrifuge tube and the single stranded DNA was precipitated by addition of 1/10 volumes of 7.8M ammonium acetate and 2.5 volumes of 95% ethanol. The mixture was vortexed and stored at -70°C for a minimum of 30 min. To pellet the DNA, the solution was centrifuged at 14,000g, 15 min, and 4°C in a microcentrifuge. The pellet and walls of the centrifuge tube were washed with 70% ethanol, and the pellet was resuspended in 20μl TE pH 8.0 and transferred to a fresh Eppendorf tube. To determine the concentration of single stranded uracil containing DNA, a small sample of the resuspension was examined on a 0.7% agarose gel alongside DNA of various known amounts.

2.20.5 Phosphorylation of the Mutagenic Oligonucleotide

Mutagenic primers were phosphorylated, using T4 polynucleotide kinase, prior to use in synthesis of the mutagenic strand. Phosphorylation was performed according to the method outlined in Muta-Gene® M13 In Vitro Mutagenesis Kit, Version 2 (Zoller and Smith, 1983). The following reagents were mixed in a 500μl microcentrifuge tube: 10μl of a 20pmol/μl stock of mutagenic oligonucleotide resuspended in sterile double distilled water for a final amount of 200pmol, 3μl of 1M Tris pH 8.0 to give a final concentration of 100mM, 1.5μl of 0.2M $MgCl_2$ to give a final concentration of 10mM, 1.5μl of 0.1M DTT to give a final concentration of 5mM, 13μl of 1mM ATP to give a final concentration of 0.4mM, and a varying volume of sterile water to a final total reaction volume of 30μl. Four and one half

units of T4 polynucleotide kinase (NEB) were added, and the solution mixed and incubated at 37°C for 45 min. The reaction was arrested by heating at 65°C for 10 min., diluted to a final oligonucleotide concentration of 6pmol/μl with TE, pH 8.0, and stored at -20°C.

2.20.6 Annealing of the Primer to the Template

The following components were mixed in a 500μl centrifuge tube: 200ng of single stranded uracil-containing phage DNA, 0.5μl of a 6pmol/μl stock of mutagenic primer, 1μl of 10X annealing buffer (20mM Tris-HCl pH 7.4, 2mM $MgCl_2$, 50mM NaCl - Bio-Rad), and a varying amount of sterile double distilled water to a final reaction volume of 10μl. A negative control reaction mixture was also made up to test for nonspecific endogenous priming. This contained all of the above ingredients except the mutagenic oligonucleotide. Reactions were placed in a 70°C heating block and allowed to cool at room temperature. Once a temperature of 30°C was reached, mixtures were placed on ice.

2.20.7 Complementary DNA Strand Synthesis

During incubation on ice, the following reagents were added in the order listed: 1μl of 10X synthesis buffer (0.4mM each dNTP, 0.75mM ATP, 17.5mM Tris-HCl pH 7.4, 3.75mM $MgCl_2$, 21.5mM DTT - Bio-Rad), 0.8μl of 2μg/μl T4 gene 32 protein for a final amount of 1.6μg, 5 units of T4 DNA ligase, and 0.5 units of T7 DNA polymerase freshly diluted from a 2X stock in enzyme dilution buffer (20mM potassium phosphate pH 7.4, 1mM DTT, 0.1mM EDTA, 50% glycerol - Bio-Rad). Reactions were mixed and incubated on ice for a further 5 min to stabilize the primer, prior to incubation at 25°C for 5 min. and at 37°C

for 90 minutes. 90μl of stop buffer (10mM Tris pH 8.0, 10mM EDTA) were added and each reaction was stored at -20°C. Reactions are stable for a period of one month for use in transformation procedures.

2.20.8 Agarose Gel Analysis of the Reaction Products

Reaction products were electrophoresed on a 1% agarose gel. Samples analyzed included the synthesis reactions, the no primer control, and 20ng of the replicative form (RF)-I of the phage to aid in identification of the covalently closed circular synthesized RF-IV DNA. This latter form is the double stranded DNA form synthesized in the above reactions and is positively supercoiled when bound to ethidium bromide. The negatively supercoiled RF-I DNA, the naturally formed isolated replicative form of phage DNA, binds more ethidium bromide than the RF-IV form and therefore travels slower on the agarose gel. The two forms also migrate closely. The single stranded uracil containing template (no primer) control, travels the furthest by agarose gel electrophoresis. The presence of a band migrating at or slightly ahead of the RF-I DNA suggested successful second strand synthesis primed by the mutagenic oligonucleotide.

2.20.9 Transformation of Synthesized Replicative Forms

Three hundred microliter aliquotes of frozen competent MV1190 cells were allowed to thaw on ice. To this was added 10μl of the synthesis reaction that was gently stirred with a sterile cold pipette tip. The no primer control was also used to transform competent cells. The mixture was placed on ice for 60 min and the cells were heat shocked at 42°C for 3 min.

Cells were placed on ice and immediately plated on H-agar plates. Prior to transformation, a 10ml overnight culture of MV1190 was prepared by inoculation with a single colony of MV1190 previously streaked on a glucose-minimal medium plate. The MV1190 overnight culture was grown at 37°C with vigorous shaking. Four 300μl aliquotes of MV1190 overnight culture were each transferred to a sterile 13ml Falcon tube. To these were added, separately, 10, 50, 100, and 140μl of the transformed cells. Three milliliters of top H-agar cooled to approximately 50°C were added to the mixture, vortexed, and immediately poured onto H-agar plates. The top agar was allowed to solidify for a period of 15 min or longer. Plates were inverted and incubated at 37°C overnight. The following morning, fresh plaques containing 10^7 or more phage were picked by insertion of a sterile Pasteur pipette through the agar surrounding the plaque and blowing the entire plug into 1ml of sterile TE pH 8.0. This was briefly vortexed to resuspend the phage. Phage stocks were stored at 4°C.

2.20.10 Screening for Mutants

To verify the presence of desired mutations, phage stocks were screened by sequencing of the replicative forms. A single well-isolated colony of MV1190 cells previously grown on a glucose minimal-medium plate was picked with a sterile toothpick and used to inoculate 20ml of LB. The culture was grown overnight at 37°C with vigorous agitation. The following morning, 1ml of the overnight culture was used to inoculate 50ml of LB and allowed to grow at 37°C for 60 min with shaking. To this was added 100μl of phage, resuspended from isolated plaques, and the culture was further incubated for 4½-5 hours. At this point, the phage was harvested according to the PEG precipitation protocol outlined in

section 2.20.3, and the entire single stranded DNA (section 2.20.4) was used for DNA sequencing. The replicative form of M13mp19G(XB) DNA was isolated from 50ml of infected MV1190 cells using the alkaline lysis method (section 2.19.1). DNA was digested with appropriate restriction endonucleases to verify the presence of properly sized inserts. Once a mutation was verified by both restriction analysis and single stranded DNA sequencing, the mutated fragment of VSV glycoprotein G was subcloned into the pXMG(AXB) vector.

2.21 DNA Sequencing

Chain termination sequencing was utilized to screen M13G(XB) mutant plaques and to confirm that desired mutants were tested in biological assays. Single stranded DNA was used as the template for screening plaques, whereas double stranded DNA was used for sequencing mutants in pXMG. Protocols for all sequencing reactions were outlined in the Sequenase Version 2.0 DNA Sequencing Kit (USB) manual and are a modification of the dideoxy chain termination sequencing reactions first described by Sanger et al. (1977). The procedure utilized the Sequenase™ Version 2.0 T7 DNA polymerase variant of bacteriophage T7 DNA polymerase. Briefly, nucleotide incorporation in a nascent DNA strand is initiated at the site of primer annealing to the template, and is terminated by incorporation of one of four dideoxy-nucleotides (ddNTPs) that does not support chain elongation. Radioactively labelled dATP is also included in the reaction, along with non-radioactive dNTPs, to facilitate visualization of terminated chain reactions following polyacrylamide gel electrophoresis.

2.21.1 Denaturation of Double Stranded DNA

To prepare the double-stranded DNA for sequencing, removing all contaminating RNA and proteins from small scale preparations of plasmid DNA was essential (section 2.18). Precipitated DNA was diluted to a final volume of 100μl with TE pH 8.0, and 1μl of 10mg/ml DNase-free RNase A was added. The solution was mixed and incubated at room temperature for a minimum of 60 min. The volume was increased to 500μl and cellular proteins and RNase A were then removed by phenol, phenol:chloroform:isoamyl alcohol (50:49:1), and chloroform:isoamyl alcohol (49:1) as in section 2.20.4 without back-extraction. To the final aqueous phase (500μl) was added 0.1 volumes of a 2M NaOH and 2mM EDTA solution. The solution was mixed and incubated at 37°C and 30 min to denature double stranded DNA. The mixture was neutralized by addition of 0.1 volumes 3M sodium acetate pH 5.2, and the DNA precipitated with two to four volumes of 95% ethanol and incubated at -70°C for a minimum of 30 min. The solution was centrifuged at 14,000g, 4°C, and 20 min to pellet the denatured DNA and the supernatant removed by aspiration. The pellet and walls of the microcentrifuge tube were washed with 70% ethanol. The ethanol was removed by aspiration and evaporation. Denatured DNA was resuspended in 7μl of sterile ddH_2O.

2.21.2 Sequencing Reaction

For annealing of the primer to the DNA, 1μl (0.5pmol) of primer was added to 7μl of DNA (200mM Tris-HCl pH 7.5, 100mM $MgCl_2$, 250mM NaCl). The reaction mixture was incubated at 65°C for of 2 min, left at room temperature to cool to less than 35°C, and then placed on ice. During the cooling period, 1.5 ml microcentrifuge tubes were filled with 2.5μl

of each termination mixture (ddG, ddA, ddT, or ddC). Each termination mixture consisted of 80μM dGTP, 80μM dATP, 80μM dCTP, 80μM dTTP, 50mM NaCl, and 8μM of the appropriate dideoxy nucleotide analogs - ddGTP, ddATP, ddTTP, or ddCTP. The tubes were capped to prevent evaporation and pre-warmed at 37°C.

To the annealed primer-template mix was added in the following order: 1μl of 0.1M DTT, 2μl of 1x labelling mix (1.5μM dGTP, 1.0μM dCTP, 1.5μM dTTP), 0.5μl of 10μCi/μl [α-^{35}S]dATP, and 2μl of a 1 in 8 dilution of Sequenase Version 2.0 T7 DNA polymerase in cold enzyme dilution buffer (20mM Tris-HCl pH 7.5, 2mM DTT, 0.1mM EDTA, 50% glycerol). If sequences less than 100 nucleotides away from the primer were required, 1μl of 0.1M $MnCl_2$ in 0.15M sodium isocitrate was added prior to the addition of sequenase. The mixture was incubated at room temperature for 2-5 min. For termination of the sequencing reactions, 3.5μl of the [α-^{35}S]dATP labelled DNA were added to each pre-warmed termination tube (ddG, ddA, ddT, or ddC) and the tubes returned to the 37°C incubation for 5 minutes. Reactions were arrested by the addition of 4μl Stop solution (95% formamide, 20mM EDTA, 0.05% Bromophenol Blue, 0.05% Xylene Cyanol FF) and stored at -20°C for a maximum period of one week. Immediately preceding gel electrophoresis, samples were heated at 75°C for 2 minutes, and 2μl of each reaction were loaded in a single lane for electrophoresis.

2.21.3 Denaturing Gel Electrophoresis

A 6% polyacrylamide gel was used for DNA fragment separation by electrophoresis. The gel consisted of 5.7g acrylamide, 0.3g bis-acrylamide and 42g urea dissolved in 1X TBE

to a final volume of 100ml. One milliliter of 10% ammonium persulfate and 25μl of TEMED were added to cross-link acrylamide chains immediately prior to pouring of the gel. Gels were pre-run at 60 watts for 15 min. before samples were loaded. In general, gels were run for four hours for 200bp long sequences. Following electrophoresis gels were dried at 80°C for 2 hrs and exposed to Kodak X-OMAT AR film at -70°C.

2.22 Maintenance of Mammalian Cells

For general purposes, COS-1 cells were grown in High Glucose Dulbecco's medium (HGD - GIBCO/BRL) supplemented with 7% (v/v) calf serum (CS), 1% penicillin/ streptomycin, 1% HEPES, 2% $NaHCO_3$, 2% L-glutamine, and 1X MEM vitamins. All media and solutions, unless otherwise stated, were pre-warmed in a 37°C water bath before use. Monolayers were grown at 37°C in a 5% CO_2 incubator.

To revive cells from stocks frozen in liquid nitrogen, the cell vial was quickly removed from liquid nitrogen and gently swirled in a 37°C water bath. Once cells were thawed, they were transferred to a 100mm culture dish containing 10ml HGD supplemented with 7% calf serum. The dish was swirled to distribute cells over its entire surface and placed at 37°C. Cells were allowed to settle during a two to three hour incubation. Media was removed by aspiration and replaced with fresh media.

To passage cell lines, growth media was removed, monolayers were washed with phosphate buffered saline, and 1ml of a 1X trypsin-EDTA solution was added to lift cells from the culture dish. Once cells were no longer adherent, the trypsin-EDTA solution was neutralized by addition of 10ml HGD supplemented with 7% calf serum. This was mixed

several times by pipetting to declump cells, and an appropriate aliquot was transferred to a fresh 100mm culture dish filled with 10ml of growth media. Cells were incubated at 37°C until a confluency of approximately 80-90% was reached, upon which cells were again passaged.

For long term storage, cells from two to three 150mm plates were washed with PBS, typsinized, and resuspended in growth media as stated above. Cells were then pooled and transferred to a 50ml conical Falcon centrifuge tube and were pelleted by centrifugation at 1,000g, 30sec, and 4°C in a swinging bucket rotor. Growth media was removed and replaced by freezing media (6ml for each 300mm plate, HGD supplemented with 7% calf serum and 10%(v/v) DMSO). One milliliter aliquotes were transferred to Nalgene cryovials and stored at -70°C for one week. An aliquot was tested for viability and the remaining stocks stored in liquid nitrogen.

2.23 Transfection of COS-1 Cells

All biological assays required to test the mutant VSV G glycoproteins were carried out on transiently transfected COS-1 cells. Cells of approximately 50-60% confluency were transfected with CsCl-purified pXM vectors carrying genes for the wild type or mutant G proteins. Transfections were carried out using the calcium phosphate method of Graham and Van Der Eb, 1973. For each 60mm culture plate, 25μl of 2.5M $CaCl_2$, a desired amount of plasmid DNA (2-30μg), and enough ddH_2O to bring the total volume to 250μl were mixed in a microcentrifuge tube. The mixture was added dropwise into 250μl of HeBS pH 7.1, in a 15ml polystyrene Falcon tube, with bubbling. The mixture was incubated at room

temperature for a 30 min. period during which old growth media was removed from COS-1 monolayers and replaced by 5ml fresh growth media. Following incubation, 500μl of the calcium-phosphate-DNA precipitate was added dropwise, and the plates swirled to distribute the precipitate. Cells were incubated for 4 hrs at 37°C before glycerol shock. Media was removed and 0.5ml of HGD supplemented with 7% calf serum and 15% glycerol (v/v) were added. Plates were swirled to cover monolayers and incubated for 2min. To dilute out the glycerol, 5ml of HGD without serum were added and the process was repeated. Five milliliters of complete growth media were added and the plates incubated overnight at 37°C to express the foreign protein. All biological assays were carried out at 24 hrs post-transfection.

2.24 Metabolic Labelling of Transfected Cells

Transfected cells were metabolically labelled with [^{35}S]methionine. Cells were washed twice with 10ml PBS and 1ml of HGD media lacking methionine (GIBCO/BRL) was added. Monolayers were starved for 1 hr at 37°C, after which 50μCi of [^{35}S]methionine were added. Cells were incubated at 37°C for 2-3 hrs, during which both cellular and transfected proteins were radioactively labelled. Plates were transferred to an ice bucket and cells were washed twice with cold PBS to remove all traces of media. Cells were lysed by the addition of 1ml, per 60mm tissue culture dish, of cold lysis buffer containing the protease inhibitors PMSF and trasylol to a final concentration of 1mM and 100units/ml, respectively. Lysates were transferred to a 1.5ml microcentrifuge tube and stored at -20°C. For pulse-chase experiments, cells were starved with media lacking methionine for one hour, pulsed with a set amount of

[^{35}S]methionine and chased for various periods at 37°C with chase media (HGD supplemented with 7% calf serum and 2.5mM methionine). Following the chase, cells were incubated on ice to arrest growth.

2.25 Immunoprecipitations

To purify wild type and mutant G proteins from the cellular lysate, immunoprecipitation with anti-G polyclonal antibody was utilized. Frozen lysates were thawed on ice and cellular debris was removed by centrifugation at 14,000g, 5 min, and 4°C. The supernatant was transferred to a fresh 1.5ml microcentrifuge tube and 1μl of crude anti-G antibody was added. The mixture was rotated in a Labquake shaker for 1 hr at 4°C. To this was added 50μl of 10% Protein-A-Sepharose beads in fresh lysis buffer, and the mixture was rotated for an additional hour. Protein-antibody complexes were pelleted by centrifugation at 14000g, 2min, and 4°C. The supernatant was removed by aspiration and the complexes were washed three times with lysis buffer containing 0.3% SDS, 1mM PMSF, and 100U/ml solution on ice. Fifteen microliters of 2X loading buffer (100mM Tris-HCl pH 6.8, 200mM DTT, 4% SDS, 0.2% bromophenol blue, 20% glycerol, 10% β-mercaptoethanol) were added and protein samples were stored at -20°C. To dissociate G proteins from antibodies, samples were boiled for 2-3 min immediately prior to electrophoresis, and loaded onto a 10% SDS-polyacrylamide gel.

2.26 SDS-Polyacrylamide Gel Electrophoresis

The discontinuous system of Laemmli (1970) was used to analyze sample proteins.

Gel molds and the electrophoresis apparatus were obtained from Bio-Rad. For each 10% polyacrylamide gel, 3ml of stacking gel and 5ml of resolving gel were prepared. Resolving gels were composed of a 1.9ml ddH_2O, 1.7ml 30% acrylamide mix (bisacrylamide/ acrylamide in a 1:29 ratio), 1.3ml of 1.5M Tris-HCl pH 8.8 and 500μl of 10% SDS solution. To cross link acrylamide chains, 50μl of 10% (w/v) ammonium persulfate and 2μl of TEMED were added. The solution was immediately poured into a gel mold and topped off with ddH_2O to form a flat surface. Once the resolving gel had solidified, the water was removed and a stacking gel was poured with a comb in place. The stacking gel consisted of 2.1ml of ddH_2O, 500μl of 30% acrylamide mix, 380μl of 1.0M Tris-HCl pH 6.8, 30μl of 10% SDS, 30μl of 10% ammonium persulfate, and 3μl of TEMED. The gel was allowed to harden and then rinsed with water to remove traces of unpolymerized acrylamide. The water was poured off and boiled samples were loaded directly into the wells. Samples were topped off with Tris-glycine electrophoresis buffer (25mM Tris, 250mM electrophoresis grade glycine, 0.1% SDS) and electrophoresed at 200V until the bromophenol dye reached the bottom of the gel.

2.27 Fluorography of Polyacrylamide Gels

Impregnation with sodium salicylate (Chamberlain, 1979) was used to enhance radioactivity of samples run on SDS-PAGE gels. Gels were briefly rinsed with water, for 5 min., to remove traces of running buffer and were soaked, while shaking, in a solution of 1M salicylic acid and 1M NaOH for 35 min. Gels were dried at 60°C for 2 hrs and exposed to Kodak X-OMAT AR film at -70°C.

2.30 Indirect Immunofluorescence

COS-1 cells grown on 18 mm square coverslips in 60mm plates were transfected as in section 2.23. At 24 hrs post-transfection, coverslips were transferred to six well plates and washed twice with PBS to remove any traces of media. Monolayers were fixed by the addition of 2ml cold 2% paraformaldehyde, in PBS pH 7.5-8.0, and incubation at 4°C for 20min. The paraformaldehyde was removed and cells were washed twice with 3ml PBS. Cells were then incubated in 3ml PBS containing 1% BSA for 15 min. at room temperature. Ammonium sulfate purified anti-G antibody was diluted in a 1:50 ratio with PBS containing 1% BSA, and 30μl of this preparation were used to overlay coverslips. Following incubation with anti-G antibody, at 37°C and 20 min., coverslips were washed with 3ml of PBS containing 1% BSA for 10 min. at room temperature. Prior to the addition of 30μl fluorescein isothiocyanate-conjugated (FITC) goat anti-rabbit antibody diluted in PBS containing 1% BSA in a 1:75 ratio, coverslips were once more incubated at 37°C for 20 min and washed with PBS containing 1% BSA for 15 min at room temperature. Traces of BSA were removed by washing with PBS for 15 min at room temperature.

Internal immunofluorescence was performed using either acetone or Triton X-100. To permeabilize cells with Triton X-100, cells fixed with 1% paraformaldehyde in PBS as above were treated with 2ml of 1% Triton X-100 in PBS for 15min at room temperature. Cells were washed twice with PBS for 5 min., and once with PBS containing 1% BSA for 10 min. Anti-G and FITC antibodies were then used to label the proteins as previously outlined for cell surface immunofluorescence. For treatment with acetone, cells were not fixed with 1% paraformaldehyde, but were instead transferred to porcelain vertical racks and immersed

in acetone for 10min at -20°C. Following fixation and permeabilization by acetone, cells were immersed in a beaker containing PBS for 5min and then transferred to a six-well plate. The coverslips were washed once more with PBS and with PBS containing 1% BSA for 10 min. Anti-G and FITC antibodies were used to label G proteins as stated above.

All coverslips were air dried and mounted onto slides using 10μl of 50% glycerol in PBS. These were examined under a Zeiss epi-fluorescence microscope and a photographic record was taken using black and white Kodak Tmax 400 film.

2.31 Lactoperoxidase Catalyzed Cell Surface Iodination

Quantification of mutant protein surface expression, as related to wild-type expression, was performed as described by Guan et al., 1984. At 24 hours post-transfection, monolayers grown on a 60mm culture plate were washed twice with phosphate buffered NaCl (PBNaCl - 10mN Na_2HPO_4, 150mM NaCl, pH 7.4) and 3ml of PB NaCl were left remaining in the plate. To this was added a mixture of 135μl of 2% glucose, 12μl of 5μg/μl lactoperoxidase (Sigma) and 250μCi of $Na^{125}I$ (Dupont NEN). The reaction was initiated by the addition of 0.5 units glucose oxidase in a volume of 10μl. Plates were swirled to distribute the reagents, and incubated for 40 min at room temperature. The solution was removed and cells were washed twice with phosphate buffered NaI (10mM Na_2HPO_4, 150mM NaI, pH 7.4) and five times with phosphate buffered NaCl. Plates were transferred to ice and lysed with lysis buffer containing 1mM PMSF and 100U/ml trasylol. The lysates were immunoprecipitated and analyzed by polyacrylamide gel electrophoresis as described in sections 2.25 and 2.26.

2.32 Cell-Cell Fusion Assay

In order to test the capacity of mutant G proteins to mediate fusion, cells expressing the glycoproteins were subjected to acidic pH (Florkiewicz and Rose, 1984) and the number of polykaryons was quantified. Cells cultured on a 60mm plate were subjected to this assay at 24 hrs post-transfection, and at greater than 80% monolayer confluency. High Glucose Dulbecco's media was removed by aspiration, and monolayers were exposed to 1ml of pre-warmed fusion media for exactly 60 seconds. Fusion media consisted of 1.85mM $NaH_2PO_4 \cdot 2H_2O$, 8.39mM Na_2HPO_4, 2.5mM NaCl, 10mM HEPES, and 10mM MES. The media was adjusted, with HCl, to pH 6.3, 6.0, 5.8, 5.6, 5.45 or 5.4, 5.2, 5.0, and 4.8. For each G protein, wild type or mutant, a single 60mm plate was exposed to only one of the above stated pHs. The fusion media was quickly removed and 3 ml of HGD including 7% calf serum were added. Plates were incubated at 37°C for 2½ hours, after which they were exposed to a second pH shock. The growth media was removed and 1ml of fusion media, of identical pH as above, was added for exactly 60 seconds. The fusion media was removed, 3ml of growth media was added, and the plates were incubated at 37°C. Following a 1½-2 hr incubation, the growth media was removed and 1ml Carnoy's solution (60% methanol, 10% acetic acid) was added. Cells were fixed, at room temperature, for 10-15 min, after which the Carnoy's solution was removed and the plates inverted to dry. Cells were stained with 1ml 0.1% crystal violet for 15 min., rinsed with water, and dried overnight. Polykaryons with greater than four nuclei in nine fields under low power magnification were counted for each 60mm plate.

2.33 Endoglycosidase H Digestion

At 24 hrs post-transfection, growth media was removed from a 60mm culture plate and monolayers were washed twice with PBS. Cells were starved by the addition of 1ml HGD lacking methionine and supplemented with 7% calf serum, and incubated at 37°C for a period of 1 hr. Seventy-five microcuries of [^{35}S]methionine were added, and plates were incubated at 37°C for 15 min. Following the pulse, cells were chased with HGD supplemented with 7% calf serum and 2.5mM methionine for either 0 or 60 min at 37°C. Monolayers were then placed on ice and immediately disrupted with lysis buffer containing 1mM PMSF and 100U/ml trasylol. The lysates were transferred to a 1.5ml microcentrifuge tube and cellular debris was pelleted by centrifugation at 14,000g, 4°C, and 5 min. The supernatant was immunoprecipitated with crude anti-G antibody and protein A-sepharose as in section 2.25. 2X sample buffer, however, was not immediately added to the immunoprecipitates. Instead, the samples were resuspended in a 20μl solution of 50mM Tris pH 6.8 and 1% SDS and boiled for 2 min. Two aliquotes of 10μl were transferred to fresh microcentrifuge tubes and 1μl of 30μg/ml Endoglycosidase H (G enzyme) was added to only one of the tubes. Both tubes were incubated overnight in a 37°C water bath. In cases where Endo H_f (NEB) was used, immunoprecipitates were resuspended in 20μl of Denaturation Buffer (0.5% SDS, 1% β-mercaptoethanol) and boiled for 10 min. Ten microliter aliquotes were transferred to a fresh microcentrifuge tube and 1μl of 10X G5 buffer (0.5M sodium citrate pH 5.5 at 25°C) was added. To only one of the tubes was added 1μl of Endo H_f (1000U/μl) and both tubes were incubated overnight at 37°C. An equal volume of 2X loading buffer was added, samples were boiled for 2 min., and loaded onto an SDS-polyacrylamide

gel. Each band on the resultant autoradiogram was scanned three times with a densitometer and the average was taken as an indication of the amount of protein present. Percent resistance to Endoglycosidase H digestion was calculated as a function of the total amount of protein present in the 60 min. enzymatically treated sample.

2.34 Oligomerization by Sucrose Gradients

This procedure was performed according to the method of Doms et al. (1987). Cells grown on a 60mm culture plate, at 24 hrs post-transfection, were starved with growth media lacking methionine for 60 min. at 37°C. The media was removed, cells were washed twice with PBS, and proteins were labelled for 30 min at 37°C with 100μCi of [^{35}S]methionine. Radioactive proteins were chased with HGD supplemented with 7% calf serum and 2.5mM methionine for 90 min. at 37°C. Plates were placed on ice and the monolayers were washed twice with PBS. Cells were lysed with 300μl of ice-cold 4X MNT (80mM MES, 120mM Tris-HCl, 400mM NaCl, 4mM EDTA, 4mM EGTA) containing 1% Triton X-100, 1mM PMSF, and 100U/ml trasylol, and buffered to a pH of either 7.4 or 5.6. Following a minimum incubation of 60 min on ice, cell lysates were transferred to a microcentrifuge tube and cellular debris was pelleted by centrifugation at 14,000g for 5min at 4°C. The supernatant was loaded onto a 5-20% sucrose gradient made in 2X MNT and containing 0.1% Triton X-100. Gradients were made up during pulse and chase periods and were stored on ice. A single gradient was used to separate BSA (4S) and aldolase (8S) that were used as markers to aid in the identification of monomer and trimer fractions. Gradients were centrifuged at 40,000rpm, 20 hrs, and 4°C in an SW41 swinging bucket rotor using a Beckman L8-70M

ultracentrifuge. Fractions containing radioactively labelled cell lysates were each neutralized by the addition of 800μl of RIPA buffer (1% NP40, 0.4% sodium deoxycholate, 12.5mM EDTA, 50mM Tris-HCl) pH 8.0 containing 2mM PMSF and 200U/ml trasylol. One microliter of crude anti-G antibody and 50μl of 10% protein-A sepharose protein were used to immunoprecipitate each fraction, as in section 2.25. The immunoprecipitates were washed three times with RIPA buffer containing 0.3% SDS, 1mM PMSF, and 100U/ml trasylol. Samples were analyzed by SDS polyacrylamide gel electrophoresis and autoradiography (sections 2.26 and 2.27).

Gradient fractions of the BSA and aldolase gradient were analyzed by the BCA* Protein Assay kit (Pierce) to identify fractions containing the proteins. Reagent A (sodium bicarbonate, sodium carbonate, BCA detection reagent, sodium tartarate in 0.1M Na OH) and reagent B (4% copper sulfate) were mixed in a 1:50 ratio to form the working reagent. This was added to a solution consisting of 50μl sample (from a single fraction) and 50μl 0.5% SDS in a 1.5ml microcentrifuge tube and vortexed. Samples were incubated at 60°C for 30 min. and cooled to room temperature. Relative protein amounts were determined by spectroscopic analysis.

2.35 Resistance to Trypsin

The following procedure was performed as described in Fredericksen and Whitt (1996). At 24 hrs post-transfection, cells (60mm plates) were starved with 1ml of growth media lacking methionine for one hour at 37°C, and subsequently pulsed with 50μCi of [^{35}S]methionine for 30 min. at the same temperature. Monolayers were washed twice with

PBS and chased with High Glucose Dulbecco's media supplemented with 7% calf serum and 2.5mM methionine. Plates were then placed on ice and cells were disrupted with the addition of 2X MNT with 1% Triton X-100 buffered to a pH of 7.4, 6.5, 6.1, or 5.6. The protease inhibitors PMSF and trasylol were not included. Following complete lysis, cells were transferred to a 1.5ml microcentrifuge tube and cellular debris was pelleted by centrifugation at 14,000g, 4°C, and 5 min. For each pH, two aliquotes of 250-300μl were transferred to microcentrifuge tubes and 10μl of 1 μg/μl TPCK-trypsin were added to only one of the tubes. Tubes were incubated at 37°C for exactly 30 min. For pH 5.6, a control sample was also included that contained 0.3% SDS. Following the 37°C incubation, samples were placed on ice and 10μl of 1U/μl aprotinin were added to each sample. Samples were spun for 2-5min., at 4°C, in a microcentrifuge and supernatants were transferred to new microcentrifuge tubes. To immunoprecipitate G proteins, 800μl of detergent lysis buffer (10mM Tris pH 7.4, 66mM EDTA, 0.4% deoxycholic acid, 0.02% sodium azide, 1% Triton X-100) containing 1.25mM PMSF and 125U/ml trasylol were added to each tube. Anti-G antibody and protein A-sepharose were used to immunoprecipitate the proteins as outlined in section 2.25. Washings were performed using detergent lysis buffer supplemented with 0.3% SDS, 1mM PMSF, and 100U/ml trasylol. Samples were analyzed by SDS-polyacrylamide gel electrophoresis (section 2.26) and autoradiograms were densitometricaly analyzed. An average of three densitometric readings was taken as an indication of the amount of proteins present in a single band. To measure resistance to trypsin at a particular pH, the amount of protein in the digested sample was taken as a percentage of that in the untreated sample.

3. RESULTS

Initial characterization of regions involved in VSV G protein mediated fusion involved linker insertion mutagenesis throughout the entire G glycoprotein gene (Li et al., 1993) to reveal four cell-cell fusion deficient mutants termed H2, H5, H10, and A4. The H2 region was first proposed as a possible fusogenic domain by Oshnishi et al., 1988, on the basis of conservation of amino acids among Indiana and New Jersey VSV serotypes. In addition, site directed mutagenesis in this region spanning amino acids 117 to 139 generated glycoproteins that were compromised in their capacity to mediate fusion and also altered the thresholds and optimum pHs required for fusion (Zhang and Ghosh, 1994; Fredericksen and Whitt, 1995, 1996). The H2 region was thus identified as a putative fusion peptide, a hypothesis that was later confirmed through hydrophobic photolabelling studies that resulted in labelling of a large peptide segment (residues 59-221) that includes the H2 region (Durrer et al., 1995) Fusion peptides of other viruses such as influenza, human immunodeficiency virus (HIV), and Semliki Forest virus (SFV) were also identified and characterized by mutational analysis of the respective spike proteins (Bosch et.al, 1989; Freed et al., 1992, 1990; Gething, et al., 1986; Levy-Mintz and Kielian, 1991). Site specific mutagenesis surrounding the H5 region did not alter the fusogenic properties of G protein (Fredericksen and Whitt, 1995). The two insertion mutants H10 and A4, at residues 410 and 415 respectively, are present within a region corresponding to residues 395 to 424 of VSV Indiana serotype that is conserved among ten rhabdoviruses (Fig. 3) (Shokralla et al., 1998). Within this region 14 of the 30 residues were

conserved in the five vesiculoviruses and three residues (P399, H423, P424) were conserved in all 10 rhabdoviruses. The region, however, was found not to interact with the target membrane (Durrer et al., 1995) and therefore functions indirectly in G mediated fusion. To characterize residues important in the function and the possible role of the H10/A4 domain, site-directed mutagenesis was employed. In addition, VSV G glycoproteins mutated in both the H2 and H10/A4 regions were constructed in order to examine if the effects exerted by both mutants are cumulative in their outcome towards fusion, or if one region dominates over the other. Such studies have been previously performed to examine enzymatic activity (Carter et al., 1984; Mildvan et al., 1992) as well as the fusogenic activity of influenza HA protein (Steinhauer et al., 1996).

Fig. 3. (A) Alignment of ten rhabdoviral G glycoproteins in the H10/A4 region of VSV Indiana serotype. Shown are VSV Indiana (IND) (Rose and Gallione, 1981), VSV New Jersey (NJ) (Gallione and Rose, 1983), Cocal virus (Bhella et al., 1998), Chandipura virus (CHP) (Masters et al., 1989), Piry virus (Brun et al., 1995), spring viremia of carp virus (SCVC) (SCVC Genbank), Sigma virus (Teninges and Bras-Herreng, 1987),infectious hematopoietic virus (IHNV) (Koener et al., 1987), Mokola virus (Tordo et al., 1993), and rabies virus CV strain (Yelverton et al., 1983). Residues conserved among all 10 rhabdoviruses are in bold. Arrowheads indicate sites of amino acid insertions of the H10 and A4 mutants. The positions of two mutants V392G and M396T of rabies virus that are compromised in acid-induced pH conformational change are indicated with arrows (Gaudin et al., 1996). (B) Mutations in the H10/A4 region of VSV Indiana glycoprotein G. Residues 395 to 424 and the corresponding nucleotide sequences are shown. Amino acids conserved in four other vesiculoviruses are underlined. Residues that are doubly underlined are conserved in all 10 rhabdoviruses. Changes in nucleotide bases are shown in lowercase letters. Mutants are designated according to the corresponding wild-type residue, amino acid position, and amino acid replacement as indicated below each mutant.

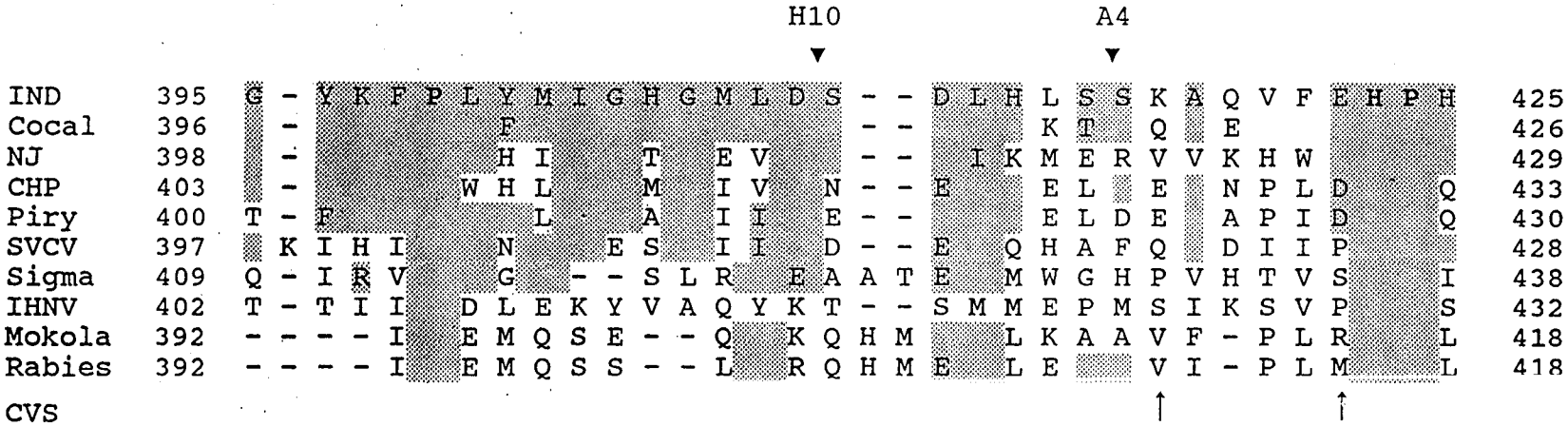
H10
A4
IND 395 G - Y K F P L Y M I G H G M L D S - - D L H L S S K A Q V F E H P H 425
Cocal 396 - F K T Q E 426
NJ 398 - H I T E V - - I K M E R V V K H W 429
CHP 403 - W H L M I V N - - E E L E N P L D Q 433
Piry 400 T - F L A I I E - - E L D E A P I D Q 430
SVCV 397 K I H I N E S I I D - - E Q H A F Q D I I P 428
Sigma 409 Q - I R V G - - S L R E A A T E M W G H P V H T V S I 438
IHNV 402 T - T I I D L E K Y V A Q Y K T - - S M M E P M S I K S V P S 432
Mokola 392 - - - - I E M Q S E - - Q K Q H M L K A A V F - P L R L 418
Rabies 392 - - - - I E M Q S S - - L R Q H M E L E V I - P L M L 418
CVS

Fig. 3A

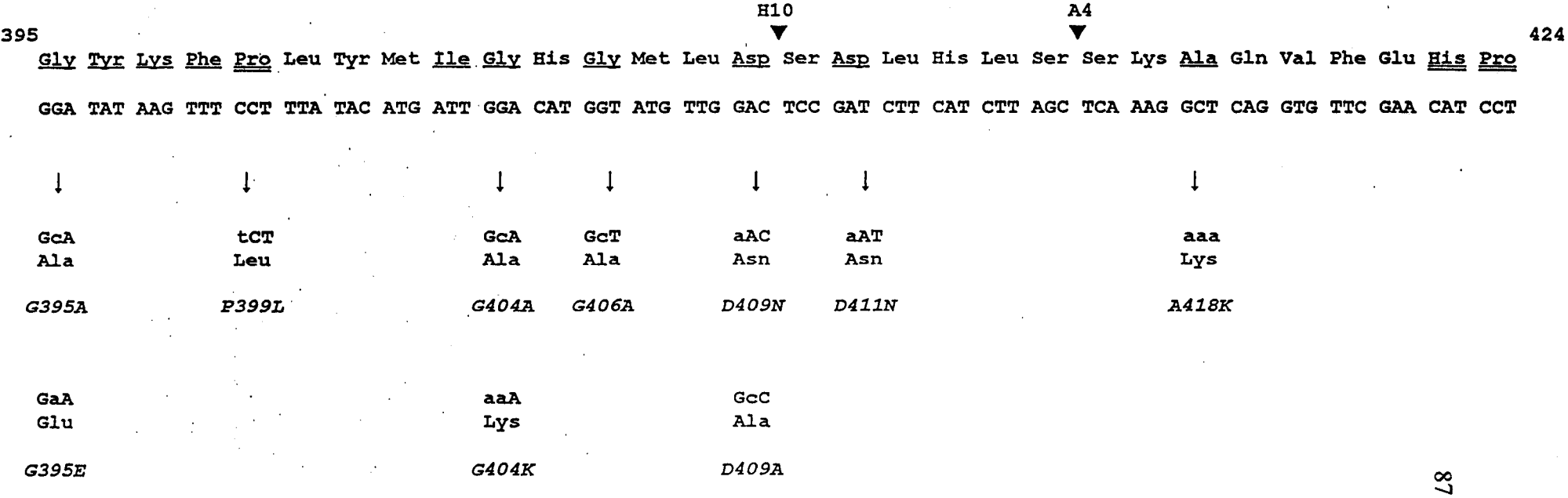
H10
A4
395
424
Gly Tyr Lys Phe Pro Leu Tyr Met Ile Gly His Gly Met Leu Asp Ser Asp Leu His Leu Ser Ser Lys Ala Gln Val Phe Glu His Pro
GGA TAT AAG TTT CCT TTA TAC ATG ATT GGA CAT GGT ATG TTG GAC TCC GAT CTT CAT CTT AGC TCA AAG GCT CAG GTG TTC GAA CAT CCT
GcA tCT GcA GcT aAC aAT aaa
Ala Leu Ala Ala Asn Asn Lys
G395A P399L G404A G406A D409N D411N A418K
GaA aaA GcC
Glu Lys Ala
G395E G404K D409A

Fig. 3B

3.1 Construction of H10/A4 Mutants

The gene encoding G protein of VSV Indiana serotype was previously subcloned into the eukaryotic expression vector pXM, at the EcoRI site, to generate the parent plasmid pXMG (Li et al., 1993). The plasmid pXMG(AXB) was constructed by E. Wanas and contains ApaI, XhoI, and BssHII sites at nucleotide positions 299, 1416, and 1473 respectively. This plasmid was tested for fusogenic activity and cell surface expression by E. Wanas and found to display wild type properties (Odell et al., 1997). The method of Kunkel et al., 1987, was used to generate ten mutants in the H10/A4 region. These were named according to the wild type residue, amino acid position, and amino acid replacement. Mutants G395A, P399L, G404A, G406A, D409N, and D411N were constructed by undergraduate students and tested for cell surface expression, polykaryon formation, transport, and oligomerization by Y. He and E. Wanas (Shokralla et al., 1998). Mutants G395E, G404K, D409A, and A418K were also constructed by M13 mutagenesis (Kunkel et al., 1987) as described in section 2.20, and using primers AB7387, AB7388, AB7389, and AB7390 listed in section 2.7. Alanine, glycine, proline, and acidic amino acids have been shown by mutagenesis to be critical for fusion peptide functions (Zhang and Ghosh, 1994; Fredericksen and Whitt, 1995, 1996). Mutagenized residues in the H10/A4 region were selected on the basis of conservation among all VSV serotypes and to examine if alanine, glycine, proline, and acidic amino acids would also be critical for H10/A4 functions.

The template used for these reactions was uracil-containing single stranded M13mp19G(XB) DNA. This contains the 629bp fragment of G gene obtained by KpnI-EcoRI restriction endonuclease digestion of pXM-GM6, with an additional BssHII site at

position 1473. Fragments obtained by KpnI-XhoI restriction endonuclease digestion of mutagenized M13mp19G(XB) plasmids were subcloned into pXMG(AXB). COS-1 cells transfected with plasmids pXMG(G395E), pXMG(G404K), pXMG(D409A), and pXMG(A418K) express G protein mutants G395E, G404K, D409A, and A418K. Clones of the mutagenized cDNAs were sequenced by the Sanger method (1977), using the sense primer AB2449 (section 2.7), and the results are presented in Fig. 4A. For mutant G395E, a glycine was replaced with a glutamine by altering a guanine to an adenine at base pair position 1213. For mutant G404K, a glycine was replaced with a lysine by altering two guanine bases, at positions 1239 and 1240, with two adenines. For mutant D409A, an aspartic acid residue was replaced with an alanine by converting an adenine at position 1255 to a cytosine. For mutant A418K, a lysine was constructed in place of an alanine by converting a guanine, cytosine, and thymine, at base pair positions 1281, 1282, and 1283 respectively, to adenosines.

Fig. 4. (A) Dideoxy-nucleotide sequencing of site-directed mutants in the H10/A4 region. Mutants were constructed by oligonucleotide mediated mutagenesis using M13 and were subcloned into the pXMG expression vector. DNA was sequenced using the sense primer AB2449. (B) Dideoxy-nucleotide sequencing of H2 inserts, with primer AB10028. At the top of each lane is indicated the chain terminator dideoxy-nucleotide utilized in the sequencing reaction. Mutagenized bases are indicated with arrowheads.

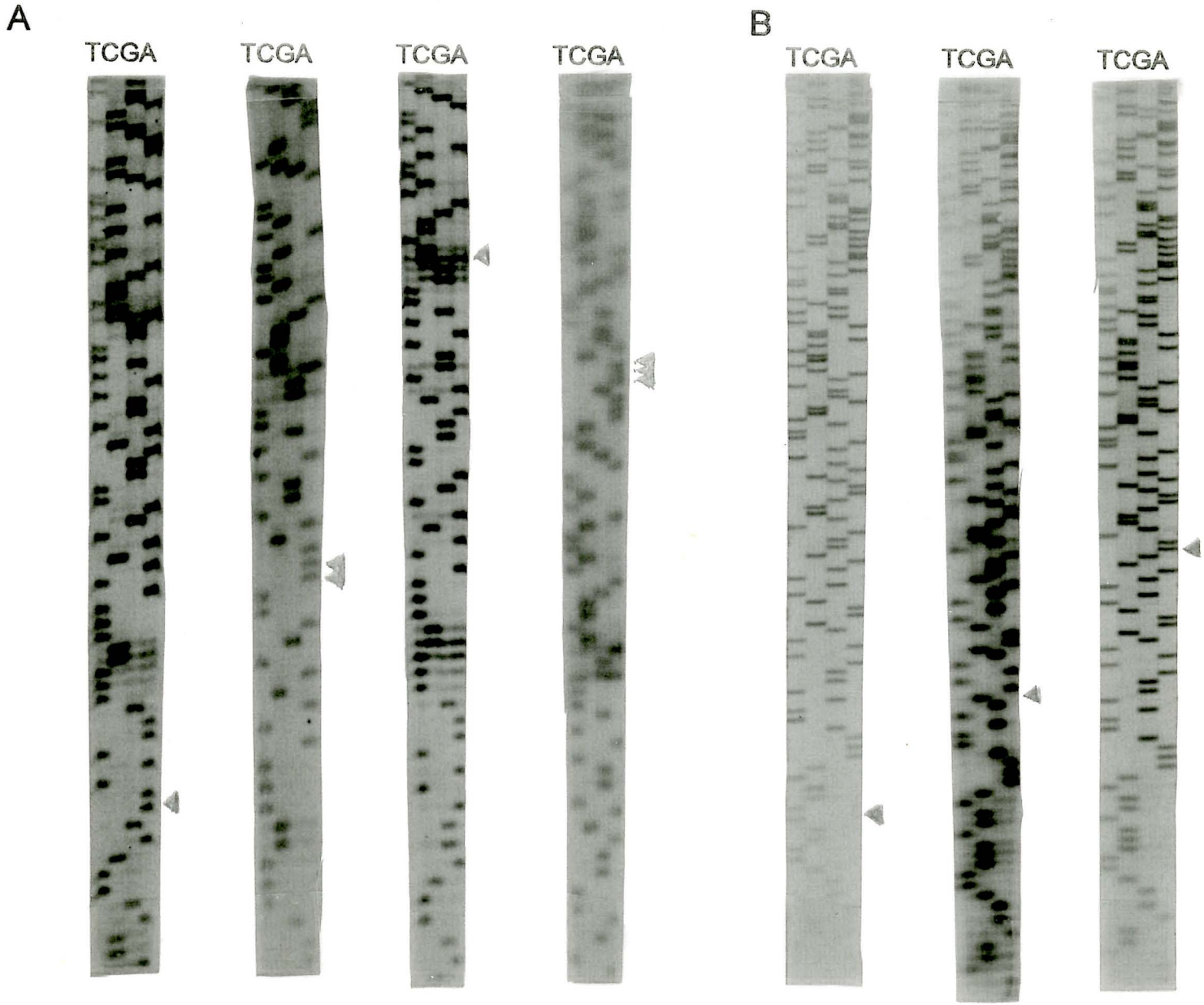
A
TCGA
TCGA
TCGA
TCGA
B
TCGA
TCGA
TCGA

3.2 Construction of H2 and H10/A4 Double Mutants

Mutants from the H2 region (Zhang and Ghosh, 1994, unpublished results) and from the H10/A4 region (Shokralla et al., 1998) were selected on the basis of their fusion profiles over the pH range of 4.8 to 6.3. The chosen mutants held profiles that were altered in their pHs of fusion thresholds and maxima (Table I). Mutants that displayed wild type or were dramatically altered in their fusion profiles were not selected. The double mutants G131A G395E, G131A D411N, and D137N D411N were constructed by R. Chernish by subcloning a 1115bp fragment of pXMG(G131A or D137N) carrying the H2 mutation into the 5681bp fragment of the pXMG(G395E or D411N) vector using BglII and KpnI restriction endonucleases. The 1115bp fragment carrying the H2 mutation replaced the corresponding wild type fragment in the H10/A4 pXMG vector. Plasmids pXMG(F125Y D411N), pXMG(P126L D411N), pXMG(G131A G404A), and pXMG(D137N G404A) were also constructed using BglII and KpnI restriction enzymes to subclone a 1115bp fragment carrying the H2 mutation into a 5681bp vector carrying the H10/A4 mutations. Inserts were sequenced, as outlined in section 2.21, using primer AB10028 (section 2.7) to verify the presence of the desired H2 mutation (Fig. 4B). For mutant P126L D411N, a cytosine at base pair position 406 was replaced with a thymine such that the proline at residue position 126 was substituted with a leucine. For mutant G131A G404A, a guanine at base pair position 421was replaced with a cytosine such that the correct insert containing an alanine substitution for glycine 131 was present. The autoradiogram for mutant D137N G404A shows an adenine substitution for guanine at base pair position 438 proving that the aspartate to asparagine mutation at residue 137 was present. Mutant F125Y D411N was sequenced by the Central

Facility of the Institute for Molecular Biology and Biotechnology, McMaster University, using primer AB10029 and automated sequencing. The autoradiogram for this mutant is therefore not shown.

3.3 Expression by Immunoprecipitation

To confirm the expression of wild type and mutant G proteins, COS-1 cells transfected with a pXM vector carrying cDNA sequences for mutant or wild type glycoproteins, were metabolically labelled with [^{35}S]methionine for a 2 hour period and lysed. Following immunoprecipitation of G proteins with rabbit polyclonal ant-G antibody, the immunoprecipitates were analyzed by SDS-polyacrylamide gel electrophoresis, and the resultant autoradiograms are shown in Figs. 5A and 5B. Mutants G395E, G404K, D409A, and A418K of the H10/A4 region co-migrate with the wild type G protein of the proper 67KDa size. Mutant A418K was tested by E. Wanas. Although size markers are not shown in these Figs., a lysate of vesicular stomatitis virus infected cells was utilized as the marker. Only VSV proteins are present in the lysate, as VSV shuts off host protein synthesis during infection. Shown are G (69KDa) and N (50 KDa) proteins of the virus as markers. Mutants F125Y D411N, P126L D411N, G131A G395E, G131A G404A, G131A D411N, D137N G404A, and D137N D411N containing mutations in both the fusion peptide (H2) and H10/A4 regions also co-migrate with wild type G protein. The intensities of both single H10/A4 and double H2-H10/A4 mutants are comparable to those of the wild-type.

Fig. 5. Expression of wild-type and (A) H10/A4 mutants (B) double mutants in the H2 and H10/A4 regions. COS-1 cells were labelled with [^{35}S]methionine for a 2 hour period and lysed. Clarified cell lysates were immunoprecipitated with rabbit anti-G antibody and analyzed by SDS-polyacrylamide gel electrophoresis. The VSV marker denotes the positions of G and N viral proteins.

B

VSV
WT
F125Y D411N
P126L D411N
G131A G395E
G131A G404A
G131A D411N
D137N G404A
D137N D411N

A

VSV
WT
G395E
G404K
D409A
A418K

3.4 Intracellular Localization and Estimates of Cell Surface Expression

It is essential that G proteins are present on the plasma membrane in order to participate in syncytia formation. Indirect immunofluorescence was used to examine cell surface expression of the mutant glycoproteins. Transfected cells were fixed with paraformaldehyde on a glass coverslip and incubated with purified rabbit anti-G antibody and fluorescein isothiocyanate-conjugated (FITC) goat anti-rabbit IgG antibody. The preparations were examined by epi-fluorescence microscopy under ultraviolet light, and photographs were taken (Figs. 6 and 7). It is evident that mutants G395E, G404K, D409A, G131A G395E, G131A G404A, G131A D411N, D137N G404A, and D137N D411N are all expressed on the cell surface. A control COS-1 immunofluorescence preparation lacking plasmid DNA transfection shows no immunofluorescence. The A418K mutant is similar in its appearance to the negative control such that it is defective in transport to the cell surface. Internal immunofluorescence experiments where cells were permeabilized using Triton X-100 showed strong internal expression of A418K protein. This data is not presented, as the expression of A418K is also shown in the immunoprecipitation experiment (Fig. 5A). Mutants F125Y D411N and P126L D411N show decreased levels of cell surface expression (Fig. 7) relative to wild-type expression. This may account for the observed reduced levels of polykaryon formation (discussed in the following section) and alterations in fusion profiles. It was previously shown that a threshold level for G glycoprotein at the cell surface is required for efficient fusion, with higher levels of G expression leading to an increase in fusion (Puri et al., 1993). That the level of polykaryon formation is dependent on the density of cell surface glycoprotein was also shown for influenza hemagglutinin (White, 1990; Gething et

al., 1986).

To quantitate the levels of cell surface expression of mutant and wild-type G protein, COS-1 cells transfected with the wild-type or mutant plasmids were subjected to iodination by a lactoperoxidase catalyzed reaction (Guan et al., 1985; Li et al., 1993; Odell et al., 1997; Shokralla et al., 1998; Zhang and Ghosh, 1994). Cells were lysed and G proteins were isolated by immunoprecipitation and analyzed by SDS-polyacrylamide gel electrophoresis. Densitometric scanning of the fluorograms (Fig. 8) was used to quantify the amount of radiated G protein. The average of two separate experiments was taken as the percent expression of wild-type. Mutant A418K was not subjected to quantitation since it was not expressed on the cell surface by indirect immunofluorescence. The percent expressions for single mutants in the H10/A4 region were 98, 103, and 177 for G395E, G404K, and D409A respectively. For double mutants in the H2-H10/A4 regions, the percent expressions were 21, 57, 148, 123, 150, 118, 199 for mutants F125Y D411N, P126L D411N, G131A G395E, G131A G404A, G131A D411N, D137N G404A, and D137N D411N respectively. All mutants, with the exception of F125Y D411N and P126L D411N, were expressed at levels similar to or above that of wild-type. Levels similar to that of P126L D411N have been previously utilized in the studies of fusion mediated by site-directed mutants, deletion mutants, and chimera of spike proteins (Li et al., 1993; Schroth-Diez et al., 1998; Bousse et al., 1994; Tanabayashi and Compans, 1996). High levels of cell surface expression indicate that alterations in the thresholds, optima, and extent of fusion by H10/A4 and H2-H10/A4 mutants are not due to under-expression of the glycoproteins.

Fig. 6. Cell surface localization of wild-type and H10/A4 mutant G proteins by indirect immunofluorescence. COS-1 cells transfected with the proper plasmids were fixed with paraformaldehyde and incubated with rabbit anti-G antibody and fluorescein isothiocyanate-conjugated (FITC) goat anti-rabbit antibody. Photographs of the preparations as viewed using a Zeiss epi-fluorescence microscope are shown.

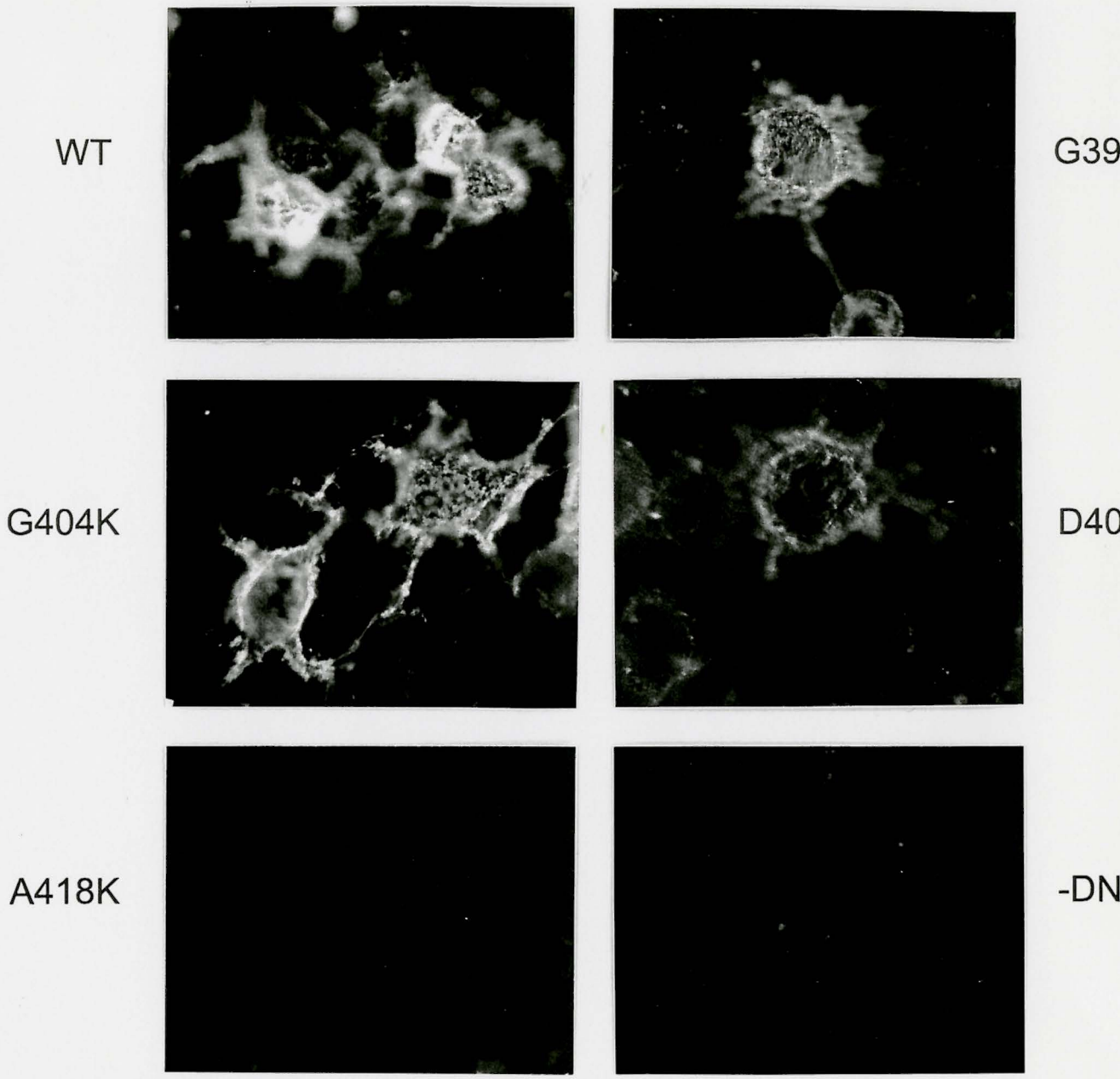
WT
G39
G404K
D40
A418K
-DN

Fig. 7. Cell surface localization of wild-type and G proteins mutated in both the H2 and H10/A4 by indirect immunofluorescence. COS-1 cells transfected with the corresponding plasmids were fixed with paraformaldehyde and incubated with rabbit anti-G antibody and fluorescein isothiocyanate-conjugated (FITC) goat anti-rabbit antibody. Photographs of the preparations as viewed using a Zeiss epi-fluorescence microscope are shown.

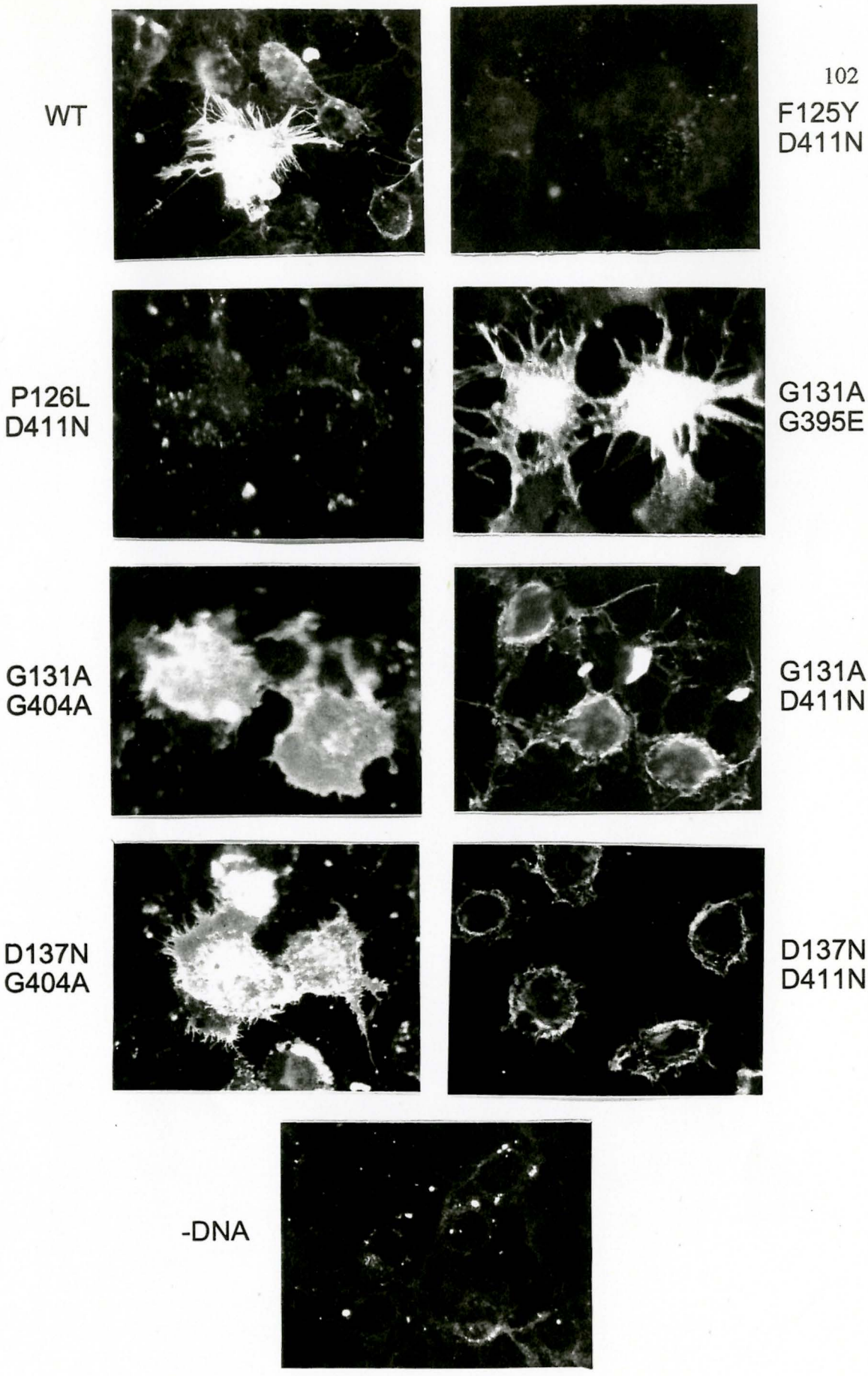
WT
F125Y
D411N
P126L
D411N
G131A
G395E
G131A
G404A
G131A
D411N
D137N
G404A
D137N
D411N
-DNA

Fig. 8. Iodination of wild-type and H10/A4 mutants (A and B), and double mutants (C). Transfected COS cells were radio-iodinated in a lactoperoxidase catalyzed reaction with ^{125}I and lysed. Immunoprecipitated G proteins were analyzed by SDS-PAGE and the fluorograms quantitated by densitometry. The average of two separate experiments was used to calculate the percent cell surface expression of mutants relative to wild-type.

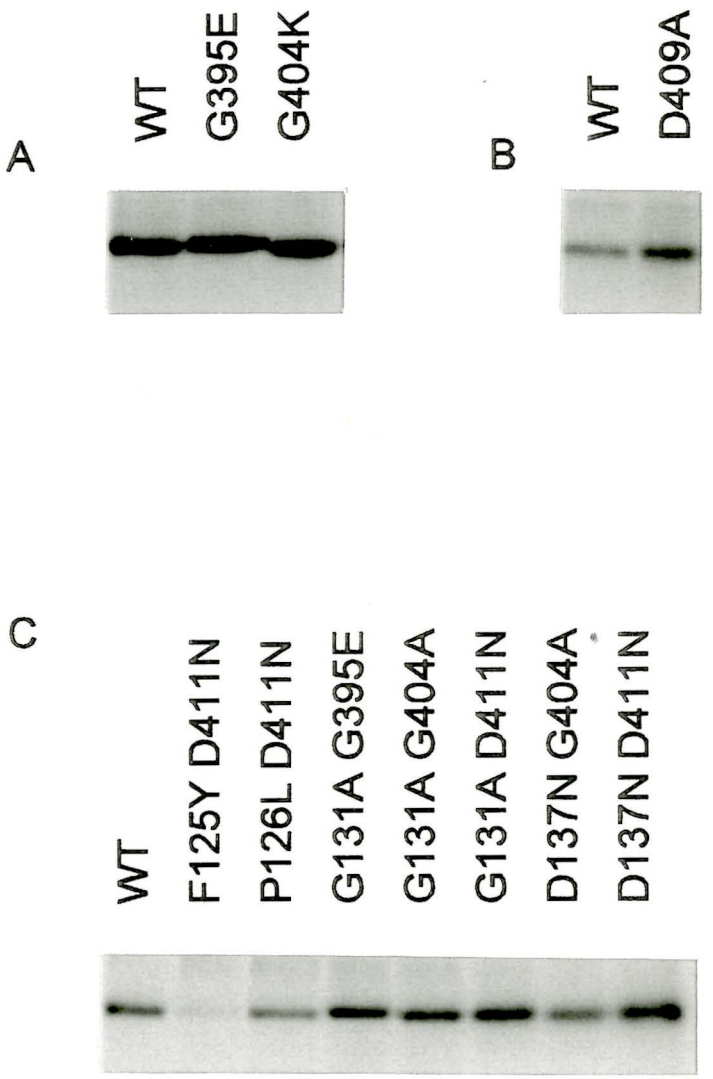
A
WT
G395E
G404K
B
WT
D409A
C
WT
F125Y D411N
P126L D411N
G131A G395E
G131A G404A
G131A D411N
D137N G404A
D137N D411N

3.5 Syncytia Formation

Cellular membrane fusion involves content mixing of internal compartments, joining of lipid membranes and thereby formation of multi-nucleated cells, also termed polykaryons or syncytia. To detect the ability of wild-type and mutant proteins to mediate fusion of target membranes, visualization of polykaryons at different pHs was employed. In the case of VSV, G is the sole viral gene product required to perform this function (Florkiewicz and Rose, 1984; Reidel et al., 1984). Mutagenesis of viral glycoproteins, including influenza hemagglutinin, Semliki Forest virus E1, human immunodeficiency virus gp41, and vesicular stomatitis virus G protein, has been previously utilized to identify regions involved in fusion (Zhang and Ghosh, 1994; Fredericksen and Whitt, 1995; Bosch et al., 1989; Freed and Myers, 1992; Freed et al., 1990; Kondor-Koch et al., 1983; Levy-Mintz and Kilean, 1991; Gething et al., 1986; Daniels et al., 1985; Skehel et al., 1995; Weis et al., 1990). COS-1 cells transfected with wild-type or mutant plasmids, at 24 hours post-transfection, were briefly exposed to acidic buffer of varying pH in the range of 6.3 to 4.8. The exposure to low-pH buffer was repeated twice for a period of 1 minute each, followed by incubations in complete media. Cells were fixed with Carnoys solution, stained with 0.1% crystal violet and polykaryons containing more than four nuclei were counted. As the wild-type protein induces the greatest number of polykaryons at the pH of 5.6 (Florkiewicz and Rose, 1984; Zhang and Ghosh, 1994; Odell et al., 1997; Shokralla et al., 1998), this was taken as the standard measure of fusion. The percent number of polykaryons formed by wild-type and mutants at all pHs was measured against 100% wild-type at pH 5.6. The fusion profiles presented in Figs. 10 and 12 are an average of two independent experiments for each pH value. Figs. 9

and 11 are photographs of syncytia formed by wild-type, H10/A4, and H2-H10/A4 mutants at the pH of 5.6.

It is evident that the syncytia formed by wild-type G protein are much larger in size and contain a greater number of nuclei than those of the mutants (Figs. 9 and 11). Mutant G395E is capable of inducing polykaryon formation at only 5% the capacity of wild-type, and the polykaryons are significantly smaller in size than those of wild-type G protein. This is also the case with mutants F125Y D411N, G131A G395E, G131A G404A, G131A D411N, and D137N G404A that are capable of inducing polykaryon formation at 1, 6, 48, 9, and 1% the capacity of wild-type protein. Polykaryon sizes are diminished in proportion to the reduction in the extents of fusion. Mutants G404K, D409A, and D137N D411N are fusion defective over the entire range of pHs tested and are similar in appearance to the untransfected control which shows no syncytia. Mutant P126L D411N that is non-fusogenic at the pH of 5.6 is also similar to the untransfected control. Mutant A418K did not form syncytia at pH 5.6 (Fig. 9) possibly due to its lack of cell surface expression.

The fusion profile of the H10/A4 mutant G395E shows a shift in both the pH threshold and pH optima of fusion with maximum fusion of 18% (Fig. 10). The glycoprotein is unable to mediate syncytia formation at pH values above 5.8, and requires a pH of 5.0 to achieve maximal fusion. This is in contrast to the wild-type threshold of a pH greater than 6.3, and a fusion optima of 5.6. Previous mutations in the H10/A4 region have also displayed a shift in the pH optima and threshold of fusion from that of wild-type (tested by Y. He as published in Shokralla et al., 1998). Shifts in thresholds and optima have also been previously observed with site-directed mutants in regions modulating fusion of influenza HA, and

Semliki Forest virus E1 (Daniels et al., 1985; Levy-Mintz and Kielian, 1991; Skehel et al., 1995; Steinhauer et al., 1995; Wiley and Skehel, 1987). The fusion peptide (H2 region) of VSV G was also characterized using site-directed mutants that caused alterations in the optimum and threshold of fusion to more acidic values, along with a decrease in the ability to form syncytia (Zhang and Ghosh, 1994; Fredericksen and Whitt, 1995). Mutants G404K and D409A are fusion defective over the entire range of 4.8 to 6.3, possibly due to an inability to assume the necessary conformation required to mediate fusion.

Fig. 9. Polykaryon formation by wild-type and H10/A4 mutant G proteins. At 24 hours post-transfection, COS-1 cells expressing the indicated glycoprotein were exposed to fusion media of pH 5.6 for a period of 60 seconds and incubated with complete media at 37°C for 2.5 hrs. Following a second exposure to fusion media, the cells were once more incubated with growth media at 37°C for a period of 1.5 hours. Cells were fixed with Carnoys solution, stained with 0.1% crystal violet and photographed.

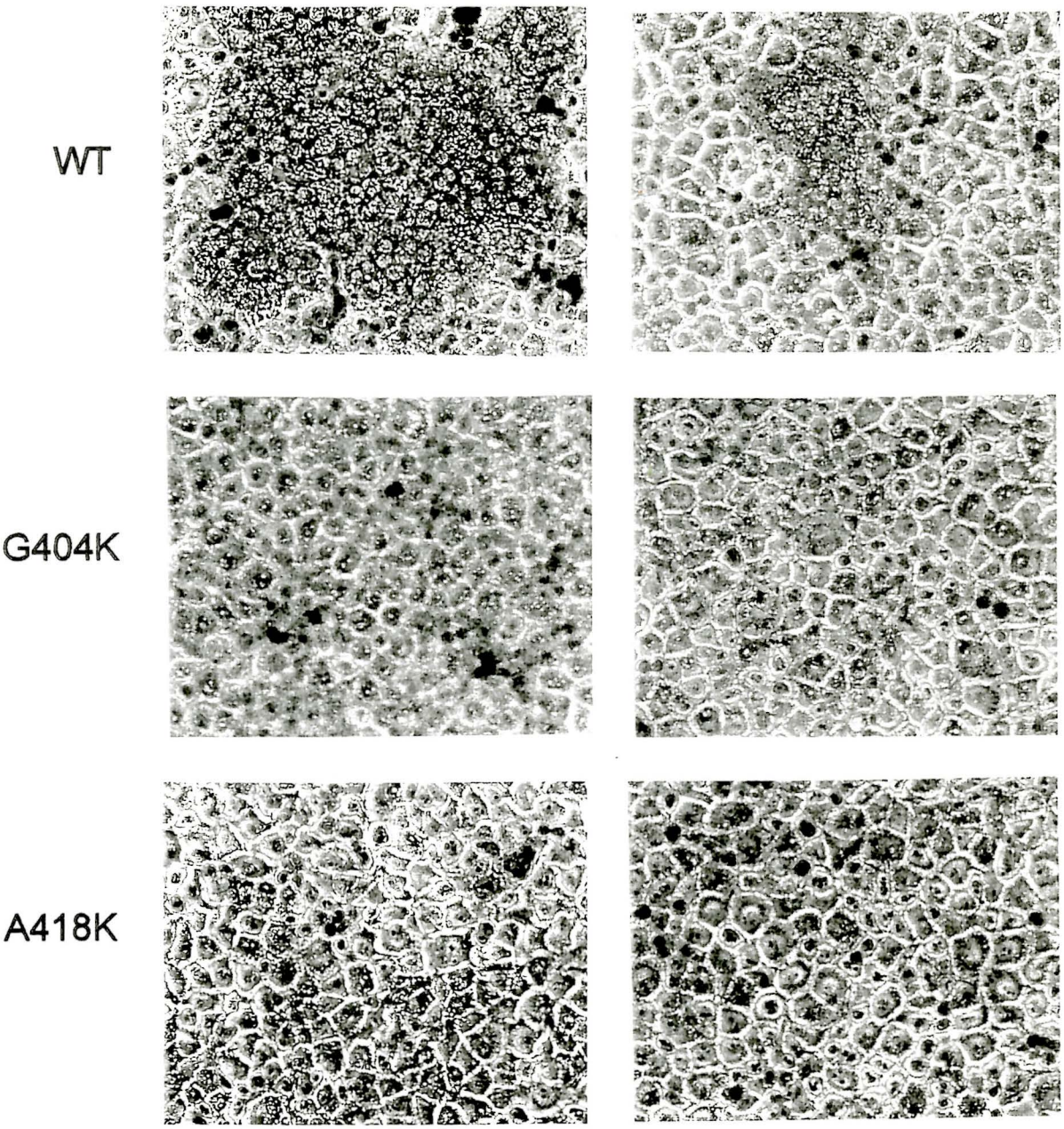
WT
G395
G404K
D409
A418K
-DNA

Fig. 10. pH dependence of cell fusion induced by expression of H10/A4 mutants. Cells transfected with wild-type or mutant plasmids were exposed to fusion media in the pH range of 4.8 to 6.3 as described in the legends to Figs. 9 and 11. Polykaryons with greater than four nuclei were counted in nine different fields and the percent number of polykaryons formed by wild-type at the pH of 5.6 was taken as the standard measure of 100%.

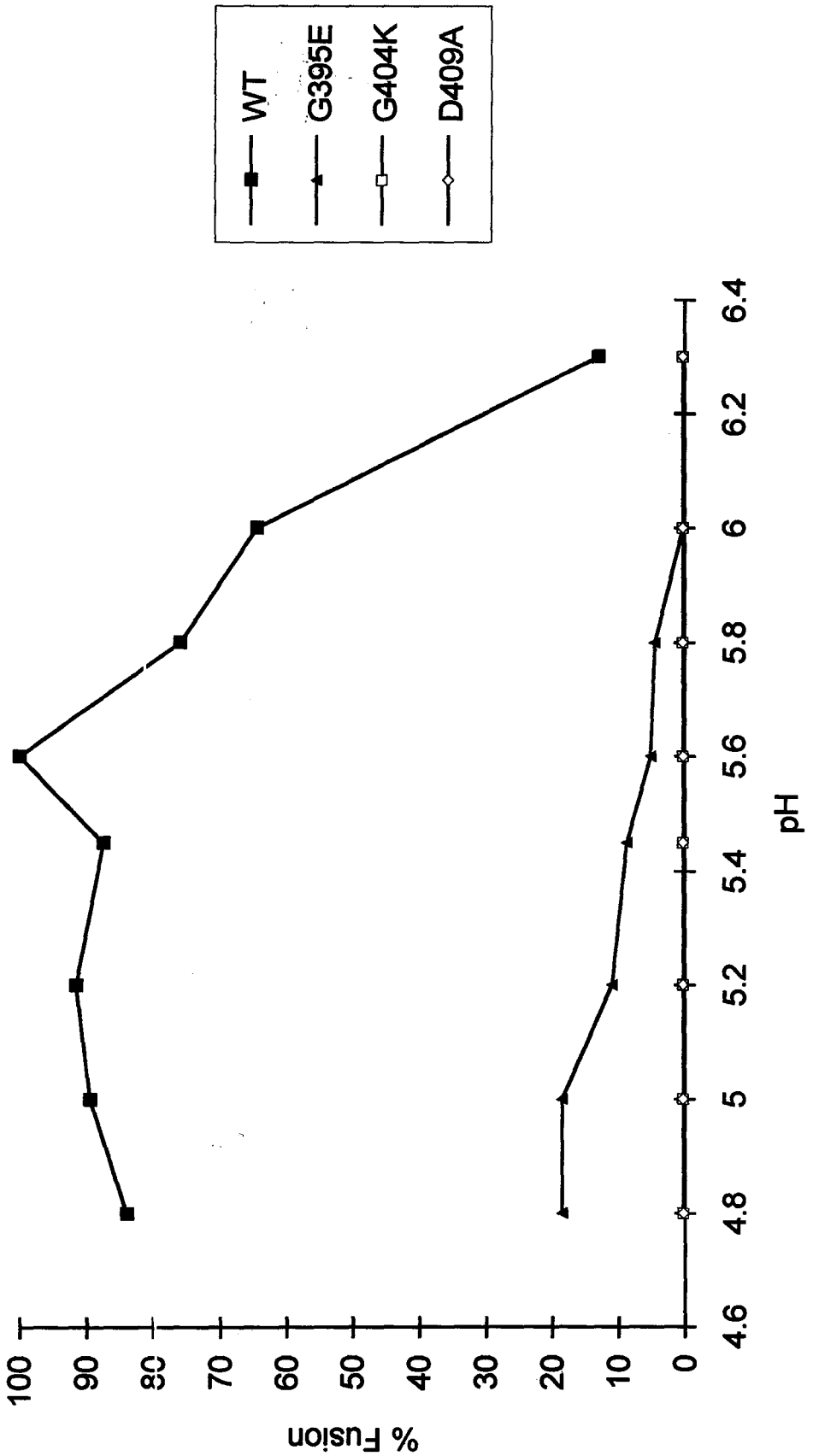
WT
G395E
G404K
D409A
% Fusion
100
90
80
70
60
50
40
30
20
10
0
4.6
4.8
5
5.2
5.4
5.6
5.8
6
6.2
6.4
pH

Mutations in multiple domains have been previously used to examine the refolding process of influenza virus hemagglutinin (Steinhauer et al., 1996), and to examine enzymatic activity (Carter et al., 1984; Mildvan et al., 1992; Shortle, 1995). Fusion profiles of G glycoproteins mutated doubly in the H2 and H10/A4 regions are presented in Fig. 12. The data for single mutants in the fusion peptide (Zhang and Ghosh, 1994, unpublished data) and H10/A4 regions (Shokralla et al., 1998) along with results of the double mutants are shown in Table I. In determining whether the effects produced by each mutant are cumulative, non-cumulative or if one domain dominates over the other, it is important to compare the pHs of fusion thresholds and optima of a double mutant with those of its H2 and H10/A4 single mutants. Mutant G131A G404A, although shifted in its optimum of fusion, is able at the pH of 5.0 to mediate fusion with only slightly reduced activity as compared to wild-type. Its pH threshold of polykaryon formation is 6.3, similar to wild-type, and above that of its constituent mutants. The optimum pH of fusion is 5.0 corresponding to that of its H2 counterpart with similar levels. Mutants G131A D411N and G131A G395E are compromised in their ability to induce fusion with an approximate 80% reduction in syncytia formation as compared to wild-type G protein. The threshold for fusion of G131A D411N is around pH 6.0, similar to that observed for both G131A and D411N mutants. Its pH optimum of 5.0, however, is similar to only the H2 mutant. G131A G395E shows a pH threshold of fusion of 5.8, corresponding to that of the G395E mutant. The maximal levels of fusion are attained at the pH of 5.0, similar to both G131A and G395E mutants, but the extent of polykaryon formation (24%) is similar to that of G395E. These mutants, with the exception of G131A G395E, have fusogenic properties that are more similar to those of the

H2 mutants rather than to the H10/A4 mutants.

The profile exhibited by D137N G404A shows a fusion threshold of pH 5.4, 0.7 units below that of wild-type, 0.4 units below the D137N mutant, and 0.6 units below G404A. The pH optima of the double mutant, however, corresponds to that of D137N with the greatest number of syncytia formed at the pH of 5.0, but with a maximal level of only 18%. Glycoprotein P126L D411N is severely reduced in fusion. Both the H2 and H10/A4 constituents (P126L and D411N, respectively) mediate fusion 0.3 pH units below wild-type, whereas the double mutant requires an even stronger acidic environment to undergo content mixing of target cells with a pH threshold of pH 5.2. The pH required for P126L D411N to achieve maximum fusion of only 5% is 5.0. This is approximately 0.6 units below that of wild-type and the D411N mutant, and 0.4 units below the P126L mutant. It is evident that both D137N G404A and P126L D411N double mutants differ from both the wild-type and single mutants, as they require increased acidity to induce a fusion competent conformation. Mutant F125Y D411N shows only about 1% fusion activity at pH 5.6, possibly due to its inadequate cell surface expression. Mutant D137N D411N is fusion defective over the entire pH range of 4.8 to 6.3. This glycoprotein, therefore, has a cumulative effect on fusion activity since the single mutants D137N and D411N each independently show shifts in fusion thresholds to a pH of 6.0. The optimal pH of D137N fusion is 5.0, whereas that of D411N is similar to wild-type. At their maximal level of fusion, D137N and D411N form approximately half the number of wild-type polykaryons. The fusion negative profile of D137N D411N depicts an additive effect induced by both the H2 and H10/A4 regions.

With the exception of G131A G395E, G131A G404A. and G131A D411N,

glycoproteins mutated in both the H2 and H10/A4 regions generally produce a fusion additive phenotype where a decrease in pH greater than that observed for the constituent single mutants is required for the double mutant to mediate polykaryon formation. Low levels or complete abolition of fusion is observed. It is also noteworthy that the optimum levels of fusion are mostly shifted to those corresponding mutations in the H2 region, whereas shifts in thresholds do not exclusively correlate with mutations in a single region, but tend to require acidity beyond that of the single mutants.

Fig. 11. Polykaryon formation of wild-type and H2-H10/A4 mutant proteins. At 24 hours post-transfection, COS-1 cells expressing the proper glycoprotein were exposed to fusion media of pH 5.6 for a period of 60 seconds and incubated with complete media at 37°C for 2.5 hrs. Following a second exposure to fusion media, the cells were once more incubated with growth media at 37°C for a period of 1.5 hours. Cells were fixed with Carnoys solution, stained with 0.1% crystal violet and photographed.

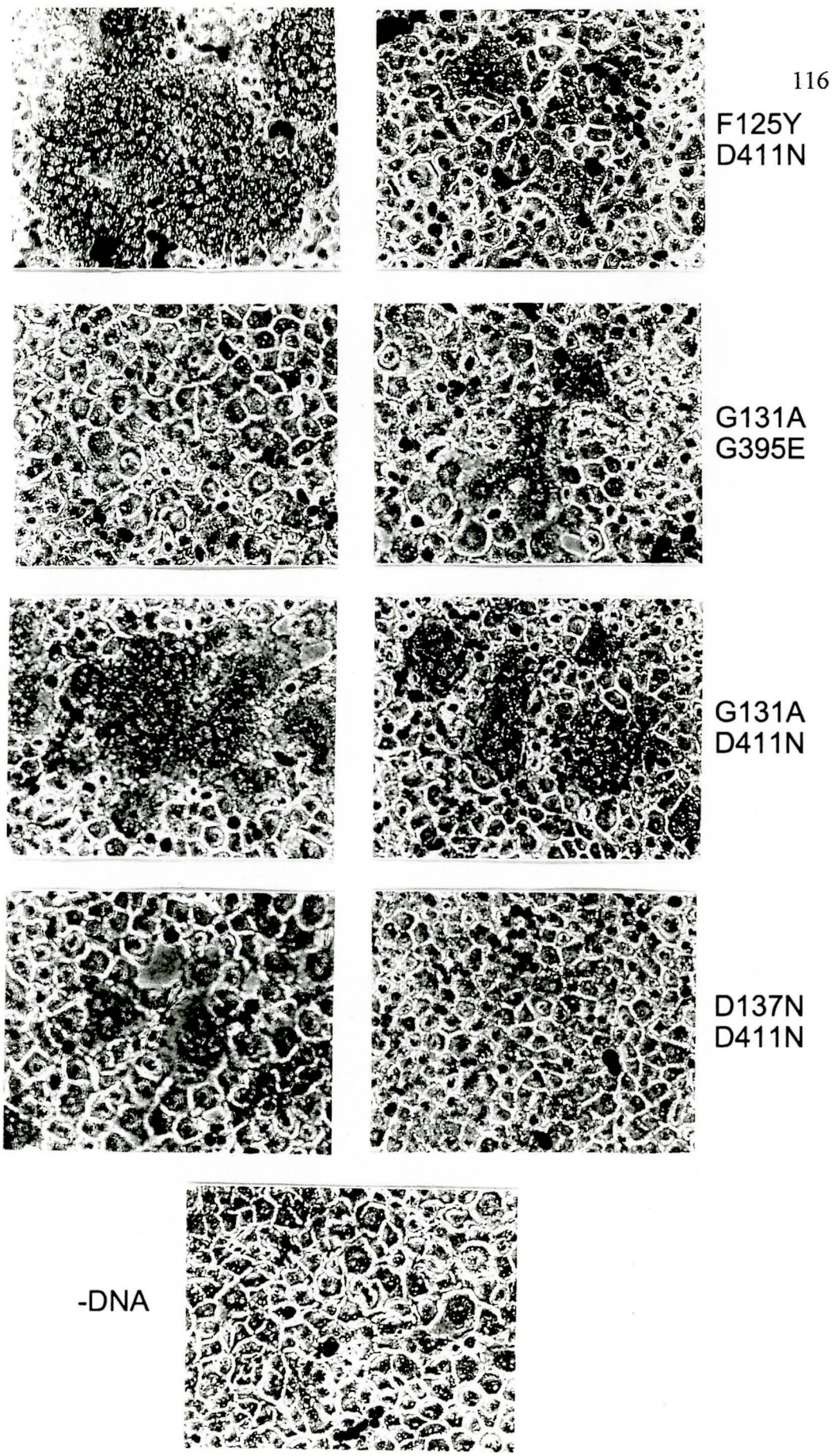
WT
F125Y
D411N
P126L
D411N
G131A
G395E
G131A
G404A
G131A
D411N
D137N
G404A
D137N
D411N
-DNA

Fig. 12. pH dependence of cell fusion induced by expression of proteins mutated in both the H2 and H10/A4 regions. Cells transfected with wild-type or mutant plasmids were exposed to fusion media in the pH range of 4.8 to 6.3 as described in the legends to Figs. 9 and 11. Polykaryons with greater than four nuclei were counted in nine different fields and the percent number of polykaryons formed by wild-type at the pH of 5.6 was taken as the standard measure of 100%.

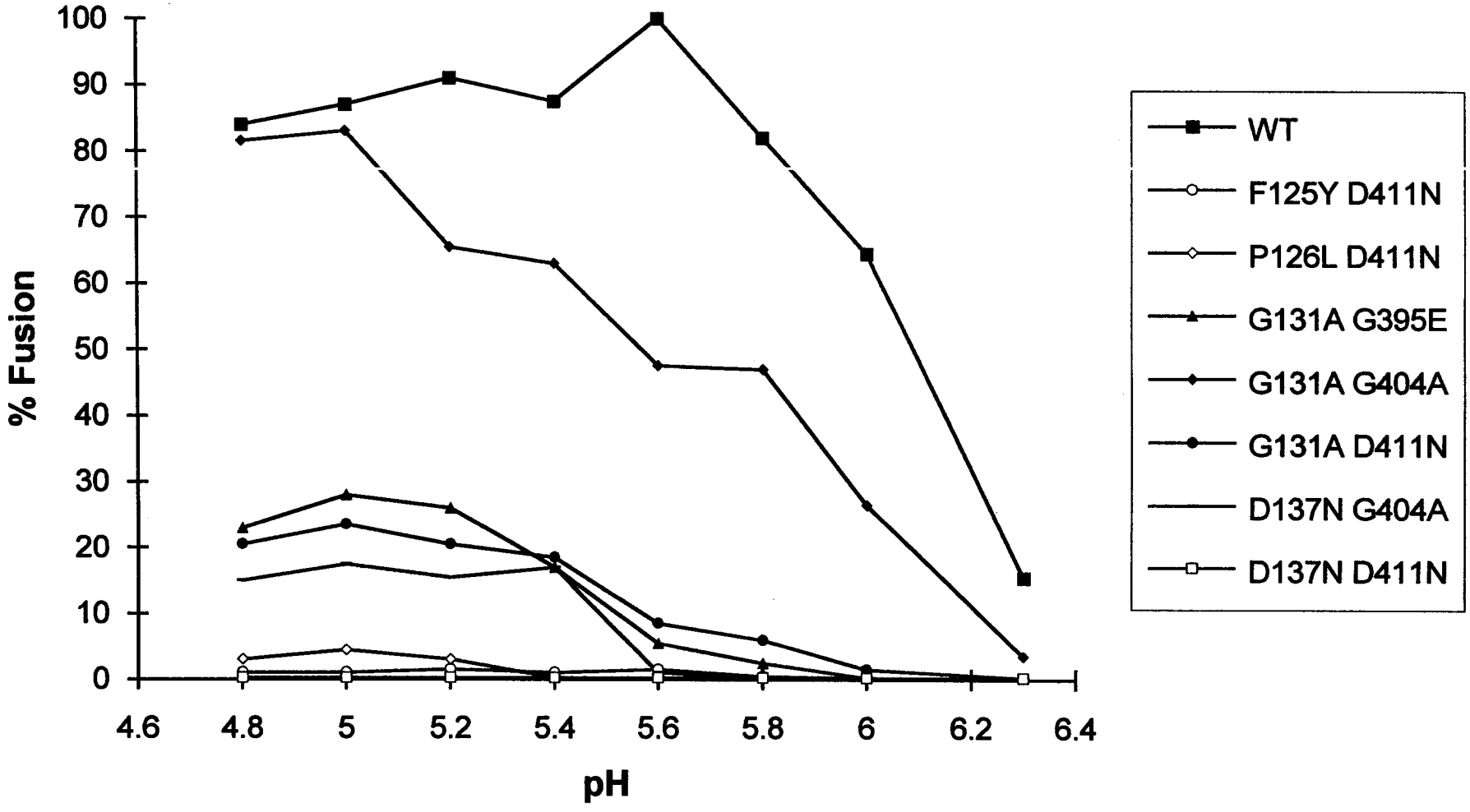
100
90
80
70
60
50
40
30
20
10
0
% Fusion
4.6
4.8
5
5.2
5.4
5.6
5.8
6
6.2
6.4
pH
WT
F125Y D411N
P126L D411N
G131A G395E
G131A G404A
G131A D411N
D137N G404A
D137N D411N

Table I. Summary of the Properties of H2 and H10/A4 Mutants Involved in Studies of Double Mutation Effects on VSV Glycoprotein G

Glycoprotein	Cell surface expression		pH threshold of fusion[c]	pH optimum of fusion[d]	Cell fusion (%)[b]	Trimer formation	Endo H resistance (%)[e]	Trypsin resistance (%)[f]
	Immuno-fluorescence	Iodination[a] (%)						
WT	+	100	6.3	5.6	100	+	100	87
F125Y	+	91	6.0	5.2	34	+	R	
P126L	+	66	6.0	5.4	52	+	R	
G131A	+	120	6.0	5.0	70	+	R	
D137N	+	126	6.0	5.0	48	+	R	
G395E	+	98	5.8	5.0	18	+	100	75
G404A	+	158	6.0	5.6	42	+	100	55
D411N	+	121	6.0	5.45	46	+	89	40
F125Y D411N	-	21	5.6	5.6	1	+	65	0
P126L D411N	-	57	5.2	5.0	5	+	80	44
G131A G395E	+	148	5.8	5.0	28	+	100	83
G131A G404A	+	123	6.3	5.0	83	+	92	34
G131A D411N	+	150	6.0	5.0	24	+	100	45
D137N G404A	+	118	5.4	5.0	18	+	100	31
D137N D411N	+	199	—[g]	—	—	+	100	52

[a]For quantitation of cell surface expression, COS cells transfected with wild type or mutant G plasmids were iodinated with ^{125}I in a lactoperoxidase-catalysed iodination reaction at 24 hours post-transfection. Results shown are the averages of two separate experiments.
[b]Cell-cell fusion at the pH optimum was determined by exposing expressed wild type or mutant proteins in COS cells, at 24 h post-transfection, to fusion media of varying acidity in the pH range of 4.8-6.3. The number of polykaryons produced by wild type G protein at pH 5.6 was taken as the standard measure of 100%.
[c,d]The pH optima and thresholds of cell-cell fusion were determined by counting polykaryons over a pH range of 4.8-6.3. Data for the H2 mutants was extrapolated from unpublished results and Zhang and Ghosh, 1994.
[e]Resistance to endoglycosidase H digestion, at 60 min of chase, was quantitated by densitometric scanning of fluorograms and the amount of glycoprotein resistant to digestion was taken as a percentage of the total amount present. R indicates resistance, although not quantified.
[f]Resistance to trypsin at pH 6.5 was determined by densitometric scanning of fluorograms and the amount of glycoprotein that is resistant to digestion by trypsin was taken as a percentage of that present in the non-trypsin treated sample.
[g]Indicates that the mutant glycoprotein is fusion defective over the pH range of 4.8 to 6.3.

3.6 Transport of G proteins

G protein is synthesized, folded, and oligomerized in the endoplasmic reticulum (Kreis and Lodish, 1986). Two N-linked oligosaccharides are co-translationally added to the newly synthesized protein and later modified in the trans-Golgi complex. (Doms et al., 1993). In order to examine transport out of the endoplasmic reticulum and to the Golgi apparatus, the susceptibility of mutant proteins to endoglycosidase H (Kornfeld and Kornfeld, 1985) was examined. The enzyme cleaves N-linked oligosaccharides when modified with high mannose sugars (Robbins et al., 1984), such that glycoproteins present in the endoplasmic reticulum are susceptible to enzymatic cleavage but not those that have been transported to the golgi complex. G protein is transported out of the endoplasmic reticulum with a t½ of 20 minutes (Balch et al., 1986; Kreis and Lodish, 1986; Doms et al., 1987, 1993). Wild-type and mutant G glycoproteins, were therefore tested for susceptibility to endoglycosidase H (Endo H) digestion at 0 and 60 minutes following radioactive protein labelling. COS-1 cells were pulsed with [^{35}S]methionine and chased with cold methionine supplemented media for a period of either 0 or 60 minutes. The lysates were immunoprecipitated, subjected to digestion by Endo H, and analyzed by SDS-polyacrylamide gel electrophoresis. The resultant autoradiogram was scanned with a densitometer and the percent resistance to enzymatic digestion, at 60 minutes of chase, was calculated as a function of the total protein in the treated sample.

Fig. 13 shows the EndoH susceptibility of wild-type and mutants G395E, G404K, D409A, and A418K. All mutants, similar to the wild-type G protein, were susceptible to enzymatic digestion at 0 minutes. Protein bands in treated samples migrate faster than those

of untreated samples due to the loss of sugar moieties. This indicates glycosylation with N-linked oligosaccharides. Complete resistance to the enzyme at 60 minutes of chase indicates transport out of the endoplasmic reticulum and to the medial Golgi compartment, as is the case with the wild-type G protein. At 60 min., both the untreated and treated samples show the same mobility indicating that wild-type G protein was transported out of the endoplasmic reticulum. Densitometric analysis of autoradiograms indicated that G395E was 100% resistant to Endo H digestion, indicating that the mutant glycoprotein was fully transported out of the endoplasmic reticulum by the 60 minute time point. Mutants G404K, D409A, A418K, however, were 70%, 82%, 40% respectively resistant to digestion. Thus, these mutants, are slower in their transport rate, possibly due to either misfolding or incorrect oligomerization. Although mutant A418K was not tested for susceptibility to Endo H at the 0 minute time point, it is assumed that the sugars are digested as they have not yet been modified by Golgi enzymes. A418K is 60% sensitive to Endo H digestion at 60 min. of chase, indicating a slow rate of transport, and thereby justifying the lack of cell surface expression by indirect immunofluorescence.

Double mutants of the H2-H10/A4 regions, namely F125Y D411N, P126L D411N, G131A G395E, G131A G404A, G131A D411N, D137N G404A, and D127N D411N, were also subjected to digestion by endoglycosidase H at 0 and 60 minutes of chase. Autoradiograms are shown in Fig. 14. As with the H10/A4 mutants, the double mutants are also completely susceptible to digestion at the 0 minute time point, indicating N-linked glycosylation. Following 60 min. of chase, mutants G131A G395E, G131A D411N, D137N G404A, and the fusion defective D137N D411N mutants were all 100% resistant to EndoH

digestion, indicating transport to the Golgi complex. Mutants F125Y D411N, P126L D411N, and G131A G404A, are 65%, 80%, and 92% resistant to digestion at the 60 minute time point, respectively. Mutant G131A G404A is only slightly transported at a slower rate than wild-type. Mutants F125Y D411N and P126L D411N, are both extremely compromised in their ability to induce COS-1 polykaryon formation, and are both expressed at the cell surface in reduced amounts by indirect immunofluorescence and iodination assays. An increase in susceptibility to endoglycosidase H digestion may be indicative of conformational alterations in protein structure preventing transport to the cell surface.

Fig. 13. Acquisition of Endoglycosidase H resistance of wild-type and H10/A4 mutant proteins. COS cells transfected with the indicated plasmid were labelled with [^{35}S]methionine for 15 minutes and chased with complete media supplemented with 2.5mM cold methionine for (A) 0 minutes and (B) 60 minutes prior to lysis. Cells were immunoprecipitated with anti-G antibody and one half was treated with Endo H (+) and the other half was not (-). Samples were analyzed by SDS-PAGE and the extent of Endo H resistance determined by densitometric scanning of the fluorograms. The percent resistance to Endo H at 60 minutes of chase was calculated as a function of the total protein in the enzymatically treated sample.

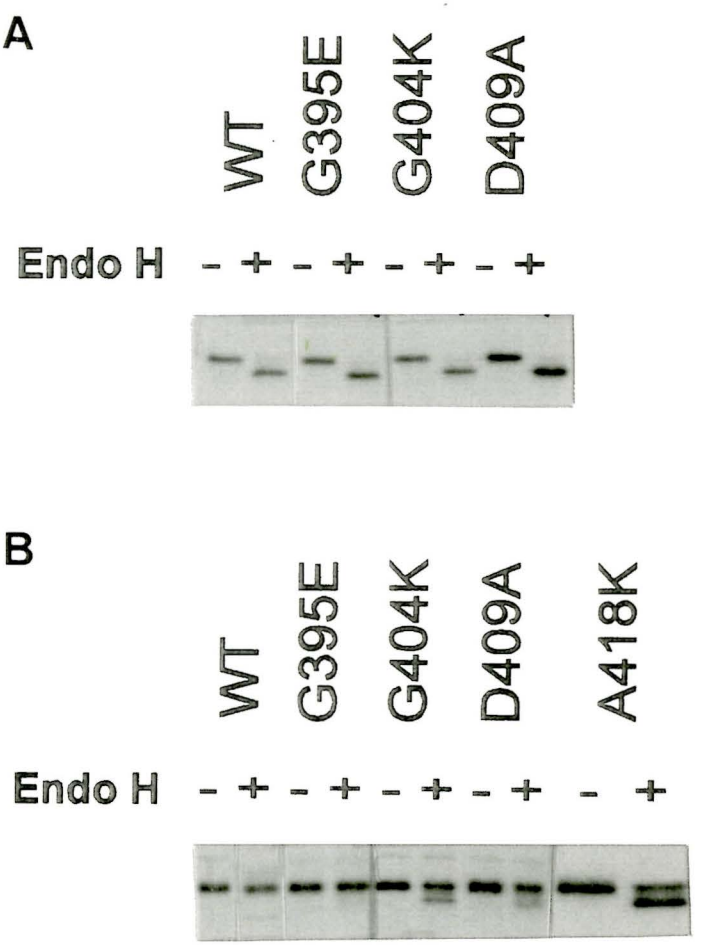
A
WT
G395E
G404K
D409A
Endo H - + - + - + - +
B
WT
G395E
G404K
D409A
A418K
Endo H - + - + - + - + - +

Fig. 14. Acquisition of Endoglycosidase H resistance of wild-type and H2-H10/A4 mutant proteins. COS cells transfected with the indicated plasmid were labelled with [^{35}S]methionine for 15 minutes and chased with complete media supplemented with 2.5mM cold methionine for (A) 0 minutes and (B) 60 minutes prior to lysis. Cells were immunoprecipitated with anti-G antibody and one half was treated with Endo H (+) and the other half was not (-). Samples were analyzed by SDS-PAGE and the extent of Endo H resistance determined by densitometric scanning of the fluorograms. The percent resistance to Endo H at 60 minutes of chase was calculated as a function of the total protein in the enzymatically treated sample.

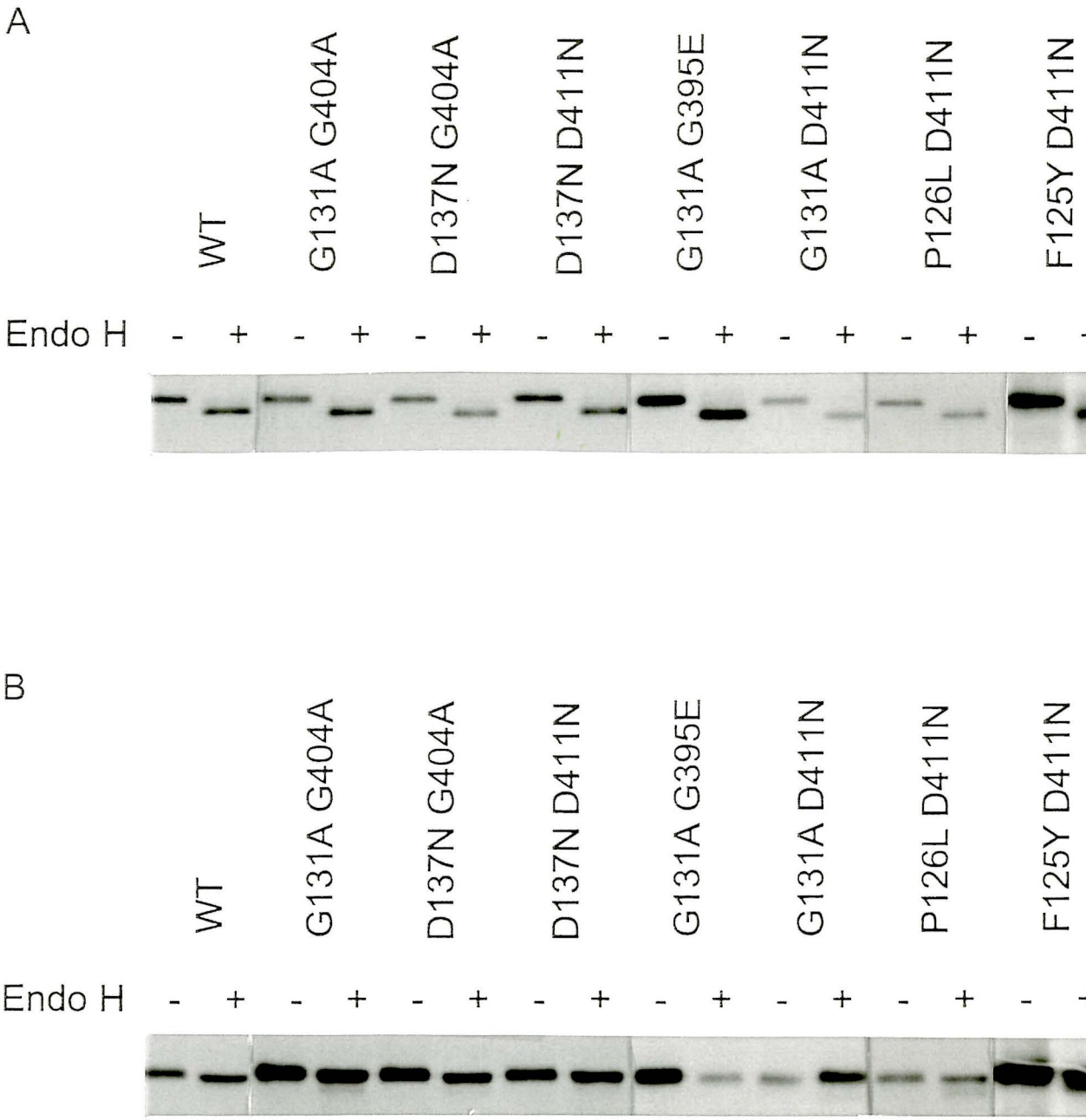
A
Endo H
- + - + - + - + - + - + - + - +
WT
G131A G404A
D137N G404A
D137N D411N
G131A G395E
G131A D411N
P126L D411N
F125Y D411N
B
Endo H
- + - + - + - + - + - + - + - +
WT
G131A G404A
D137N G404A
D137N D411N
G131A G395E
G131A D411N
P126L D411N
F125Y D411N

3.7 Oligomerization Into Trimers

Oligomerization of G protein takes place in the rough endoplasmic reticulum, after which the protein is transported to the cell surface in the form of a trimer (Kreis and Lodish, 1986; Doms et al., 1987, 1993; Dubovi and Wagner, 1990). To determine if the defects in fusion were due to improper oligomerization, G proteins were subjected to sedimentation in a 5%-20% sucrose gradient. As well, G proteins sediment as trimers only under a low-pH environment, and as monomers when exposed to neutral pH (refer to the wild-type control in Figs. 15 and 16). There exists, therefore, a correlation between the oligomeric form rendered under the experimental conditions, and those of G protein fusion (Fredericksen and Whitt, 1995). This may be indicative of a conformational change that generates a more stable G trimer under a pH of 5.5. The assay has been previously used to test trimer formation in original VSV G studies and by mutants and chimera of the glycoprotein (Shokralla et al., 1998; Odell et al., 1997; Fredericksen and Whitt, 1995; Zhang and Ghosh, 1994; Li et al., 1993; Whitt et al., 1990; Crise et al., 1989; Guan et al., 1988; Doms et al., 1988, 1987).

COS-1 cells transfected with the proper wild-type or mutant G protein expressing plasmid were pulsed with [^{35}S]methionine and chased with growth media supplemented with cold methionine for 90 minutes. Cells were lysed with 4X MNT lysis buffer containing 1% Triton X-100 at either pH 5.5. Clarified lysates were loaded onto a 5%-20% sucrose gradient of either pH 5.5 or 7.4 and sedimented by centrifugation. The gradient was fractionated into 18 fractions from the bottom, such that the first fraction is the densest among all fractions. Fractions were immunoprecipitated with rabbit polyclonal anti-G antibody and analysed by SDS-polyacrylamide gel electrophoresis. A single gradient was used to analyze the bovine

serum albumin (BSA) and aldolase markers. Aldolase sedimented in fraction 9, while BSA sedimented in fraction 13.

As can be seen from Figs. 15 and 16, the wild-type protein sediments in the region of 4S as a monomer at pH 7.4 in fractions 13-17. At the pH of 5.5, wild-type G sediments in the region of 8S as a trimer in fractions 9-11. This is in accordance with previously published results (Zhang and Ghosh, 1994; Li et al., 1993; Shokralla et al., 1998). The single H10/A4 mutants G395E, G404K, D409A, and A418K also sediment in fractions 9-11. A small portion of A418K protein is also present in the monomeric fraction 13. Double mutants F125Y D411N, P126L D411N, G131A G395E, G131A G404A, G131A D411N, D137N G404A, D137N D411N also sediment in fractions 9-11 at pH 5.5, indicating similar oligomerization properties as the wild-type G protein. Thus, the observed differences in fusogenic activities of the double mutants are not due to defects in their oligomerization.

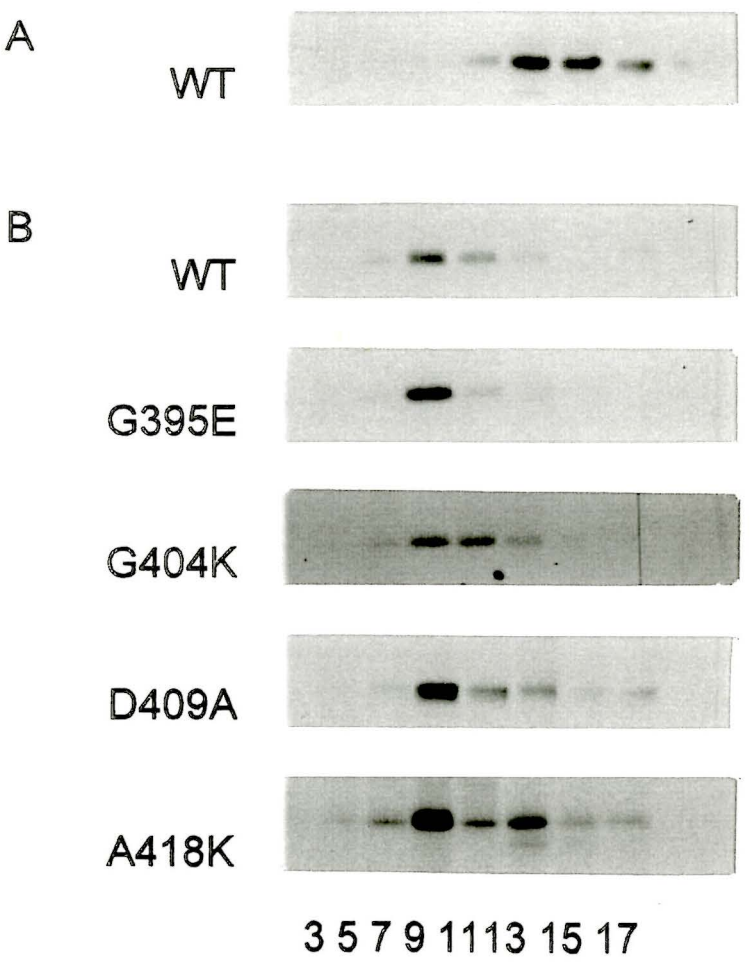
A
WT
B
WT
G395E
G404K
D409A
A418K
3 5 7 9 1113 15 17

Fig. 16. Oligomer formation of wild-type and H2-H10/A4 double mutant G proteins. COS cells transfected with the indicated plasmid were labelled with [^{35}S]methionine for 30 minutes and chased with complete media supplemented with 2.5mM methionine for 90 minutes. Cells were lysed in 4X MNT buffer containing 1% Triton X-100 at either pH 7.4 (A) or 5.5 (B). Clarified lysates were loaded onto a 5%-20% sucrose gradient of either pH 7.4 or 5.5. Eighteen fractions were collected from the bottom. Odd fractions were immunoprecipitated with anti-G antibody and analyzed by SDS-PAGE. The bottom fraction is to the left. Sedimentation markers aldolase (8S) and bovine serum albumin (4S) sedimented in fractions 9 and 13, respectively.

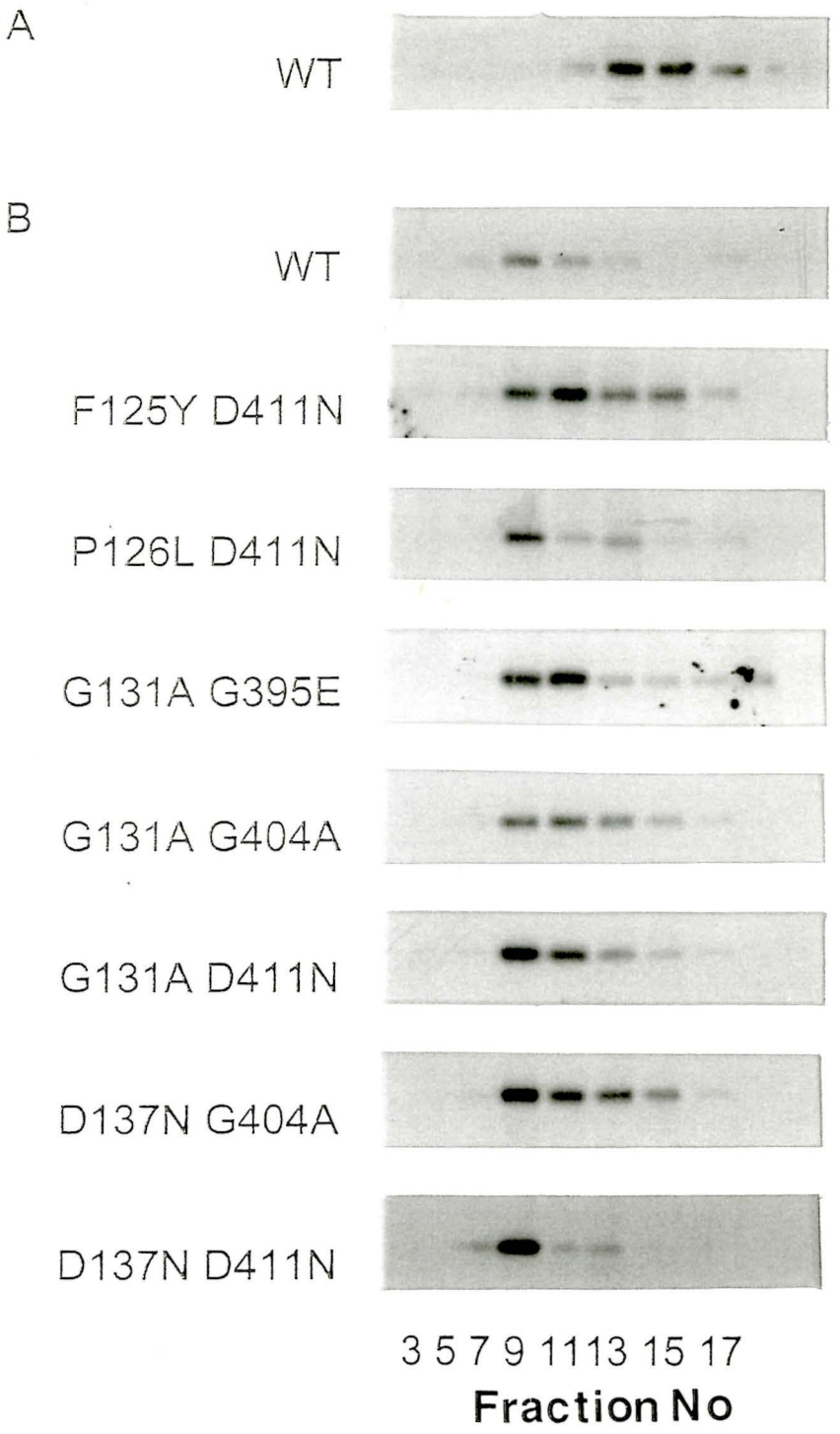
A
WT
B
WT
F125Y D411N
P126L D411N
G131A G395E
G131A G404A
G131A D411N
D137N G404A
D137N D411N
3 5 7 9 1113 15 17
Fraction No

3.8 pH Dependent Resistance to Trypsin

Viruses that mediate fusion at a low pH undergo conformational changes from the native state present at neutral pH to a fusion active one at low pH (Bullough et al., 1994; Hernandez et al., 1996; Carr and Kim, 1993; Crimmins et al., 1983; Gaudin et al., 1995; Hughson, 1995; White, 1990; Wiley and Skehel, 1987). The transition from one state to the next has been previously detected using a variety of techniques including sensitivity to tryptic digestion of influenza HA and rabies G (Doms et al., 1985; Skehel et al., 1995; Wharton et al., 1988; Wiley and Skehel, 1987; Gaudin et al., 1993, 1995, 1995a) where the spike proteins had become increasingly sensitive to proteolysis with increasing acidity. Recently, Fredericksen and Whitt (1995) developed a trypsinization assay for detection the of conformational changes in VSV glycoprotein G following exposure to low pH. The results are similar to those of Kielian and Helenius (1985) using Semliki Forest virus glycoprotein E1 in that both proteins become increasingly resistant to digestion by trypsin with decreasing pH.

COS-1 cells were transfected with wild-type or mutant proteins, pulsed with [^{35}S] methionine and chased with complete media supplemented with cold methionine. Cells were lysed with 2X MNT of pH 7.4, 6.5, 6.1, or 5.6. Two aliquotes of equal volume, from each clarified sample, were incubated at 37°C in the presence or absence of TPCK-trypsin. A control sample of pH 5.6 included 0.3% SDS and trypsin to ensure complete susceptibility to digestion under denaturing conditions. Glycoproteins were isolated by immuno-precipitation with polyclonal anti-G antibody and analyzed by SDS-polyacrylamide gel electrophoresis. Fluorograms, presented in Figs. 17 and 19, were subjected to densitometry

and the percent resistance to trypsinization as a function of pH was determined (Figs. 18 and 20).

Wild-type G protein (Figs. 17 and 19) is most sensitive to trypsin at the pH of 7.4 and approximately 90% resistant to digestion at the pH of 6.5 and below. As well, the protein is completely sensitive at the pH of 5.6 with added sodium dodecyl sulfate, indicating that the loss of susceptibility is not due to a reduction in trypsin activity at acidic pH. All single mutants of the H10/A4 region (Shokralla et al., 1998), namely G395A, G395E, G404A, G404K, G406A, D409A, D409N and D411N whose fusogenic, oligomeric, transport, and cell surface functions are also summarized in Table II, were tested for conformational alterations. Glycoproteins G395A and G395E were comparable to wild-type in their tryptic profile (Fig. 18). At the pH of 6.5, the mutants differ in their susceptibility to digestion. Glycoproteins G404A and G406A were 55% resistant, whereas D409A, D409N, and D411N were approximately 40% resistant. The most dramatic alteration from wild-type is that of the fusion deficient mutant G404K with complete susceptibility to digestion at the pH of 6.5. All mutants gained increasing resistance to tryptic digestion with decreasing pH, as did the wild-type G protein. Deviations from wild-type, therefore indicate differences in conformation between mutant and wild-type G proteins.

Analysis of the double mutants by tryptic digestion (Figs. 19 and 20), showed that only mutant F125Y D411N is completely susceptible to digestion at the pH of 6.5. As has been shown, this protein is expressed at the cell surface at levels (21%) lower than that of the wild-type G, and is only 65% resistant to digestion by endoglycosidase H at 60 minutes of chase. Thus, the conformational change detected by trypsinization may be accounted for in

terms of improper folding that retards the majority of the protein from reaching the plasma membrane. Similar to the G395E mutant, glycoprotein G131A G395E also displays a digestion profile that is similar to wild-type with 83% resistance to proteolytic digestion at pH 6.5. This mutant also shows a fusion profile which is similar to the G395E mutant. All other mutants are compromised in their susceptibility to trypsin. Mutants G131A D411N, P126L D411N, D137N D411N are approximately 50% resistant, and G131A G404A and D137N G404A are near 35% resistant to trypsin at the pH of 6.5. All double mutants become increasingly resistant to trypsin with decreasing pH, as does the wild-type. That the mutants differ in their susceptibility to trypsin suggests that they may have altered conformations as compared to the wild-type G protein. This is in accord with the observed alterations in fusion profiles.

Fig. 17. Tryptic digestion of wild-type and H10/A4 mutant G proteins. COS cells transfected with the indicated plasmid were pulsed with [^{35}S]methionine for a period of 30 minutes and chased with complete media supplemented with 2.5mM methionine for 60 minutes. Cells were lysed with 2X MNT in the presence of 1% Triton X-100 at the indicated pH of 7.4, 6.5, 6.1, or 5.6. Lysates were incubated in the presence (+) or absence (-) of 10μg TPCK-trypsin at 37°C for 30 minutes. To the control sample (C) of pH 5.6, 0.3% SDS in addition to trypsin was also included. Proteins were immunoprecipitated with anti-G antibody and analyzed by SDS-polyacrylamide gel electrophoresis.

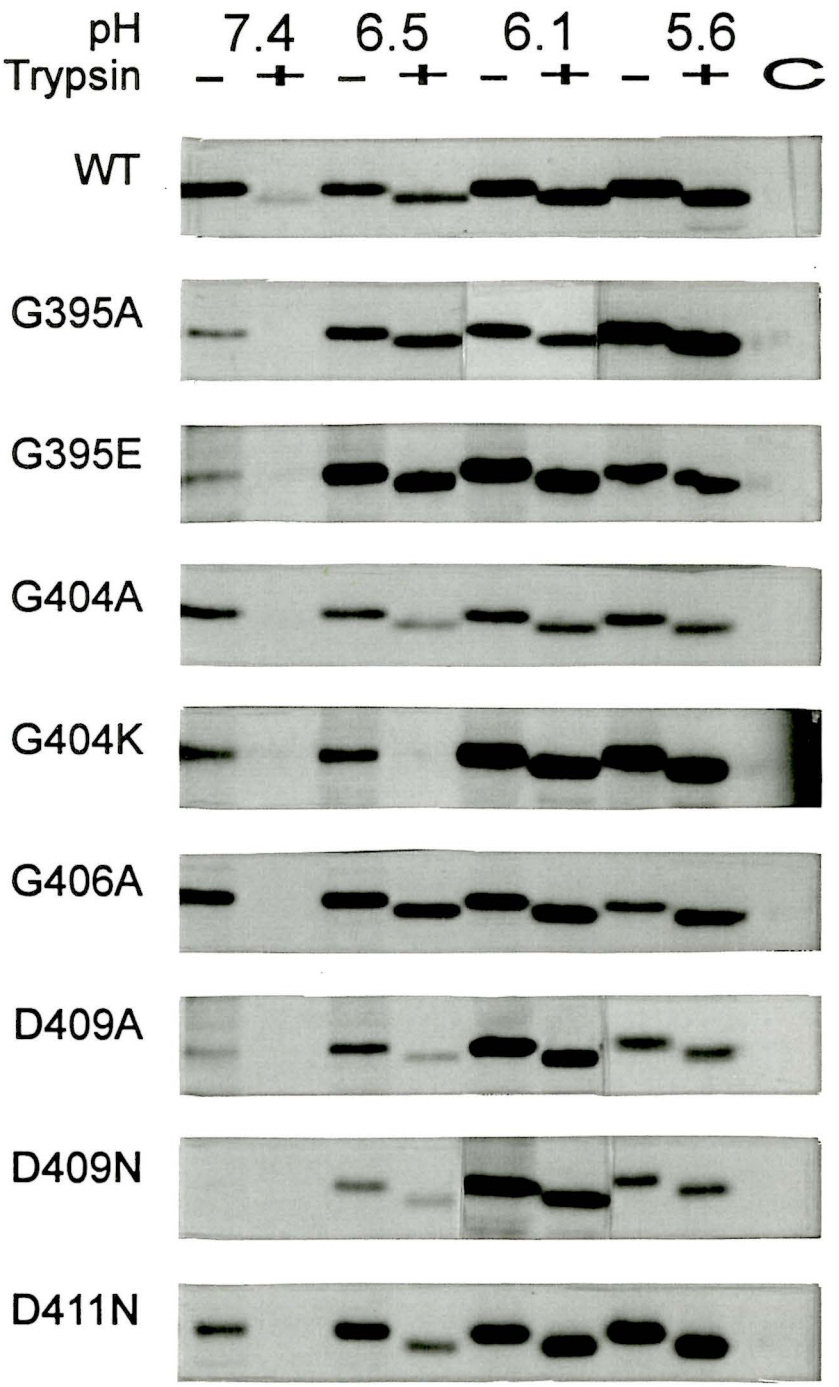
pH
7.4
6.5
6.1
5.6
Trypsin
– + – + – + – +
C
WT
G395A
G395E
G404A
G404K
G406A
D409A
D409N
D411N

Fig. 18. pH dependent resistance of wild-type and H10/A4 mutant proteins. Samples were prepared as in the legends to Figs. 17 and 19. Densitometric scanning of fluorograms was utilized to quantitate the percent trypsin resistance at pHs 7.4, 6.5, 6.1, and 5.6, with the band intensity of treated samples taken as a percentage of untreated sample intensity. Data plotted is the average of two independent experiments at each pH point.

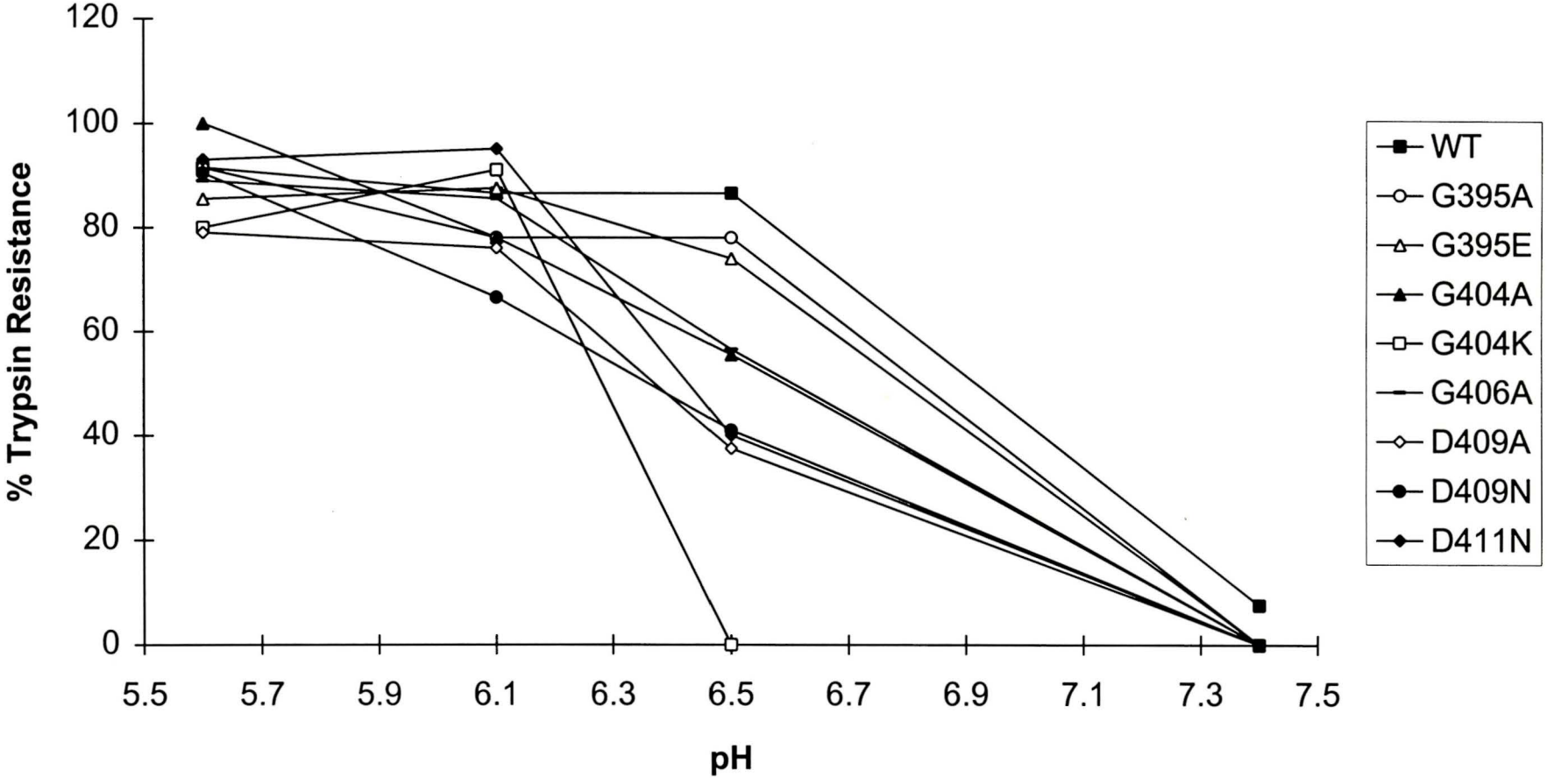
120
100
80
60
40
20
0
% Trypsin Resistance
5.5
5.7
5.9
6.1
6.3
6.5
6.7
6.9
7.1
7.3
7.5
pH
WT
G395A
G395E
G404A
G404K
G406A
D409A
D409N
D411N

Table II. Summary of the Properties of Site-Directed Mutants in theH10/A4 Region of VSV Glycoprotein G

Glycoprotein	Cell surface expression		pH threshold of fusion[c]	pH optimum of fusion[d]	Cell fusion (%)[b]	Trimer formation	Endo H resistance (%)[e]	Trypsin resistance (%)[f]
	Immuno-fluorescence	Iodination (%)[a]						
WT	+	100	6.3	5.6	100	+	100	87
G395A	+	136	6.3	5.45	77	+	100	80
G395E	+	98	5.8	5.0	18	+	100	75
P399L	-							
G404A	+	158	6.0	5.6	45	+	100	55
G404K	+	103	—	—	—	+	70	0
G406A	+	133	5.8	5.2	16	+	100	55
D409A	+	177	—	—	—	+	82	37
D409N	+	230	5.8	5.0	29	+	100	40
D411N	+	121	6.0	5.45	49	+	89	40
A418K	-					+	40	

[a]For quantitation of cell surface expression, COS cells transfected with wild type or mutant G plasmids were iodinated with ^{125}I in a lactoperoxidase-catalysed iodination reaction at 24 hours posttransfection. Results shown are the averages of two separate experiments.
[b]Cell-cell fusion at the pH optimum was determined by exposing expressed wild type or mutant proteins in COS cells, at 24 h post-transfection, to fusion media of varying acidity in the pH range of 4.8-6.3. The number of polykaryons produced by wild type G protein at pH 5.6 was taken as the standard measure of 100%.
[c,d]The pH optima and thresholds of cell-cell fusion were determined by counting polykaryons over a pH range of 4.8-6.3.
[e]Resistance to endoglycosidase H digestion, at 60 min of chase, was quantitated by densitometric scanning of fluorograms and the amount of glycoprotein resistant to digestion was taken as a percentage of the total amount present.
[f]Resistance to trypsin at pH 6.5 was determined by densitometric scanning of fluorograms and the amount of glycoprotein that is resistant to digestion by trypsin was taken as a percentage of that present in the non-trypsin treated sample.
[g]Indicates that the mutant glycoprotein is fusion defective over the pH range of 4.8 to 6.3.

Fig. 19. Tryptic digestion of wild-type and the double mutant G proteins. COS cells transfected with the indicated plasmid were pulsed with [^{35}S]methionine for a period of 30 minutes and chased with complete media supplemented with 2.5mM methionine for 60 minutes. Cells were lysed with 2X MNT in the presence of 1% Triton X-100 and of either pH 7.4, 6.5, 6.1, or 5.6. Lysates were incubated in the presence (+) or absence (-) of 10μg TPCK-trypsin at 37°C for 30 minutes. To the control sample (C) of pH 5.6, 0.3% SDS in addition to trypsin was also included. Proteins were immunoprecipitated with anti-G antibody and analyzed by SDS-polyacrylamide gel electrophoresis.

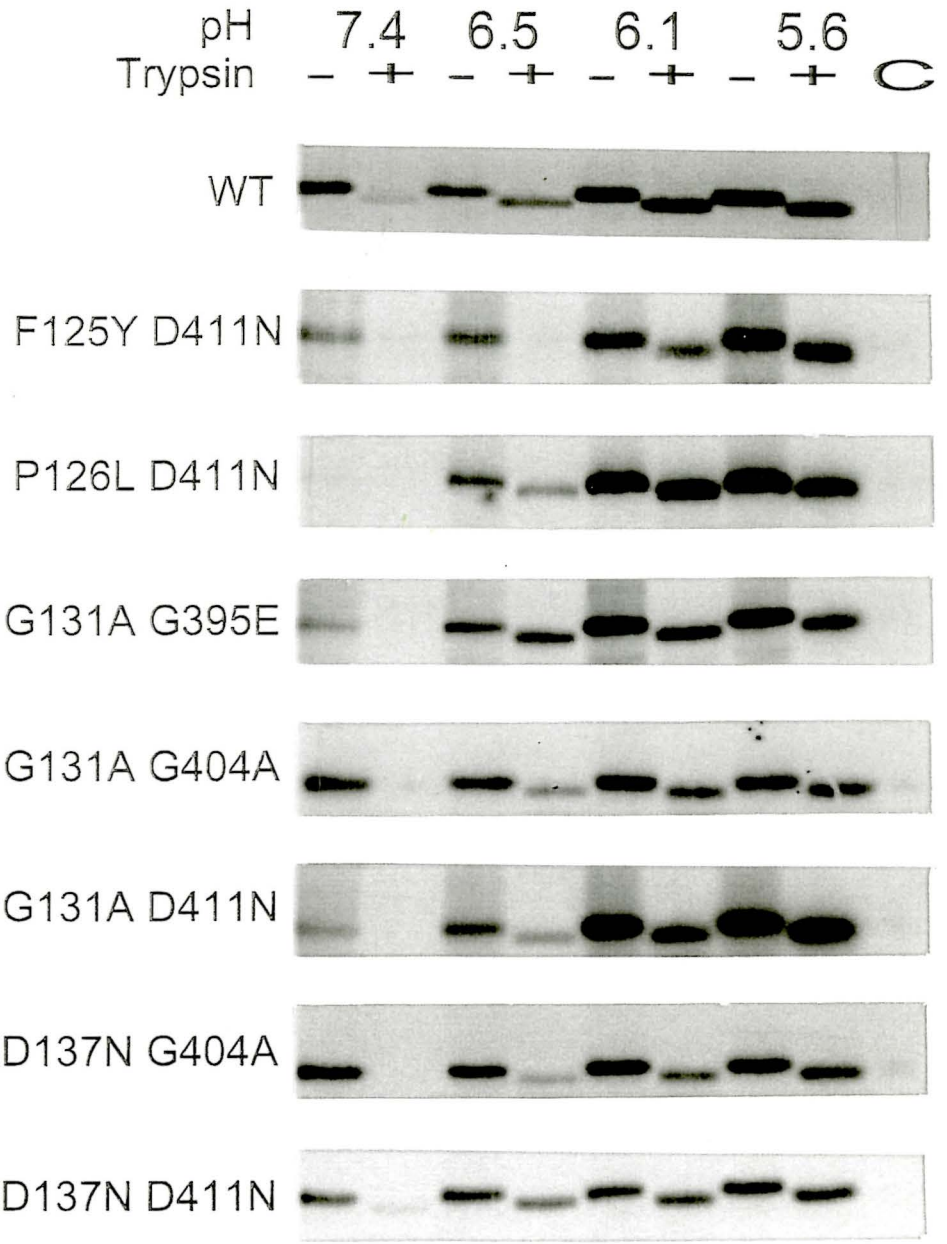
pH
7.4
6.5
6.1
5.6
Trypsin
– + – + – + – +
C
WT
F125Y D411N
P126L D411N
G131A G395E
G131A G404A
G131A D411N
D137N G404A
D137N D411N

Fig. 20. pH dependent resistance of wild-type and double mutant proteins. Samples were prepared as in the legends to Figs. 17 and 19. Densitometric scanning of fluorograms was utilized to quantitate the percent trypsin resistance at pHs 7.4, 6.5, 6.1, and 5.6, with the band intensity of treated samples taken as a percentage of untreated sample intensity. Data plotted is the average of two independent experiments at each pH point.

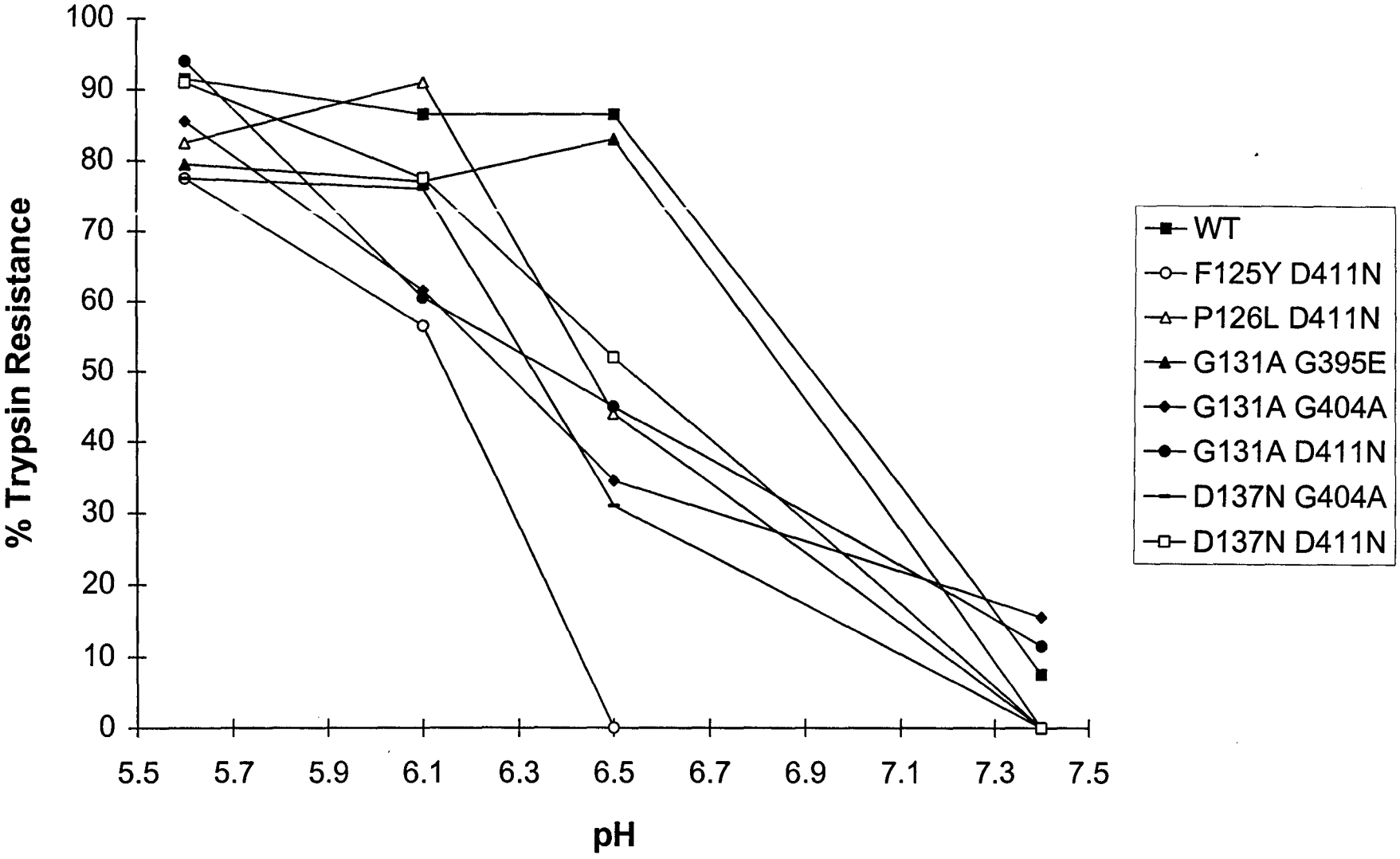
% Trypsin Resistance
100
90
80
70
60
50
40
30
20
10
0
5.5
5.7
5.9
6.1
6.3
6.5
6.7
6.9
7.1
7.3
7.5
pH
WT
F125Y D411N
P126L D411N
G131A G395E
G131A G404A
G131A D411N
D137N G404A
D137N D411N

4. DISCUSSION

As opposed to glycoproteins of other viruses, little is known about the fusion mechanism of vesicular stomatitis virus G protein. Mutagenic, hydrophobic photolabelling, and peptide inhibition studies of influenza virus and HIV have identified multiple domains in their spike proteins having either direct or indirect effects on fusion (reviewed in Hernandez et al., 1996; Durell et al., 1997). These include the fusion peptide, amino and carboxy-terminal heptad repeats, and a loop region for influenza virus. X-ray crystallography has resolved the fusion-active conformations of human immunodeficiency, Moloney murine leukemia, and influenza viruses (Bullough et al., 1994; Weissenhorn et al., 1997; Chan et al., 1997; Fass et al., 1996). The crystal structure of the inactive conformation of influenza virus has also been solved (Wilson et al., 1981). The structure of VSV G is not yet available, and the only region proven to affect fusion in the extracellular domain of G is the fusion peptide (residues 118-136). Linker insertion mutagenesis at various locations in G was first utilized to identify regions in the protein that may modulate fusion without abolishing transport or oligomerization of the protein (Li et al., 1993). The region surrounding the H2 insertion mutant was later postulated by site directed mutagenesis to be the fusion peptide (Zhang and Ghosh, 1994; Fredericksen and Whitt, 1995, 1996), and found to interact with lipid bilayers by hydrophobic photoreactive crosslinking reagents (Durrer et al., 1995). The conserved region surrounding the H10 and A4 insertion mutants (at positions 410 and 415) was not labelled, and therefore has an indirect effect on membrane fusion.

This work, along with previous analysis, has resulted in the identification of residues 395 to 424 (H10/A4 region) as a region modulating the fusogenic function of VSV G. The region is conserved among vesiculoviruses (Fig. 2A), and was thus speculated to be of functional importance to G protein. Previous site directed mutagenesis in this region, namely mutants G404A, G406A, D409N, and D411N, caused a reduction in the fusogenic capacity of G protein without affecting transport, oligomerization, or cell surface expression (Table II). Conservative substitution of G395 to alanine did not severely affect low-pH induced fusion or conformation of G protein (Shokralla et al., 1998). Mutants G404A, D409N, and D411N required an increase in acidity, relative to wild-type, for syncytia formation. The pH optima of fusion for mutants G406A and D409N were also more acidic as compared to wild-type. More drastic substitutions of residues G404 and D409 to lysine and alanine, respectively, completely abolished fusion. Mutation of G395 to glutamate also severely altered the fusion profile. The pH threshold and optimum of fusion were shifted to pH 5.8 and 5.0, respectively, and a maximum fusion of only 18% wild-type was achieved. Alterations from wild-type fusion were not due to lack or reduction in cell surface expression or to oligomerization deficiencies. Mutants P399L and A418K were not detected on the cell surface by immunofluorescence. Mutant A418K was also retarded in transport out of the endoplasmic reticulum. A small fraction of the protein was also observed to be monomeric by sucrose density centrifugation analysis. As with A418K, the conformation of P399L may be also drastically altered such that the proteins are no longer able to transport to the cell surface but are instead retained within the endoplasmic reticulum. All residues examined in this study are conserved within the vesiculoviruses (Fig. 2). In addition, P399 is invariant

within all ten rhabdoviruses. Residues 340 through 418 are predicted to form a putative amphipathic alpha helix for all ten rhabdoviruses (Gaudin et al., 1996).

Proteolytic sensitivity has been previously used to examine acid-induced conformational changes of influenza HA, rabies G, and VSV G (Doms et al., 1985; Skehel et al., 1995; Wharton et al., 1988; Wiley and Skehel, 1987; Gaudin et al., 1993, 1995, 1995a; Fredericksen and Whitt, 1996). All mutants, with the exceptions of G395A and G395E, were more susceptible than the wild-type to tryptic digestion at the pH of 6.5. The fusion defective mutant G404K was completely sensitive, suggesting a dramatic conformational alteration from wild-type. Mutant D409A was also unable to mediate syncytia formation at the pH range of 6.3 to 4.8, and was only 37% resistant to trypsin at pH 6.5. The slower rate of transport of these mutants also suggests differences from wild-type conformation. Conversion of residues G404, G406, D409, and D411 to alanine, alanine, asparagine, and asparagine respectively, not only decreased fusion but also rendered the mutant glycoproteins approximately 45%-60% sensitive to trypsin. Mutants G395A and G395E were similar to wild-type with approximately 75%-90% resistance to trypsin at pH 6.5. Recently, using photosensitized labelling, it has been shown that interaction of the fusion peptide with lipid bilayers initially takes place at approximately pH 6.4 (Durrer et al., 1995; Pak et al., 1997). Thus, mutations in H10/A4 may affect pH-dependent conformational changes leading to fusion.

Rabies G has been shown to shift in equilibrium between the native, inactive, and

active forms (Gaudin et al., 1993, 1991). These are analogous to the tense, desensitized, and relaxed forms of VSV G. The native form is present at the cell surface at pHs above 7.0. Once the protein is exposed to acidic pH, a more hydrophobic "active" state develops and is thought to mediate fusion. Prolonged exposure of G protein to acidic pH results in inhibition of fusion and coincides with the appearance of lengthened inactive spikes. Monoclonal antibodies recognizing the inactive state of rabies virus G glycoprotein, were recently used to select mutants resistant to acid-induced neutralization (RAIN mutants) (Gaudin et al., 1996). Sequence alignment of VSV with rabies virus (Fig. 2A) shows that two of these mutants map to the H10/A4 region, and correspond to positions 417 and 422 of VSV G. The first is adjacent to the VSV G A4 linker insertion mutant, at amino acid position 415, and to the conformationally defective A418K mutant. RAIN mutants are delayed in attainment of the inactive conformation, and shift the equilibrium between the native and inactive states during prolonged acidic incubations toward the native state. Therefore this region has been postulated to be involved in control of the inactive conformation (Gaudin et al., 1996). In contrast to the H10/A4 mutants, the fusion properties of RAIN mutants are similar to wild-type. Mutants in the H10/A4 region, may stabilize the inactive (desensitized) conformation of VSV G, thereby compromising the ability of G protein to acquire its native (tense) form at the cell surface. The inactive state is thought to prevent premature fusion of G during transport through acidic Golgi vesicles (Gaudin et al., 1995).

Double mutants of the H2 and H10/A4 regions were constructed to examine if effects exerted by both mutants are additive in their outcome toward fusion, or if one region

dominates over the other. Such studies have been previously performed in the examination of enzymatic functions and influenza hemagglutinin (Wells, 1990; Mildvan et al., 1992; Steinhauer et al., 1996). The pH threshold of mutant D137N G404A exceeds the sum of its single mutant counterparts, suggesting a requirement for an increase in acidity to overcome barriers preventing lipid mixing. Conformationally the protein may be more compromised than either of its constituent mutant glycoproteins. This is even more apparent for mutants F125Y D411N, P126L D411N, and D137N D411N. Mutant D137N D411N is completely void of polykaryon formation capabilities over the entire pH range of 4.8 to 6.3, even at approximately 200% wild-type levels of cell surface expression. Each of its component mutants could only induce maximal levels of fusion near to 50% of that of wild-type G, with the fusion profiles exhibiting shifts in both the pH optima and thresholds of fusion. The mutant is also altered in its conformation with approximately 50% resistance to trypsin and 80% resistance to endo H at 60 minutes of chase. Mutant P126L D411N is shifted in its pH threshold and pH optimum of fusion to values beyond those of both the P126L and D411N mutants. The pHs required to induce and to reach maximal fusion are greater than the sum of those belonging to the single mutants. F125Y D411N, although capable of syncytia formation, is 65% resistant to EndoH digestion, is expressed at the cell surface at 21% wild-type levels, and is completely sensitive to trypsin at pH 6.5. The protein is structurally altered on a global level that prevents its transport to the cell surface and renders it more susceptible to proteolytic digestion than the single mutant D411N. Mutant F125Y was not tested for resistance to trypsin. These double mutants appear to act in an additive manner. The pH threshold of fusion for G131A G404A is that of wild-type, and is more alkaline than either

G131A or G404A. Mutations in the H2 and H10/A4 regions, therefore, do not act at a local level but induce structural perturbations that affect one another.

Whereas effects on the pH limits for polykaryon formation were mostly dependent on both the H2 and H10/A4 mutants, the impact on the optimum pH of fusion was mostly governed by the parental H2 mutant. Glycoproteins G131A G404A, G131A D411N, and D137N G404A all result in fusion profiles that peak at the pH of 5.0, similar to the G131A and D137N H2 mutants. Tryptic digestion patterns of these mutants display an increase in susceptibility to digestion ranging from approximately 50% to 65% at the pH of 6.5. As well, mutant G131A D411N exhibits a profile more in common with its H2 counterpart than its H10/A4 single mutant, since its pH optimum and thresholds are identical to the G131A protein. Studies with influenza hemagglutinin have also shown that mutations in regions near to the fusion peptide override those toward the C-terminal end (Steinhauer et al., 1996). Only G131A G395E exhibited an H10/A4 dominant profile. It should be noted, however, that the pH optimum of fusion exhibited by the double mutant not only correlates to G395E, but also to G131A. G395E is located outside the alpha helical structure of H10/A and therefore may not cause alterations within the protein that would affect exposure of the fusion peptide as do residues found within the alpha helix.

Glycines have been proven important in the fusion peptides of influenza, HIV, SFV, and VSV, since mutations in these residues drastically affect fusion and cause shifts in pH limits and optima of fusion. Although residues in the fusion peptides of influenza, HIV, and

SIV are mostly variable, amino acid sequence alignment shows conservation of glycines (Durell et al., 1997). The fusion peptides of HIV and influenza are found at amino termini of transmembrane bound subunits. The H2 region of vesicular stomatitis virus is an internal fusion peptide. A comparison of the sequence of H2 with the Semliki Forest virus (SFV) internal fusion peptide shows a similarity in terms of the spatial locations of glycines, prolines, and aspartic acids, including effects of G131A and D137N (Zhang and Ghosh, 1994). Mutagenesis of these residues similarly affected the fusogenic properties of VSV G and SFV E1 proteins causing shifts in the pH thresholds and optima of fusion to more acidic values (Zhang and Ghosh, 1994; Levy-Mintz and Kielian, 1991). Mutagenesis of SFV E1 G91, which aligns with VSV G G131, to alanine resulted in the reduction of fusion and shift of the threshold of fusion to more acidic pH values (Levy-Mintz and Kielian, 1991). Mutagenesis of the same residue to aspartate completely blocked cell-cell fusion (Levy-Mintz and Kielian, 1991). The SFV glycoprotein consists of three non-covalently attached subunits (E1, E2, E3). E1 and E2 are transmembrane bound with the E1 subunit containing the fusion peptide. Once exposed to a low-pH environment, interactions between the E1 and E2 heterodimer weaken and a fusion active E1 homotrimer is instead formed (Fuller et al., 1995; Bron et al., 1993). Whereas mutant G91A could form homotrimers, albeit at a lower efficiency than wild-type, mutant G91D was completely incapable of homotrimer formation (Kielian et al., 1996). Similar to VSV G, E1 proteins become increasingly resistant to tryptic digestion with decreasing pH. The G91A mutant showed a reduction and shift in resistance to trypsin, whereas G91D was almost completely susceptible to trypsin (Kielian et al., 1996). This is also similar to the G404 residue of the H10/A4 region, since mutagenesis of this residue to

alanine results in a reduction in the extent of fusion, a shift in the pH threshold of fusion, and an increase in the susceptibility to tryptic digestion at the pH of 6.5. Replacement of glycine 404 with lysine resulted in the abolition of fusion and complete susceptibility to trypsin at pH 6.5. The flexible nature of glycines may be important in allowing maneuverability to fusion peptides as the entire protein undergoes conformational alterations from a native to an active form. It may also aid in structural transitions from the inactive to native form, presumably governed by the H10/A4 region. Shifts in the pH thresholds of double mutants to values more acidic than the those of their constituant single mutants, may correlate with the ability of the glycoproteins to make available the fusion peptide. Thus the double mutants would be more structurally compromised, than either of their component mutants, and would require greater acidity to induce the proper fusogenic conformation.

Although deviations from the wild-type conformation may account for the observed differences in fusion, substitution of residues within fusion peptides can also affect interactions with target bilayers and subsequent steps in pore formation. Mutation of G4 of influenza HA to glutamate resulted in a reduction of cell-cell fusion and shift in the pH threshold of fusion (Gething et al., 1986). Mutation of E11 to glycine also resulted in the reduction of cell-cell fusion. Both glycoproteins were capable of acid-induced conformational change, membrane binding and small pore formation, but were compromised at the level of pore enlargement (Gething et al., 1986; Schoch and Blumenthal, 1993). The amino terminus of the more fusogenic Sendai F1 G12A mutant was found to be more proximal to its target membrane than wild-type, suggesting a closer to parallel and more oblique angle of insertion

(Rapaport and Shai, 1994). In addition to conformational alterations within double mutant glycoproteins, these factors may also contribute to the observed shifts in pH optima.

Low-pH induced viral glycoproteins of influenza, alphaviruses, and rhabdoviruses contain acidic amino acids in their fusion peptides. Substitution of these residues with uncharged residues also resulted in shifts of pH thresholds and optima of cell-cell fusion (Zhang and Ghosh, 1994; Gething et al., 1986; Levy-Mintz and Kielian, 1991). Protonation of negatively charged residues at low-pH is presumed to account for greater membrane binding affinity and decrease in electrostatic repulsion of the fusion peptide with respect to a target membrane (Ohnishi, 1988). Shifts in the fusion profile of VSV G D137N, and double mutants containing the H2 mutant, may result from a decrease in hydrophobicity due to loss of protonation. Protonation of VSV G causes low-pH induced conformational changes of the entire glycoprotein (Puri et al., 1988; Clague et al., 1990; Pak et al., 1997). Thus, replacement of acidic residues with uncharged ones may result in loss of cooperative folding within the protein. The D112G mutant of influenza HA, located near the base of the HA2 central coiled coil, causes an upward shift in the threshold pH of fusion (Daniels et al., 1985). X-ray crystallization of the mutant revealed that hydrogen bonds previously stabilizing burial of the fusion peptide were lost upon replacement of aspartate with glycine (Weis et al., 1990). For VSV G, loss of protonable residues within the H10/A4 region may cause stabilization of the inactive conformation and thereby an increase in acidity to drive the protein into the native conformation.

Two regions of heptad repeats, corresponding to residues 134 to 161 and 328 to 369 of VSV G Indiana serotype, have recently been proposed in a number of rhabdoviruses (Coll, 1995a). These are situated after the fusion peptide and toward the carboxy terminus of the ectodomain and are reminiscent of the long and short heptad repeats of influenza, human immunodeficiency virus, moloney murine leukemia virus, and simian immunodeficiency virus (Carr and Kim, 1993; Chan et al., 1997; Lu et al., 1995; Weissenhorn et al., 1997; Blacklow et al., 1997). The second heptad repeat precedes the H10/A4 region. With the exception of influenza, the above-mentioned viruses undergo fusion with a target membrane under neutral pH conditions. Synthetic peptides corresponding to the heptad repeats of HIV-1 were shown independently to inhibit fusion, the carboxy-terminal heptad repeat being a more potent inhibitor (Lu et al., 1995). The inhibitory activity of C-terminal heptad repeat is, however, reduced when stoichiometric amounts of the N-terminal heptad repeat are added suggesting an association of the two repeats. Exposure of influenza hemagglutinin to low-pH induces a structural change in the loop region connecting the two heptad repeats, converting it to a coiled coil, and thrusting the fusion peptide away from its initial location presumably toward a target bilayer (Bullough et al., 1994; Carr and Kim, 1993). A structural rearrangement also takes place at the carboxylic heptad repeat that disrupts the coiled coil structure to form a connection joining the coiled coil to a short alpha helix (Bullough et al., 1994). The short alpha helices surround a trimeric central coiled coil in an antiparallel manner. The heptad repeats of human immunodeficiency and moloney murine leukemia viruses have also been shown to pack in an antiparallel manner with the amino terminal repeats forming a central coiled coil surrounded by carboxy-terminal helices (Chan et al., 1997; Weissenhorn et al.,

1997; Fass et al., 1996). Thus, the predicted amino and carboxy helical regions of vesicular stomatitis virus G protein may also interact in an anti-parallel orientation.

The H10/A4 region is able to modify fusion without insertion into the target bilayer (Durrer et al., 1995), as shown by reductions in the extent of fusion and shifts in the pH thresholds and optima of fusion. These mutants are also altered in their ability to undergo low-pH induced conformational changes as indicated by an increased susceptibility to tryptic digestion. The H10/A4 region may define a domain influencing the low-pH induced conformational changes of the vesicular stomatitis virus glycoprotein. Mutants of the fusion peptide are also capable of reductions in the extent of fusion and shifts in the pH threshold and optimum of wild-type G protein. In general, glycoproteins mutated in the H2 and H10/A4 region are more severely compromised in their fusogenic functions than the single mutants with alterations in protein conformation as detected by endoglycosidase H and protease digestions. Given the structural data of influenza HA, HIV-1 gp41, and MoMuLV TM and the possibility of a common fusion active conformation, it is not unlikely that the two regions may influence each other through alterations in protein structure.

5. REFERENCES

Atkinson, P., and Lee, J.T. (1984). Co-translational excision of alpha-glucose and alpha-mannose in nascent vesicular stomatitis virus G protein. *J. Cell Biol.* **98,** 2245-2249.

Balch, W.E., Elliott, M.M., and Keller, D.S. (1986). ATP-coupled transport of vesicular stomatitis virus G protein between the endoplasmic reticulum and the Golgi. *J. Biol. Chem.* **261,** 14681-14689.

Balch, W.E., McCaffery, J.M., Plutner, H., and Farquhar, M.G. (1994). Vesicular stomatitis virus glycoprotein is sorted and concentrated during export from the endoplasmic reticulum. *Cell,* **76,** 841-852.

Bhella, R.S., Nichol, S.T., Wanas, E., and Ghosh, H.P. (1998). Structure, expression, and phylogenetic analysis of the glycoprotein gene of Cocal virus. *Virus Res.* **54,** 197-205.

Birnboim, H.C., and J. Doly. (1979). A Rapid Alkaline Extraction Procedure for Screening Recombinant Plasmid DNA. *Nucleic Acids Res.* 7, 1513-1523.

Blacklow, S.C., Lu M., and Kim, P.S. (1995) A trimeric subdomain of the simian immunodeficiency virus envelope glycoprotein. *Biochemistry* **34,** 14955-14962.

Blumenthal, R., Bali-Puri, A., Walter, A., Corell, D., and Eidelman, O. (1987). pH dependent fusion of vesicular stomatitis virus with Vero cells. *J. Biol. Chem.* **262,**13614-13619.

Bosch, M.L., Earl, P. L., Fargnoli, K., Picciafuoco, S., Giombini, F., Wong-Staal, F., and Franchini, G. (1989). Identification of the fusion peptide of primate immunodeficiency viruses. *Science* **244,** 694-697.

Bousse, T., Takimoto, T., Gorman, W.L., Takahashi, T., and Portner, A. (1994). Regions on the hemagglutinin-neuraminidase proteins of human parainfluenza virus type-1 and Sendai virus important for membrane fusion. *Virol.* **204,** 506-514.

Brand, C.M., and Skehel, JJ. (1972). Crystalline antigen from influenza virus envelope. *Nature New Biol.***238,** 145-147.

Bron, R., Wahlberg, J.M., Garoff, H., and Wilschut, J. (1993). Membrane fusion of Semliki Forest virus in a model system: correlation between fusion kinetics and structural changes in the envelope glycoprotein. *EMBO J.* **12,** 693-701.

Brun, G., Bao X. K., and Prevec, L. (1995). The relationship of Piry virus to other vesiculoviruses: a re-evaluation based on the glycoprotein gene sequence. *Intervirology* 38, 274-282.

Bullough, P.A., Hughson, F. M., Skehel, J.J., Wiley, D.C. (1994). Structure of influenza hemagglutinin at the pH of membrane fusion. *Nature* **371,** 37-43.

Carr, C.M., and Kim, P.S. (1993). A spring-loaded mechanism for the conformational change of influenza hemagglutinin. *Cell* **73,** 823-832.

Carr, C.M., and Kim, P.S. (1994). Flu virus invasion: halfway there. *Science* **266,** 234-236.

Carter, P., Winter, G., Wilkinson, A.J., and Fersht, A.R. (1984). The use of double mutants to detect structural changes in the active site of the tyrosyl-tRNA synthetase (Bacillus stearothermophilus). *Cell* **38,** 835-840.

Chan, D.C., Fass, D., Berger, J.M., and Kim, P.S. (1997). Core structure of gp41 from the HIV envelope glycoprotein. *Cell* **89,** 263-273.

Chambers, P., Pringle, C.R., and Easton, A.J. (1990). Heptad repeat regions are located adjacent to hydrophobic regions in several types of virus fusion glycoproteins. *J. Gen. Virol.* **71,** 3075-3080.

Chamberlain, J.P. (1979). Fluorographic Detection of Radioactivity in Polyacrylamide Gels with the Water Soluble Fluor, Sodium Salicylate. *Anal. Biochem.* **98,** 132-135.

Chong, L.D., and Rose, J.K. (1993). Membrane association of functional vesicular stomatitis virus matrix protein *in vivo*. *J. Virol.* **67,** 407-414.

Chong, L.D., and Rose, J.K. (1994). Interactions of normal and mutant vesicular stomatitis virus matrix proteins with the plasma membrane and nucleocapsids. *J. Virol.* **68,** 713-719.

Clague, M.J., Schoch, C., Zech, L., and Blumenthal, R. (1990). Gating kinetics of pH-activated membrane fusion of vesicular stomatitis virus with cells: stopped-flow measurements by dequenching of octadecylrhodamine fluorescence. *Biochem.* **29,** 1303-1308.

Coll, J.M. (1995). The glycoprotein G of rhabdoviruses. *Arch. Virol.* **140,** 827-851.

Coll, J.M. (1995a). Heptad repeat sequences in the glycoprotein of rhabdoviruses. *Virus Genes* **10,** 107-114.

Crimmins, D., Mehard, W., and Schlesinger, S. (1983). Physical properties of a soluble form of the glycoprotein of vesicular stomatitis virus at neutral and acidic pH. *Biochem.* **22**, 5790-5796.

Crise, B., Ruusala, A., Zagouras, P., Shaw, A., and Rose, J.K., (1989). Oligomerization of glycolipid-anchored and soluble forms of the vesicular stomatitis virus glycoprotein. *J. Virol.* **63,** 5328-5333.

Daniels, R.S., Downie, J.C., Hay, A.J. Knossow, M., Skehel, J.J., Wang, M.L., and Wiley, D.C. (1985). Fusion mutants of the influenza virus hemagglutinin glycoprotein. *Cell* **40,** 431-439.

de Silva, A.M., Balch, W.E., and Helenius, A. (1990). Quality control in the endoplasmic reticulum: folding and misfolding of vesicular stomatitis virus G protein in cells and in vitro. *J. Cell Biol.* **111,** 857-866.

de Silva, A.M., Braakman, I., and Helenius, A. (1993). Post-translational folding of vesicular stomatitis virus G protein in the ER: involvement of noncovalent and covalent complexes. *J. Cell Biol.* **120,** 647-655.

Doms, R.W., Helenius, A., and White, J. (1985). Membrane fusion activity of the influenza virus hemagglutinin: the low pH-induced conformational change. *J. Biol. Chem.* **260,** 2973- 2981.

Doms, R.W., Keller, D.S., Helenius, A., and Balch, W.E. (1987). Role of adenosine triphosphate in regulating the assembly and transport of vesicular stomatitis virus G protein trimer. *J. Cell Biol.* **105,** 1957-1969.

Doms, R.W., Lamb, R.A., Rose, J.K., and Helenius, A. (1993). Folding and assembly of viral membrane proteins. *Virology* **193,** 545-562.

Doms, R.W., Ruusala, A., Machamer, C., Helenius, J., Helenius, A., and Rose, J.K. (1988). Differential effects of mutations in three domains on folding, quaternary structure, and intracellular transport of vesicular stomatitis virus G protein. *J. Cell Biol.* **107,** 89-99.

Dubovi, E.J., and Wagner, R.R. (1990). Spatial Relationship of the proteins of vesicular stomatitis virus: induction of reversible oligomers by cleavable protein cross linkers and oxidation. *J. Virol.* **22,** 500-509.

Durell, S.R., Martin, I., Ruysschaert, J.-M., Shai, Y., and Blumenthal., R. (1997). What studies of fusion peptides tell us about viral envelope glycoprotein mediated membrane fusion (review). *Mol. Membr. Biol.* **14,** 97-112.

Durrer, P., Gaudin, Y., Ruigrok, R.W., Graf, R., and Brunner, J. (1995). Photolabeling identifies a putative fusion domain in the envelope glycoprotein of rabies and vesicular stomatitis viruses. *J. Biol. Chem.* **270,** 17575-17581.

Fass, D., Harrison, S.C., and Kim, P.S. (1996) Retrovirus envelope domain at 1.7Å resolution. *Nature Struct. Biol.* **3,** 465-469.

Fass, D., and Kim, P.S. (1995). Dissection of a retrovirus envelope protein reveals structural similarity to influenza hemagglutinin. *Curr. Biol.* **5,** 1377-1383.

Fredericksen, B.L., and Whitt, M.A. (1995). Vesicular stomatitis virus glycoprotein mutations that affect membrane fusion activity and abolish virus infectivity. *J. Virol.* **69,** 1435-1443.

Fredericksen, B.L., and Whitt, M.A. (1996). Mutations at two conserved acidic amino acids in the glycoprotein of vesicular stomatitis virus affect pH-dependent conformational changes and reduce the pH threshold for membrane fusion. *Virology* **217,** 49-57.

Florkiewicz, R.Z., and Rose, J.K. (1984). A cell line expressing vesicular stomatitis virus glycoprotein fuses at low pH. *Science* **225,** 721-723.

Freed, E.O. and Martin, M.A. (1995). The role of human immunodeficiency virus type 1 envelope glycoproteins in virus infection. *J. Biol. Chem.* **270,** 23883-23886.

Freed, E.O., and Myers, D.J. (1992). Identification and characterization of fusion and processing domains of the human immuno-deficiency virus type 2 envelope glycoprotein. *J. Virol.* **66,** 5472-5478.

Freed, E.O., Myers, D.J., and Risser, R. (1990). Characterization of the fusion domain of the human immunodeficiency virus type 1 envelope glycoprotein gp41. *Proc. Natl. Acad. Sci. USA* **87,** 4650-4654.

Fuller, S.D., Berriman, J.A., Butcher, S.J., and Gowen, B.E. (1995). Low pH induces swivelling of the glycoprotein heterodimers in the Semliki forest virus spike complex. *Cell* **81,** 715-725.

Gallione, C.J., and Rose, J.K. (1983). Nucleotide sequence of a cDNA clone encoding the entire glycoprotein from the New Jersey serotype of vesicular stomatitis virus. *J. Virol.* **46,** 162-169.

Gaudin, Y., Ruigrok, R., Knossow, M., and Flamand, A. (1993). Low-pH conformational changes of rabies virus glycoprotein and their role in membrane fusion. *J. Virol.*, **69,**

1435-1443.

Gaudin, Y., Ruigrok, R.W.H., and Brunner, J. (1995). Low-pH induced conformational changes in viral fusion proteins: implications for the fusion mechanism. *J. Gen. Virol.* **76,** 1541-1556.

Gaudin, Y., Tuffereau, C., Durrer, P., Flamand, A., and Ruigrok, R. (1995a). Biological function of the low-pH, fusion-inactive conformation of rabies virus glycoprotein (G): G is transported in a fusion-inactive state-like conformation. *J. Virol.*, **69,** 5528-5534.

Gaudin, Y., Tuffereau, C., Segretain, D., Knossow, M., and Flamand, A. (1991). Reversible conformational changes and fusion activity of rabies virus glycoprotein. *J. Virol.* **65,** 4853- 4859.

Gaudin, Y., Raux, H., Flamand, A., and Ruigrok, R.W.H. (1996). Identification of amino acids controlling the low-pH-induced conformational change of rabies virus glycoprotein. *J. Virol.* **70,** 7371-7378.

Gething, M.J., Doms, R.W., York, D., and White, J. (1986). Studies of the mechanism of membrane fusion: Site-specific mutagenesis of the hemagglutinin of influenza virus. *J. Cell Biol.* **102,** 11-23.

Graham, F.L., and A.J. Van Der Eb. (1973). A new technique for the assay of infectivity of human adenovirus 5 DNA. *Virology* **52,** 456-457.

Guan, J.-L., Machamer, C.E., and Rose, J.K. (1985). Glycosylation allows cell surface transport of an anchored secretory protein. *Cell* **42,** 489-496.

Guan, J.-L., and Rose J.K. 1984. Conversion of a secretory protein into a transmembrane protein results in its transport to the Golgi complex but not to the cell surface. *Cell,* **37,** 779-787.

Guan, J.-L., Ruusala, A., Cao, H., and Rose, J.K. (1988). Effects of altered cytoplasmic domains on transport of the vesicular stomatitis virus glycoprotein are transferable to other proteins. *Mol. Cell. Biol.* **8,** 2869-2874.

Hammond, C., and Helenius, A. (1994). Quality control in the secretory pathway: retention of a misfolded viral membrane glycoprotein involves cycling between the ER, intermediate compartment, and golgi apparatus. *J. Cell Biol.* **126,** 41-52.

Hanahan, D. (1985). Techniques for transformation of *E. coli.* In: DNA Cloning: A

Practical Approach, Vol 1, D. M. Glover, ed, p. 109-135. IRL Press, Oxford.

Hart, T.K., Kirsch, R., Ellens, H., Sweet, R.W., Lambert, D.M., Petterway, S.R., Jr., Learly, J., and Bugelski, P.J. (1991). Binding of soluble CD4 proteins to human immunodeficiency virus type1 and infected cells induces release of envelope glycoprotein gp120. *Proc. Natl. Acad. Sci. USA* **88,** 2189- 2193.

Harter, C., James, P., Bächi, T., Semenza, G., and Brunner, W.J. (1989). Hydrophobic binding of the ectodomain of influenza hemagglutinin to membranes occurs through the "fusion peptide". *J. Biol. Chem.* **264,** 6459-6464.

Herrmann, A., Clague, M.J., Puri, A., Morris, S.J., Blumenthal, R., and Grimaldi, S. (1990). Effect of erythrocyte transbilayer phospholipid distribution on fusion with vesicular stomatitis virus. *Biochem.* **29,** 4054-4058.

Hernandez, L.D., Hoffman, L.R., Wolfsberg, T.G., and White, J.M. (1996). Virus-cell and cell-cell fusion. *Annu. Rev. Cell Dev. Biol.* **12,** 627-661.

Hughson, F.M. (1995). Molecular mechanisms of protein-mediated membrane fusion. *Curr. Opinion Struct. Biol.* **5,** 507-513.

Hughson, F.M. (1997). Enveloped viruses: a common mode of membrane fusion? *Curr. Biol.* **7,** R565-R569.

Ish-Horowicz, D., and J.F. Burke. (1981). Rapid and Efficient Cosmid Cloning. *Nucleic Acids Res.* **9,** 2989-2998.

Iverson, L.E., and Rose, J.K. (1981). Localized attenuation and discontinuous synthesis during vesicular stomatitis virus transcription. *Cell* **23,** 477-484.

Jiang, S., Lin, K., Strick, N., and Neurath, A.R. (1993). HIV-1 inhibition by a peptide. *Nature* **365,** 113.

Justice, P.A., Sun, W., Li, Y., Ye., Z., Grigera, P.R., and Wagner, R.R. (1995). Membrane vesiculation function and exocytosis of wild-type and mutant matrix proteins of vesicular stomatitis virus. *J. Virol.* **69,** 3156-3160.

Kemble, G.W., Daniele, T., and White, J.M. (1994). Lipid-anchored influenza hemagglutinin promotes hemifusion, not complete fusion. *Cell* **78,** 383-391.

Kielian, M. (1993). Membrane fusion activity of alpha-viruses. In: Viral fusion mechanisms, J. Bentz, ed, p. 386-412. CRC Press, Boca Raton, Fla.

Kielian, M.C., and Helenius, A. (1985). pH induced alterations in the fusogenic spike protein of Semliki Forest virus. *J. Cell Biol.* **101,** 2284-2291.

Kielian, M., Klimjack, M.R., Ghosh, S., and Duffus, W.A. (1996). Mechanisms of mutations inhibiting fusion and infection by Semliki Forest virus. *J. Cell Biol.* **134,** 863-872.

Kim, C.-H., Macosko, J.C., and Shin, Y.-K. (1998). The mechanism for low-pH induced clustering of phospholipid vesicles carrying the HA2 ectodomain of influenza hemagglutinin. *Biochem.* **37,** 137-144.

Knipe, D.M., Baltimore, D., and Lodish, H.F. (1977). Separate pathways of maturation of the major structural proteins of vesicular stomatitis virus. *J. Virol.* **21,** 1128-1139.

Koener, J.F., Passavant, C.W., Kurath, G., and Leong, J. (1987). Nucleotide sequence of a cDNA clone carrying the glycoprotein gene of infectious hematopoietic necrosis virus, a fish rhabdovirus. *J. Virol.* **61,** 1342-1349.

Kondor-Koch, C., Burke, B., and Garoff, H. (1983). Expression of Semliki Forest virus proteins from cloned complementary DNA. I. The fusion activity of the spike glycoproteins. *J. Cell Biol.* **97,** 644-651.

Kornfeld, R., and Kornfeld, S. (1985). Assembly of asparagine-linked oligosaccharides. *Ann. Rev. Biochem.* **54,** 631-664.

Kreis, T.E., and Lodish, H.F. (1986). Oligomerization is essential for transport of vesicular stomatitis virus glycoprotein to the cell surface. *Cell* **46,** 929-937.

Kunkel, T., Roberts, J.D., and Zakour, R.A. (1987). Rapid and efficient site-specific mutagenesis without phenotypic selection. *Methods Enzymol.* **154,** 367-387.

Laemmli, U.K. (1970). Cleavage of Structural Proteins During the Assembly of the Head of Bacteriophage T4. *Nature* **227,** 680-685.

Lazarowitz, S.G., Compans, R.W., and Choppin, P.W. (1971). Influenza virus structural and nonstructural proteins in infected cells and their plasma membranes. *Virology* **46,** 830-843.

Lenard, J. (1993). Vesicular stomatitis virus fusion. In: Viral Fusion Mechanisms, J. Bentz, ed., p. 425-435. CRC Press, Boca Raton, Fla.

Levy-Mintz, P., and Kielian, M. (1991). Mutagenesis of the putative fusion domain of the Semliki Forest virus spike protein. *J. Virol.* **65,** 4292-4300.

Li, Y., Drone, C., Sat, E., and Ghosh, H.P. (1993). Mutational analysis of the vesicular stomatitis virus glycoprotein G for membrane fusion domains. *J. Virol.* **67,** 4070-4077.

Li, Y., Luo, L., Schubert, M., Wagner, R.R., and Kang, C.-Y. (1993a). Viral liposomes released from insect cells infected with recombinant baculovirus expressing the M protein from vesicular stomatitis virus. *J. Virol.*, **67,** 4415-4420.

Lu, M., Blacklow, S.C., and Kim, P.S. (1995) A trimeric structural domain of the HIV-1 transmembrane glycoprotein. *Nature Struct. Biol.* **2,** 1075-1082.

Machamer, C.E., Doms, R.W., Bole, G.B., Helenius, A., and Rose, J.K. (1990). BiP recognizes incompletely disulfide-bonded forms of vesicular stomatitis virus G protein. *J. Biol. Chem.* **265,** 6879-6883.

Masters, P.S., Bhella, R.S., Butcher, M., Patel, B., Ghosh , H.P., and Banerjee, A.K. (1989). Structure and expression of the glycoprotein gene of Chandipura virus. *Virology* **171,** 285-290.

Mathieu, M.E., Grigera, P.R., Helenius, A., and Wagner, R.R. (1996). Folding, unfolding, and refolding of the vesicular stomatitis virus glycoprotein. *Biochem.* **35,** 4084-4093.

Mebatsion, T., Konig, M., and Conzelmann, K.-K. (1996). Budding of rabies virus particles in the absence of the spike glycoprotein. *Cell* **84,** 941-951.

Melikyan, G.B., White, J.M., and Cohen, F.S. (1995). GPI-anchored influenza hemagglutinin induces hemifusion to both red cell and planar bilayer membranes. *J. Cell Biol.* **131,** 679-691.

Mildvan, A.S., Weber, D.J., and Kupiopulos A. (1992). Quantitative interpretations of double mutations of enzymes. *Arch. Biochem. Biophys.* **294,** 327-340.

Moore, J.P., McKeating, J.A., Weiss, R.A., and Sattentau, Q.J. (1990). Dissociation of gp120 from HIV-1 virions induced by soluble CD4. *Science* **250,** 1139-1142.

Morris, S., Sarkar, D., White, J., and Blumenthal, R. (1988). Kinetics of pH-dependent fusion between 3T3 fibroblasts expressing influenza hemagglutinin and red blood cells. *J. Bol. Chem.* **264,** 3972-3978.

Odell, D., Wanas, E., Yan, J., and Ghosh, H.P. (1997). Influence of membrane anchoring and cytoplasmic domains on the fusogenic activity of vesicular stomatitis virus glycoprotein G. *J. Virol.* **71,** 7996-8000.

Ohnishi, S.-I. (1988). Fusion of viral envelopes with cellular membranes. *Curr. Top. Membr. Transp.* **32,** 257-298.

Owens, R.J., and Rose, J.K. (1993). Cytoplasmic domain requirement for incorporation of a foreign envelope protein into vesicular stomatitis virus. *J. Virol.* **67,** 360-365.

Pak, C.C., Puri, A., and Blumenthal, R. (1997). Conformational changes and fusion activity of vesicular stomatitis virus glycoprotein: [^{125}I]iodonapthyl azide photolabeling studies in biological membranes. *Biochem.* **36,** 8890-8896.

Puri, A., Drumbigel, M., Dimitrov, D., and Blumenthal, R. (1993). A new approach to measure fusion activity of cloned viral envelope proteins: fluorescence dequenching of octadecylrhodamine- labelled plasma membrane vesicles fusing with cells expressing vesicular stomatitis virus glycoprotein. *Virol.* **195,** 855-858.

Puri, A., Winick, J., Lowy, J.R., Covell, D., Eidelman, O., Walter, A., and Blumenthal, R. (1988). Activation of vesicular stomatitis virus fusion with cells by pretreatment at low pH. *J. Biol. Chem.* **263,** 4749-4753.

Rapaport, D., and Shai, Y. (1994). Interaction of fluorescently labelled analogues of the amino-terminal fusion peptide of Sendai virus with phospholipid membranes. *J. Biol. Chem.* **269,** 15124-15131.

Reidel, H., Kondor-Koch, C., and Garoff, H. (1984). Cell surface expression of fusogenic vesicular stomatitis virus G protein from cloned cDNA. *EMBO J.* **3,** 1477-1483.

Robbins, P., Timble, R.B., Wirth, D.F., Hering, C., Maley, F., Maley, G.F., Das, R., Gibson, B.W., Royal, N., and Bilmann, K. (1984). Primary structure of the Streptomyces enzyme endo-beta-N-acetylglucosaminidase H. *J. Biol. Chem.* **259,** 7577-7583.

Rolls, M.M., Haglund, K., Rose, J.K. (1996). Expression of additional genes in a vector derived from a minimal RNA virus. *Virol.* **218,** 406-411.

Rose, J.K., and Bergmann, J.E. (1983). Altered cytoplasmic domains affect intracellular transport of the vesicular stomatitis virus glycoprotein. *Cell* **34,** 513-524.

Rose, J.K., and Gallione, C.J. (1981). Nucleotide sequences of the mRNA's encoding the vesicular stomatitis virus G and M proteins determined from cDNA clones containing the complete coding regions. *J. Virol.* **39,** 519-528.

Rose, J.K., Doolittle, R.F., Anilionis, A., Curtis, P.J., and Wunner, W.H. (1982). Homology between the glycoproteins of vesicular stomatitis virus and rabies virus. *J. Virol.* **43,**

361-364.

Sambrook, J., Fritsch, E.F., and Maniatis, T. (1989). Molecular Cloning. A Laboratory Manual, 2nd Edition. Cold Spring Harbor Laboratory Press, Cold Spring Harbor, N.Y.

Sanger, F., Nickelen, S., and A.R. Coulson. (1977). DNA sequencing with chain terminating inhibitors. *Proc. Natl. Acad. Sci. USA*, **74,** 5463-5467.

Schlegel, R., Tralka, T. S., Willingham, M. C., and Pastan, I. (1983). Inhibition of VSV binding and infectivity by phosphatidylserine: Is phosphatidylserine a VSV binding site? *Cell* **32,** 639-646.

Schloemer, R. H., and Wagner, R. R. (1975). Cellular adsorption function of the sialoglycoprotein of vesicular stomatitis virus and its neuraminic acid. *J. Virol.* **15,** 882-893.

Schnell, M.J., Buonocore, L., Boritz, E., Ghosh, H.P., Chernish, R., and Rose, J.K. (1998). Requirement for a non-specific glycoprotein cytoplasmic domain sequence to drive efficient budding of vesicular stomatitis virus. *EMBO J.* **17,** 1289-1296.

Schoch, C., and Blumenthal, R. (1993). Role of the fusion peptide sequence in initial stages of influenza hemagglutinin-induced cell fusion. *J. Biol. Chem.* **268,** 9267-9274.

Schroth-Diez, B., Ponimaskin, E., Reverey, H., Schmidt, M.F.G., and Herrmann, A. (1998). Fusion activity of transmembrane and cytoplasmic domain chimeras of the influenza virus glycoprotein hemagglutinin. *J. Virol.* **72,** 133-141.

Shokralla, S., He, Y., Wanas, E., and Ghosh, H.P. (1998). Mutations in a carboxy-terminal region of vesicular stomatitis virus glycoprotein G that affect membrane fusion activity. *Virology* **242,** 39-50.

Shortle, D. (1995). Staphylococcal nuclease: a showcase of m-value effects. *Adv. Protein Chem.* **46,** 217-247.

Skehel, J.J., Bizebard, T.,Bullough, P.A., Hughson, F.M., Knossow, M., Steinhauer, D.A., Wharton, S.A., and Wiley, D.C. (1995). Membrane fusion by influenza hemagglutinin. *Cold Spring Harbor Symp. Quant. Biol.* **60,** 573-580.

Skehel, J.J., and Waterfield, M.D. (1975). Studies on the primary structure of the influenza virus hemagglutinin. *Proc. Natl. Acad. Sci. USA* **72,** 93-97.

Stegmann, T., Doms, R.W., and Helenius, A. (1989). Protein-mediated membrane fusion. *Annu. Rev. Biophys. Bioyphis. Chem.* **18,** 187-211.

Steinhauer, D., Martin, J., Pu Lin, Y., Wharton, S., Oldstone, M., Skehel, J., and Wiley, D. (1996). Studies using double mutants of the conformational transitions in Influenza hemagglutinin required for its membrane fusion activity. *Proc. Natl. Acad. Sci. USA* **93**, 12873-12878.

Steinhauer, D., Wharton, S., Skehel, J., and Wiley, D. (1995). Studies of the membrane fusion activities of fusion peptide mutants of influenza virus hemagglutinin. *J. Virol.* **69**, 6643-6651 48.

Tabas, I., and Kornfeld, S. (1984). The synthesis of complex-type oligosaccharides. III. Identification of an alpha-D-mannosidase activity involved in a late stage of processing of complex type oligosaccharides. *J. Biol. Chem.* **253**, 7779-7786.

Tanabayashi, K., and Compans, R. (1996). Functional interaction of paramyxovirus glycoproteins: identification of a domain in Sendai virus HN which promotes cell fusion. *J. Virol.* **70**, 6112-6118.

Teninges, D., and Bras-Herreng, F. (1987). Rhabdovirus sigma, the hereditary CO_2 sensitivity agent of Drosophila: nucleotide sequence of a cDNA clone encoding the glycoprotein. *J. Gen. Virol.* **68**, 2625-2638.

Tordo, N., Bourhy, H., Sather, S., and Ollo, R. (1993). Structure and expression in baculovirus of the Mokola virus glycoprotein: an efficient recombinant vaccine. *Virology* **194**, 59-69.

Wagner, R.R., and Rose, J.K. (1996). Rhabdoviridae: the viruses and their replication. In: Fundamental Virology, Fields, ed. p. 561-575. Lippincott-Raven Publishers, Philadelphia.

Weis, W., Brown, J., Cusack, S., Paulson, J.C., Skehel, J.J., and Wiley, D.C. (1988). The structure of the influenza virus hemagglutinin complexed with its receptor, sialic acid. *Nature* **33**, 426-431.

Weis, W., Cusack, S., Brown, J., Daniels, R., Skehel, J., and Wiley, D. (1990). The structure of a membrane fusion mutant of the influenza virus hemagglutinin. *EMBO J.* **9**, 17-24.

Weissenhorn, W., Dessen, A., Harrison, S.C., Skehel, J.J., and Wiley, D.C. (1997). Atomic structure of the ectodomain from HIV-1 gp41. *Nature* **387**, 426-430.

Wells, J.A. (1990). Additivity of mutational effects in proteins. *Biochem.* **29**, 8509-8517.

Wharton, S.A., Ruigrok, R.W.H., Martin, S.R., Skehel, J.J., Bayley, P.M., Weis, W., and Wiley, D.C. (1988). Conformational aspects of the acid-induced fusion mechanisms of influenza virus hemagglutinin. *J. Biol. Chem.* **263,** 4474-4480.

White, J.M. (1992). Membrane fusion. *Science* **258,** 917-924.

White, J.M. (1990). Viral and cellular membrane fusion proteins. *Annu. Rev. Physiol.* **52,** 675-697.

Whitt, M.A., Buonocore, L., Prehaud, C., and Rose, J.K. (1991). Membrane fusion activity, oligomerization, and assembly of the rabies virus glycoprotein. *Virol.* **185,** 681-688.

Whitt, M.A., Chong, L., Rose, J.K. (1989). Glycoprotein cytoplasmic domain sequences required for rescue of a vesicular stomatitis virus glycoprotein mutant. *J. Virol.* **63,** 3569-3578.

Whitt, M.A., Zagouras, P., Crise, B., and Rose, J.K. (1990). A fusion-defective mutant of the vesicular stomatitis virus glycoprotein. *J. Virol.* **64,** 4907-4913.

Wild, C.T., Oas, T., McDanal, C.B., Bolognesi, D., and Matthews, T.J. (1992). A synthetic peptide inhibitor of human immunodeficiency virus replication: correlation between solution structure and viral inhibition. *Proc. Natl. Acad. Sci. USA* **89,** 10537-10541.

Wild, C.T., Shugars, D.C., Grenwell, T.K.,, McDanal, C.B., and Matthews, T.J. (1994). Peptides corresponding to a predictive α-helical domain of human immunodeficiency virus type 1 gp41 are potent inhibitors of virus infection. *Proc. Natl. Acad. Sci. USA* **91,** 9770-9774.

Wiley, D.C., and Skehel, J.J. (1987). The structure and function of the hemagglutinin membrane glycoprotein of influenza virus. *Ann. Rev. Biochem.* **56,** 365-394.

Wilkinson, D. (1996). HIV-1: co-factors provide the entry keys. *Curr. Biol.* **6,**1051-1053

Wilson, I.A., Skehel, J.J., and Wiley, D.C. (1981). Structure of the hemagglutinin membrane glycoprotein of influenza virus at 3 Å resolution. *Nature* **289,** 366-373.

Woodgett, C., and Rose, J.K. (1986). Amino-terminal mutation of the vesicular stomatitis virus glycoprotein does not affect its fusion activity. *J. Virol.* **59,** 486-489.

Yamada, S., and Ohnishi, S.-I. (1986). Vesicular stomatitis virus binds and fuses with phoshpolipid domain in target cell membranes. *Biochem.* **25,** 3703-37.

Zagouras, P., Ruusala, A., and Rose, J. (1991). Dissociation and reassociation of oligomeric viral glycoprotein subunits in the endoplasmic reticulum. *J. Virol.* **65,** 1976-1984.

Zhang, L., and Ghosh, H.P. (1994). Characterization of the putative fusogenic domain in vesicular stomatitis virus glycoprotein G. *J. Virol.* **68,** 2186-2193.

Zoller, M.J., and M. Smith. (1983). Oligonucleotide-directed mutagenesis of DNA fragments cloned into M13 vectors. *Methods Enzymol.* **100,** 468-500.